Architected Acoustic Metamaterials: an integrated design perspective

G. Comandini[a],[1] **M. Ouisse**,[2] **V. P. Ting**,[1,3] and **F. Scarpa**[1]
[1]*Bristol Composite Institute (BCI), School of Civil, Aerospace and Mechanical Engineering (CAME), University of Bristol, Bristol, UK*
[2]*SUPMICROTECH, Université de Franche-Comté, CNRS, Institut FEMTO-ST, 25000, Besançon, France*
[3]*Research School of Chemistry, Australian National University, Canberra, ACT, 2601, Australia*

[a]*Corresponding author email: gianni.comandini@bristol.ac.uk*

The review focuses on architected acoustic metamaterials to manipulate airborne sound waves, with only limited discussions on elastic metamaterials related to solid media. We review the design of acoustic metamaterials and the physical mechanisms underpinning their performance and related manufacturing methodologies, while also examining potential issues and challenges affecting the use of metamaterials in acoustics. The complexities of several metamaterial architectures are discussed. A new classification system is proposed to distinguish metamaterial configurations based on the typology of the channels inside the acoustic meta-atom. Several types of acoustic metamaterials architectures like perforated and micro-perforated panels, acoustic foams, resonators, various geometrical paths, and piezoelectric patches, are also discussed.

The fundamental acoustic mechanisms of these classes of metamaterials are identified and commented on. The paper also describes the main measurement techniques used for acoustic metamaterials and the physical quantities evaluated, providing a guide to characterise and assess their performance. The fundamental challenges of the current metamaterials designs are discussed with a focus on the complex synergy between architectural patterns of acoustic metamaterials and their thickness. We clarify the distinction between acoustic and elastic metamaterials, emphasizing the design and applications of materials that manipulate sound waves in fluid media. The paper also offers further comments about the need for practical design tools to allow the use of acoustic metamaterials in real-world applications.

CONTENTS

I. INTRODUCTION

Acoustic metamaterials (AMs) provide an innovative approach to interacting with acoustic waves, surpassing the constraints of conventional porous materials and presenting new opportunities for sound and noise management.
This review concentrates on acoustic metamaterials in fluids, distinguishing them from elastic metamaterials that affect mechanical waves in solids.
Acoustic metamaterials are specifically engineered to control and manipulate the propagation of sound waves. They can be classified geometrically into several distinct categories, as shown in Fig. 1. Each type of metamaterial has unique or shared characteristics and applications. This geometrical classification provides a comprehensive framework for a better understanding of their design and offers insights into their potential applications in various fields.
Acoustic Metamaterials have gathered considerable attention in the field of material science and technological design, due to their various applications in areas such as noise mitigation[1], energy harvesting[2], and medical imaging[3].
AMs are characterised by their extraordinary properties, such as unusual bulk modulus and density[4], which can interact with acoustic waves innovatively; however, it is important to note that these characteristics are only applicable when equivalent fluid models are used to describe these metamaterials, a condition that does not universally apply.
These unusual or artificially-generated properties have led to various real-world applications, like minimising noise in hospital rooms during the recent pandemic[5], or making the external chiller unit of air conditioning systems more silent[6].

Amongst all the possible geometries, the fractal (Fig. 1*a*) is one of the most commonly and effectively used[1,8–19]. The advantage of using fractal geometries relies on the adoption of self-repeating patterns, which exhibit multi-scale structures[20]. Amongst all the space-filling fractal geometries, the Hilbert fractal appears to be one of the most robust and thoroughly investigated in terms of acoustic wave modulation.
Another architecture widely used in acoustic metamaterials is the coiled or space-coiling one (Fig. 1*b*). These geometries control the propagation of sound waves through the number of zigzag units inside the periodic unit area. Coiled structures can also be designed with tapered channels[21] and openings, allowing the further modulation of their acoustic properties for wider broadband effects.

Architected acoustic metamaterials can provide, in particular, tailored transmissibility[12,22–26] and focused acoustic wave projection capability[1,27–31]. AMs can also provide multifunctional capabilities, like structures with soundproofing and air passage capabilities to help reduce noise pollution without blocking ventilation[32–40], generating a more comfortable and sustainable built environment.
Their utility can span various industries, addressing heating, ventilation, and air conditioning (HVAC) noise[41] in buildings[42–45]. In terms of multifunctionality, some acoustic metamaterials can be used to enable sound insulation at extreme temperatures[46–49], opening up new possibilities for aeronautics and high-temperature machining. Acoustic metamaterials have been applied to combustion engine mufflers[50–53] or turbojets noise passing through an aeroplane fuselage[54].
Noise barriers[55]represent one of the most promising applica-

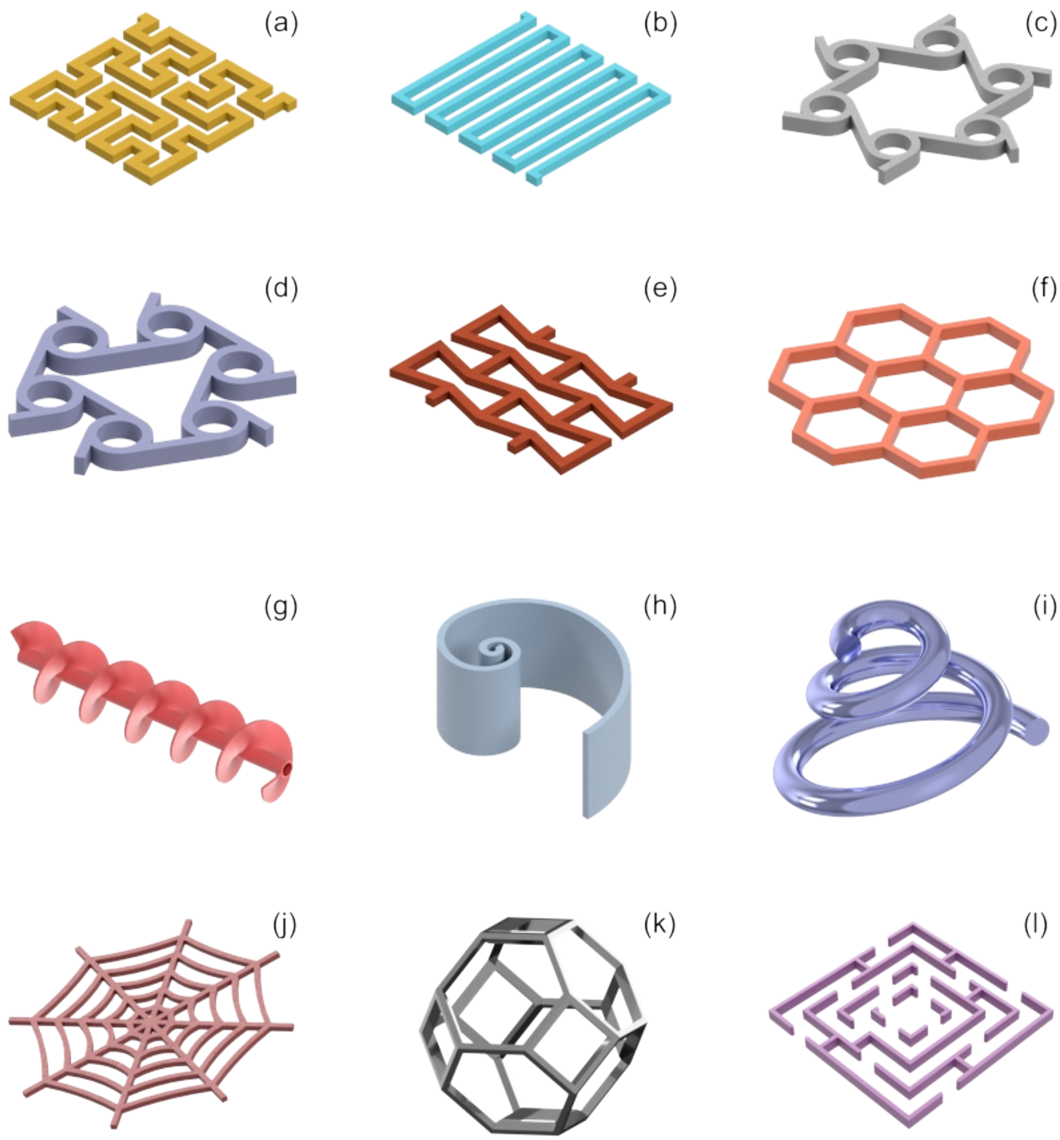

FIG. 1. Examples of the main geometries used in acoustic metamaterials: fractal (a), coiled or zigzag (b), chiral (c), antichiral (d), auxetic (e), honeycomb or hexagonal (f), helicoidal (g), spiral (h), cochlea (i), spider (j), Kelvin cell (k), and labyrinthine or maze (l). G. Comandini, *Hilbert Fractal Acoustic Metamaterials*, University of Bristol, 2024; licensed under a Creative Commons Attribution (CC BY) license[7].

tions of acoustic metamaterials. Those barriers function by attenuating noise pollution, thereby fostering a quieter environment (Fig. 2). The design of AMs barriers often involves the creation of materials that can absorb a wide spectrum of noise frequencies.

Beyond these, AMs seem to have found applications in everyday life, like reducing toilet flushing noise[56] in condominium buildings, where the turbulent water noise can interfere with other people's sleep and peace of mind. Acoustic meta-absorber prototypes have also shown their efficiency in reducing the noise of stage machinery in theatres and opera houses[35], thus improving the acoustic quality of performances and enhancing the overall experience in those leisure activities.

Architected acoustic metamaterials have also been used to exploit the tunnelling effect[22] in non-destructive testing[57–63] of structural and non-structural parts for SHM[64] in a non-destructive way. Acoustic metamaterials also demonstrate some promising energy harvesting capacity, transforming seemingly disruptive noise into a renewable energy source[2,65–70]. They can convert ambient acoustics into electrical energy through resonance processes that exploit the acoustic modes of the metamaterials, paving the way for sustainable and renewable energy sources (Fig. 3).

Quite interestingly, the exploration of the design and performance space of AMs is not solely limited to noise mitigation and energy usage. Biomedical applications have also been developed; examples are the improvement of the efficiency and effectiveness of hearing aids technologies[71–76] or more effective noise-cancelling headphones[17,77,78] for the mass market.

By manipulating the acoustic signals, acoustic metamaterials provide improved sound quality and clarity.
(Insert Fig. 2 here)
(Insert Fig. 3 here)
Similarly, an artificial cochlea[71], has been designed with a selective frequency picking along its architecture and modelled after the mammalian hearing organ (Fig. 1*i*), further advancing the field of audiology. Another biomedical application of AMs is related to the improvement of imaging technologies[45,58,60,79–87], for which the presence of a higher accuracy of image diagnostic would improve patient care[88].
One of the metamaterial effects, responsible for this enhanced image accuracy, is the tunnelling effect (Fig. 4), that can improve the visible features of interior structures [89]. This meta behaviour lets acoustic waves travel through a metamaterial, mimicking the diode effect [90]. Along an acoustic tunnel, it is possible to determine which one of the two potential orientations is restricted for the acoustic wave, using the reflection modulated by acoustic tunnel walls [90]. Thus, as a consequence, a decreased wave scattering [22] is obtained, thanks to its quasi-diode behaviour. The tunnelling effect (Fig. 4), can also increase image resolution for biological applications, such as body scans through ultrasounds, by reducing the presence of undesired reflection and refraction of the waves, augmenting, as a consequence, the image resolution quality. Moreover, the tunnelling effect could also be helpful in acoustic underwater communications[91], for which traditional radio techniques do not work properly.
The use of acoustic metamaterials can improve the quality of water, due to ultrasonic treatments[92–95] that enable more efficient and sustainable solutions to decontaminate waste and drain waters from pollutants. This application employs high-frequency sound waves to eliminate impurities from water, improving its overall quality with fewer chemical agents added to the water to purify it.
Furthermore, acoustic metamaterials have been used for acoustic cloaking[96–106] to effectively manipulate sound waves around an object and making it acoustically invisible because of the minimum amount of reflected or refracted waves[107](Fig. 5). This feature has promising applications in defence applications: an acoustic metamaterial skin could be applied to a stealth submarine[108] to make it acoustically invisible to enemy sonar.
Surprisingly, AMs can also be designed to act as transistors[109–112] to perform math operations with acoustic signals for acoustic computing applications[112]. This latter will form the basis of an acoustic calculator that can solve ordinary differential equations and more in environments where, due to harsh and strong electromagnetic fields, a traditional computational system would not work.
Further exciting applications of acoustic metamaterials include acoustic levitation (Fig. 6), with ultrasound[82,113–120] to manipulate extremely hot, reactive or toxic chemical compounds in a contactless manner.
Architectural acoustics is another domain exploiting the benefits of acoustic metamaterials, leveraging their soundproofing abilities to create quieter spaces. Urban planning applications constitute another possible field that would benefit from adopting acoustic metamaterials. Applying fractal geometries to architectural forms[121,122] can lead to a higher noise diffusion within cities, with a consequent drop in noise pollution and improved life quality of all the urban residents.
Another unique attribute facilitates their use in sensors that detect[87] and respond[123] to sound. The use of AMs as antennae[80,87,123–131] allows for the enhancement of weak acoustic signals within random noise, which could help with diagnostics in rotating and complex mechanisms to avoid imminent catastrophic failures. Broadband acoustic sensing (Fig. 7), for instance, allows for capturing both low-level and high-level features of audio signals, offering opportunities in various sectors such as surveillance[127] and healthcare[132]. Acoustic sensors can be classified in two types: directional[87] and non-directional[80] acoustic antennas. Directional antennas are useful to spot specific frequencies in a noisy environment. For instance, the diagnostics of a different frequency from the one generated by an imminent failure can help avoid stopping production in an assembly line. On the other hand, the non-directional antenna can spot the noise direction in a 3D environment. This feature can be useful in robotics to detect a generic noise source position (Fig. 8). In the field of wave propagation, acoustic metamaterials with chiral Archimedean spirals[133] or other coiled geometries can modify the wavefront[134], allowing for precise control of propagation with limited or null waves refracted or reflected. This application of metamaterials could lead to the creation of acoustic barriers[135], which would direct sound waves into designated areas where noise is not a concern.

A. Topological

A significant innovation within this domain is the study of topological acoustic metamaterials. These systems utilise concepts from topological physics to generate edge states that exhibit resistance to defects and irregularities. These topologically protected modes allow for directional sound propagation without backscattering, offering substantial benefits for the development of durable acoustic waveguides and devices[136]. For example, research on adjustable acoustic acceleration beams illustrates the application of topological ideas to achieve precise manipulation of the propagation of sound waves[137]. Incorporating topological principles into metamaterials not only strengthens their durability and efficiency, but also sets the stage for creating devices capable of maintaining functionality despite structural flaws. This research highlights the transformative potential of topological acoustic metamaterials to advance sound manipulation technologies, providing innovative solutions to intricate acoustic problems.

B. Non-reciprocal

Non-reciprocal acoustic metamaterials signify a major breakthrough in controlling sound, facilitating directional sound propagation, and fostering groundbreaking uses such as acoustic diodes and isolators. These systems leverage non-reciprocity, a phenomenon in which sound waves propagate in a single direction while being restricted in reverse, thus optimising sound control in critical settings such as recording studios and concert halls[138–140]. Recent advances have highlighted diverse strategies for performing non-reciprocal acoustic propagation, including spatiotemporal modulation and magnetoelastic effects, which successfully disrupt the time-reversal symmetry[139,141]. Furthermore, the creation of acoustic metamaterials that feature extensive band gaps has proven effective in isolating sound over broad frequency ranges, making them ideal for scenarios that require meticulous acoustic control[142]. Incorporating these innovations not only improves sound isolation, but also sets the stage for the design of functional acoustic devices specifically adapted to unique acoustic settings[140,143,144].

C. Multifunctional

The field of multifunctional acoustic metamaterials has gained prominence, focusing on the design of materials capable of performing several tasks at once. Examples include merging sound-damping properties with structural support or combining acoustic wave control with heat regulation[145,146]. The achievement of multiple functionalities in a single-material system enhances performance and minimises the requirement for separate components, resulting in more streamlined and cohesive designs. Alongside advances in active and programmable metamaterials, interest has grown in hybrid metamaterials that integrate diverse functionalities. Recent investigations have highlighted the feasibility of acoustic metamaterials acting as both noise barriers and energy generators. By embedding piezoelectric elements within the metamaterial framework, researchers have engineered systems capable of transforming sound energy into electrical energy, enabling dual-purpose noise mitigation and energy production[68,147,148]. This innovation is especially applicable in urban areas where noise pollution is a significant issue, presenting an eco-friendly solution for both noise reduction and energy harvesting. Such developments underscore the movement toward the creation of materials with versatile applications, increasing their practicality in real-world scenarios.

D. Artificial Intelligence & Machine Learning

The incorporation of artificial intelligence (AI) and machine learning (ML) techniques has experienced a remarkable growth in advancing the creation of innovative metamaterials. These computational approaches reveal groundbreaking design possibilities that may surpass human intuition, thus expediting the development of state-of-the-art acoustic technologies[149]. Using generative models within machine learning aids in exploring expansive design spaces, uncovering unique metamaterial configurations that human designers may overlook[150,151].

For example, machine learning tools can process experimental data to uncover relationships between structural characteristics and acoustic properties, refining design specifications through data-driven insights[152,153]. Furthermore, AI-powered optimisation methods can be utilised to boost the effectiveness of acoustic metamaterials in practical applications, such as adaptive noise control systems that modify their properties dynamically in response to variable acoustic conditions[154,155]. Additionally, combining AI and ML with acoustic metamaterials has enabled the creation of multifunctional devices capable of tackling diverse acoustic challenges at the same time. For example, recent studies have highlighted the potential for acoustic metamaterials to integrate both soundproofing and energy harvesting functions, uniting two traditionally separate functions into a material system[147,156]. This multifunctionality offers significant benefits in fields such as architectural acoustics, where materials must operate efficiently over a wide range of frequencies and environmental factors[157,158].

E. Fabrication Techniques

Advancements in acoustic metamaterials encompass not only their functional aspects but also the approaches used for their production. Developments in additive manufacturing and 3D printing have allowed the creation of intricate metamaterial designs with tailored acoustic features[159,160]. These innovations allow for the realisation of complex configurations that were previously challenging to achieve through conventional fabrication methods. Among the most promising techniques is two-photon lithography, which facilitates the production of microacoustic metagratings designed to function at extremely high frequencies. This method provides precise control over the geometry and spatial arrangement of the structure, which is crucial to attaining the desired acoustic effects such as sound focussing and negative refraction[161]. The capability of manipulating microstructures with such precision facilitates the creation of advanced acoustic lenses and devices that can guide sound waves in unconventional ways. Additive manufacturing, along with two-photon lithography, has become a critical method for producing acoustic metamaterials. This technology supports the fabrication of intricate structures that are often unachievable with standard manufacturing techniques. For example, 3D printing has been used to create acoustic metamaterials based on tetrakaidecahedron cells, which exhibit notable sound absorption properties[162]. The versatility of additive manufacturing not only enables the construction of complex shapes, but also allows the tailoring of material properties to address specific acoustic demands[163]. Furthermore, the use of soft metamaterials, which can be manufactured by 3D printing, has revealed exceptional acoustic characteristics, including the ability to exhibit negative acoustic indices. This proves especially advantageous for applications such as underwater acoustics, where the distinct features of soft metamaterials enhance sound transmission and absorption[156].

F. Tunable Passive & Active

The domain of acoustic metamaterials has seen remarkable progress in recent years, especially with innovations in tunable and active acoustic metamaterials. Tunable acoustic metamaterials enable modifications of acoustic responses through external factors such as mechanical strain, temperature changes, or magnetic influences, expanding their applicability in scenarios that require adaptable acoustic filtering or focus[164]. Incorporating origami-based structures into metamaterials, for example, offers substantial design flexibility to create programmable and responsive systems, underlining the critical role of tunability in contemporary acoustic technologies[165–167]. Active acoustic metamaterials leverage active components, including actuators and smart materials, to dynamically adjust their acoustic characteristics in real time under external stimuli. This real-time adaptability supports uses such as adaptive noise suppression and reconfigurable acoustic devices, which are becoming increasingly important in technological applications[168]. The programmable capabilities of these materials provide advanced functionalities that are unattainable with passive designs[169]. For example, the use of dynamic actuators to regulate the effective surface mass density of membrane-based acoustic metamaterials illustrates how active features achieve specific acoustic results[170,171]. This strategy facilitates the creation of materials that adapt to changing acoustic conditions, addressing needs in areas such as noise mitigation and soundproofing.

G. Programmable

The advent of programmable metamaterials has facilitated the modulation of their properties. By altering geometric structures or employing materials with, for instance, electronically tunable attributes, these metamaterials can be customised to produce specific acoustic outcomes as required. This capability is particularly beneficial in dynamic acoustic environments characterised by rapid fluctuations[172,173]. This flexibility is vital for applications in noise mitigation, sensing, and communication systems[173,174].

Recent progress has highlighted the capabilities of active acoustic metamaterials, which can dynamically modify their sound-dampening properties via intrinsic tuning mechanisms[175]. For example, incorporating piezoelectric components allows real-time adjustments to acoustic characteristics, thereby broadening their applicability in various settings[176]. Furthermore, the development of modular acoustic metamaterials has exhibited the potential to achieve precise noise control, resulting in notable advances in design effectiveness and overall performance[177].

(Insert Fig. 4 here)
(Insert Fig. 5 here)
(Insert Fig. 6 here)
(Insert Fig. 7 here)
(Insert Fig. 8 here)
(Insert Fig. 9 here)

Acoustic metamaterials constitute a step up in the application and understanding of already well-known materials for acoustic/sound management[178–182] and inspire scientific and industrial stakeholders to reconsider the use and functionality of conventional materials[183–187]. Fueled by the need for lighter and more efficient acoustic devices, the potential applications of AMs extend well beyond the confines of traditional noise control techniques.

From solving complex mathematical problems to their role in aerodynamic noise reduction and acoustic imaging, acoustic metamaterials represent truly multifunctional platforms of materials systems. Within the present review, we will examine the most frequently encountered metamaterial architectures that make up these unique constructs. We will then delve into these individual and combined configurations. The synergy between traditional acoustic components like resonators[188–192], foams[193–197] and porous panels[198–202], with the aforementioned AMs geometries will also be described.

This study will also cover materials commonly used in manufacturing AMs and provide an outline of the cutting-edge technologies that facilitate their production.

Our journey through the acoustic metamaterial landscape will continue by describing the main physical mechanisms behind the performance of AMs and also discussing various measurement tools capable of capturing their effects.

The final paragraph contains the Authors' perspective on the main obstacles and complexities associated with the development and use of acoustic metamaterials.

II. MAIN PHYSICAL MECHANISMS AND ARCHITECTURES

A. Distinction Between Acoustic and Elastic Metamaterials

Acoustic metamaterials (AMs) and elastic metamaterials (EMs) are designed for specific wave manipulation purposes, targeting sound waves and elastic waves, respectively. AMs are specialised for the control of sound waves in fluids, using methods such as resonance and impedance tuning to improve noise reduction and sound absorption[203–205]. Their diverse applications include architectural sound management and medical imaging, showcasing their ability to handle airborne pressure waves effectively[206]. On the other hand, EMs devices are designed to influence elastic waves within solids, addressing longitudinal and transverse waves that are critical for uses such as vibration isolation and seismic shielding[207,208]. Although these two types of metamaterial focus on different waveforms, they are based on shared principles such as periodic structures and localised resonances, resulting in effects such as negative effective mass density[204,209]. A clear grasp of these differences is essential to delineate their applications and the core physical principles that drive their functionality[203,206].

B. Influence of Geometric Structures on Acoustic Metamaterials

Acoustic metamaterials have become a key research focus due to their distinctive ability to control sound waves through specially designed structures that possess characteristics absent in traditional materials. The configurations used in acoustic metamaterials, including fractals, coiled designs, chiral and antichiral formations, auxetic structures, honeycomb patterns, helicoidal shapes, spirals, cochlea-inspired forms, spider web configurations, Kelvin cells, and labyrinthine designs, each provide unique physical principles and acoustic functionalities suitable for diverse applications.

1. *Fractals*

Fractal geometries (Fig. 1*a*), known for their self-similar patterns and intricate structures, repeat on varying scales. These features enhance wave manipulation and sound absorption by increasing the surface area-to-volume ratio. Studies show that fractal metamaterials enable broadband focus, essential for applications that require precise acoustic control, such as acoustic sensing and medical imaging[210]. The distinctive characteristics of fractals facilitate the creation of acoustic lenses capable of focussing sound waves with greater efficiency than conventional designs, thereby boosting the performance of devices such as ultrasonic transducers[210].

2. *Coiled or space-coiling geometries*

Coiled configurations (Fig. 1*b*), such as space coil designs, employ spiral structures to control sound waves by adjusting their phase and amplitude. These metamaterials enable concurrent modulation of various acoustic properties, making them effective for tasks such as sound filtration and wavefront alteration[58]. The crafting of coiled designs at scales smaller than the wavelength enhances their acoustic capabilities, especially in underwater scenarios where conventional materials often fail[211]. The remarkable ability of coiled geometries to manipulate waves has been shown to substantially increase the performance of acoustic technologies[58].

3. *Chiral geometries*

Chiral metamaterials (Fig. 1*c*) exhibit asymmetrical configurations that interact distinctively with sound waves, resulting in effects such as acoustic rotation and amplified sound transmission. By tailoring chiral characteristics, it becomes possible to create devices capable of directing sound propagation, offering valuable applications in fields such as acoustic imaging and sensing[212]. Research has recently shown that chiral designs can be customised to produce negative refractive indices, facilitating the innovation of advanced acoustic lenses and cloaking systems[212]. This potential smooths the way for breakthroughs in stealth technologies and sound control solutions.

4. *Antichiral geometries*

Antichiral configurations (Fig. 1*d*), characterised by their mirrored symmetry relative to chiral structures, are also capable of effectively manipulating sound waves. These designs can be customised to achieve distinctive acoustic characteristics, such as improved sound absorption and transmission, making them highly applicable for noise mitigation purposes[212]. The dynamic interaction between chiral and antichiral attributes facilitates the creation of cutting-edge acoustic devices that innovatively control sound and opens the door to advancements in acoustic cloaking and sound filtration technologies[212].

5. *Auxetic geometries*

Auxetic materials (Fig. 1*e*), exhibit a negative Poisson's ratio, which means that they expand laterally when pulled. This distinctive attribute is used in acoustic metamaterials to increase sound absorption and transmission[212]. Auxetic configurations can be customised to construct structures that efficiently capture and dissipate sound energy, making them well suited for noise reduction and soundproofing applications[212]. The adjustable properties of auxetic materials enable the creation of adaptive acoustic devices capable of responding to changes in sound frequencies and intensities, thus enhancing their overall functionality[212].

6. *Honeycomb or hexagonal geometries*

Honeycomb configurations (Fig. 1*f*) are renowned for their lightweight nature and the exceptional specific mechanical attributes, which make them advantageous for acoustic purposes. These patterns can be customised to make acoustic metamaterials with improved properties for sound absorption and transmission[213]. The hexagonal layout supports efficient wave propagation and can be adjusted to target particular frequency ranges, making it ideal for use in architectural acoustics and noise mitigation[213]. The adaptability of honeycomb structures allows their integration into various acoustic technologies, including sound barriers, acoustic liners, and sophisticated acoustic lenses[213].

7. *Helicoidal geometries*

Helicoidal designs (Fig. 1*g*), featuring spiral or helical configurations, influence sound waves by leveraging their distinct geometric characteristics. These metamaterials are tailored to produce targeted acoustic effects, such as focussing or scattering of sound waves[213]. The helicoidal configuration facilitates the development of devices capable of managing sound

transmission in three-dimensional space, making them ideal for use in medical imaging and ultrasound therapy[213]. The capacity to fabricate helicoidal structures at the microscale increases their efficiency in directing sound waves across various applications[213].
(Insert Fig. 9 here)

8. Spiral geometries

Spiral configurations (Fig. 1*h*) are employed to fabricate acoustic devices capable of distinctive wave manipulation properties. These designs focus on sound waves and improve sound transmission through their specific geometric arrangements[214]. Incorporating spiral patterns into acoustic metamaterials facilitates the creation of devices with exceptional sound control, which is critical for use in telecommunications and audio systems[214]. The adjustable nature of spiral geometries supports the development of adaptable acoustic devices that can accommodate changes in sound frequencies and intensities[214].

9. Cochlea-inspired geometries

Cochlea-inspired designs (Fig. 1*i*) replicate the intricate architecture of the human ear, facilitating effective sound manipulation and processing. These structures can be customised to improve sound absorption and transmission, making them highly applicable for use in acoustic sensors and hearing aids[213]. The biomimetic approach of cochlea-inspired geometries enables the creation of sophisticated acoustic devices that emulate biological systems, enhancing their capability for sound detection and processing[213](Fig. 8). Incorporating cochlea-inspired configurations into acoustic devices has the potential to drive remarkable progress in auditory technologies[213].

10. Spider web geometries

Spider web formations (Fig. 1*j*) possess remarkable mechanical and acoustic characteristics, which can be utilised in the design of metamaterials. The complex architecture of spider webs facilitates efficient sound absorption and propagation, making them ideal for noise mitigation and soundproofing applications[213]. The customisation of spider web geometries on a microscale enhances their ability to influence sound waves in various functionalities[213]. The lightweight and adaptable properties of spider web structures support their integration into various acoustic technologies, ranging from soundproof barriers to sophisticated acoustic lenses[213].

11. Kelvin cell geometries

Kelvin cell structures (Fig. 1*k*) exhibit a distinctive geometric configuration that can be tailored to achieve superior acoustic functionality. These designs can deliver targeted acoustic results, including improved sound absorption and transmission properties[215]. Incorporating Kelvin cells into acoustic metamaterials facilitates the creation of systems adept at capturing and dissipating sound energy, making them highly suitable for applications such as noise mitigation and sound insulation[215]. The adjustable nature of Kelvin cell geometries supports the development of adaptive acoustic systems capable of responding to different frequencies and intensities of sound, thus improving their efficiency[215].

12. Labyrinthine or maze-like geometries

Labyrinthine designs (Fig. 1*l*) offer innovative solutions to build acoustic devices with exceptional wave control properties. These configurations are designed to improve sound absorption and propagation through their complex layouts[213]. Incorporating maze-like patterns into acoustic metamaterials facilitates the creation of devices capable of capturing and dissipating sound energy effectively, making them ideal for noise reduction and soundproofing applications[213]. The adaptability of labyrinthine structures makes them applicable in a range of acoustic technologies, from noise barriers to sophisticated acoustic lenses[213].

C. Key Physical Principles

Fifteen main physical mechanisms underpinning the behaviour of acoustic metamaterials can be defined. Acoustic impedance match/mismatch between two media is essential for controlling the reflection and transmission of sound waves. Bragg scattering blocks specific frequency bands, shaping the sound wave propagation. Mie and Fabry-Pérot resonances affect wave interactions and specific resonance effects. Fano-like interference offers some unique acoustic profiles through asymmetric responses. Double open-ended and open-closed resonators fine-tune the resonance behaviour within the material. Helmholtz resonators control sound by manipulating the vibration of air, while thermoviscous losses affect sound propagation by converting acoustic energy into heat. Together, all these physical mechanisms contribute to creating the metamaterials' unique acoustic properties.

Moreover, essential physical concepts like band theory, effective medium theory, generalised Snell's law, topological phonon edge states, parity-time (PT) symmetry, and non-Hermitian acoustics are crucial in shaping the design and analysis of acoustic metamaterials. These frameworks facilitate novel control over sound waves, unlocking applications that range from noise isolation to cutting-edge acoustic technologies.

1. Acoustic impedance

The acoustic impedance is related to the resistance offered by a material against impinging sound waves (Fig. 10a). For a given sound wave, the impedance is calculated as the ratio derived from the sound pressure about the particle velocity at a specific point within the material. Factors that determine the acoustic impedance include the geometry of the metamaterial and its boundary conditions.

The principle of impedance matching[49] facilitates the efficient transfer of acoustic energy from the medium to the metamaterial. Impedance matching can be beneficial in the case of sound cloaking since a good impedance match will generate a limited amount of reflected acoustic energy.

A different scenario arises with the presence of impedance mismatch[216] when the material and the medium differ significantly in terms of acoustic properties. This situation leads to the reflection of the acoustic waves until no acoustic waves can successfully pass through the acoustic metamaterial, resulting in an entirely reflective effect. Impedance mismatch, however, is intentionally utilised in designing acoustic metamaterials. For instance, impedance mismatch can create a sonic barrier, which can obstruct specific frequencies, such as those generated by HVAC systems, thereby making them less noisy[217].

The acoustic impedance Z is expressed as:

$$Z = \sqrt{k\rho} \tag{1}$$

where Z represents the acoustic impedance (units: Pa s/m), ρ denotes the density of the medium (in kg/m^3), and k signifies the bulk modulus (Pa). This equation demonstrates that the acoustic impedance is determined by the square root of the product between the density of the medium and its compressibility resistance. This principle plays a crucial role in applications such as ultrasound imaging and acoustic engineering, where achieving impedance matching is vital to reduce reflections at boundaries between different materials.[218,219].

2. Bragg scattering

Bragg scattering (Fig. 10b) is a crucial occurrence in acoustics and happens when sound waves encounter a periodic structure. This interaction heavily affects the wave propagation. The core of this interaction is the "Bragg condition[220]", represented mathematically as $\Delta L = \lambda/2$, which represents a particular case of the Laue equations[221]. In the Bragg equation, ΔL stands for the typical length scale of the periodic structure, while λ refers to the wavelength of the sound wave. The condition is usually fulfilled when the wavelength is double the distance between the scattering elements. When this scenario occurs, the scattering of the waves from the periodic structure leads to destructive interference that creates a band gap. This band gap represents a particular frequency range in which waves are prevented from propagating through the material, effectively blocking sound at those frequencies from penetrating the acoustic metamaterial. Fig.10b represents the mutual effect of a series of scatters at a distance ΔL on the incident acoustic wave. As a consequence, a band gap is generated on the opposite side of the metamaterial.

Bragg's Law can be written in mathematical form as:

$$2d \sin\theta = n\lambda \tag{2}$$

where d represents the spacing between scattering planes, defining the structural periodicity, θ denotes the angle of incidence (the angle at which the wave interacts with the scattering planes), n indicates the diffraction order (an integer specifying how many wavelengths fit within the path difference), and λ stands for the wavelength of the incoming wave. Bragg scattering plays a pivotal role in controlling wave behaviour within periodic structures, facilitating the development of materials that can selectively reflect or transmit particular wavelengths. This concept is crucial in areas such as acoustic filters and noise suppression systems, where structural periodicity is designed to form band gaps, thus blocking certain frequencies while permitting others to propagate[222,223].

3. Mie resonance

An acoustic wave infiltrating a metamaterial can encounter scattering elements present within the metamaterial architecture. When the frequency of the incoming sound wave coincides with the scatterers' natural frequency, Mie resonance[63] may be initiated due to interference between the resonant frequency of the material and the medium's monopolar, or multipolar resonance.

The arrangement of scatterers can facilitate diverse and useful effects. A notable consequence is the formation of multiple band gaps within the frequency spectrum.

The rise of Mie resonances can be triggered when the size of the metamaterial's components is comparable to the wavelength of the incoming sound wave as illustrated in Fig. 10c, in which the dimension of the scatter and the acoustic wavelength are the same.

Mie resonances in acoustic metamaterials result from the interaction between acoustic waves and sub-wavelength scatterers, which resembles Mie scattering observed in electromagnetic contexts. The resonance condition for a spherical scatterer is given by $ka = \frac{\omega a}{c}$, where k denotes the wave number, ω represents the angular frequency, c is the speed of sound and a refers to the radius of the scatterer. This equation is crucial to comprehending how acoustic waves interact with objects smaller than their wavelength, producing distinctive resonant effects that can be harnessed in various applications, such as sound absorption and cloaking[224,225]. The theoretical framework used to examine these resonances mirrors electromagnetic Mie theory, as both involve resolving wave equations constrained by the geometrical and material properties of scatterers. This parallel enables the application of scattering theories to anticipate and control acoustic wave interactions within engineered materials[226,227]. The significance of Mie resonance is far-reaching, introducing novel approaches to influence sound and light, particularly in the fields of optics and materials science[228–230].

4. Fabry-Pérot resonance

A Fabry-Pérot resonator[231,232] operates by implementing two reflective planes positioned in a parallel configuration. An incoming wave is subjected to repeated reflections between these surfaces, thereby producing a series of increasingly reflected waves. Constructive interference is observed in the transmitted waves when the width of the resonator aligns with an integer multiple of half the wavelength. This type of interference maximises the transmission coefficient[233]. The phase synchronisation among the reflections generates an improved transmitted wave.

A Fabry-Pérot resonator can function as a frequency filter. It facilitates the efficient transmission of waves at particular frequencies while causing at the same time significant attenuation of waves in other parts of the spectrum[234]. This selective frequency transmission serves many applications, including the design of acoustic devices, sensors and systems dedicated to noise management. As shown in Fig. 10d, the parallel walls of the acoustic duct generate constructive interference. A similar phenomenon is exploited in the design of laser systems.

Fabry-Pérot resonance in acoustics arises from the constructive and destructive interference of sound waves bouncing between two parallel boundaries, resulting in distinct resonance frequencies that satisfy the resonance condition:

$$2nL = m\lambda \tag{3}$$

where n denotes the refractive index of the medium in the cavity, L represents the cavity length, m is the integer mode number, and λ is the wavelength of the sound. The propagation of sound waves through the cavity is described by the transmission function:

$$T(\omega) = T_0\left(1 + F\sin^2\left(\frac{\delta}{2}\right)\right) \tag{4}$$

In this expression, $T(\omega)$ signifies transmission at angular frequency ω, T_0 is the peak transmission, F refers to the finesse coefficient and $\delta = \frac{2\omega L}{v}$ represents the phase shift per round trip, where v is the speed of sound. This resonance mechanism facilitates the selective amplification or attenuation of specific frequencies, which is useful in devices such as filters and sensors[235,236].

5. Fano-like interference

Fano-like interference[55] happens when acoustic waves impact a multifaceted configuration that supports an array of oscillation modes. A single mode can be narrow and well-defined, like the resonance of a tuning fork, for instance. The remaining modes generate however a broad and almost continuous spectrum of resonances. The simultaneous excitation of the discrete resonance and the continuum by the sound waves leads to interference, culminating in a highly irregular scattering profile (Fig. 10e). This effect shows up as asymmetric transmission peaks, which occur when resonant and non-resonant wave modes interact[237].

Fano-like interference has particular relevance in the field of acoustic metamaterials to design open or ultra-open sound insulators[34] for HVAC systems, for instance.

In acoustics, Fano-like interference emerges from the interaction between discrete resonant states and a continuum of states, resulting in an asymmetric profile in the transmission or absorption spectrum. This phenomenon is captured by the Fano formula:

$$f(\varepsilon) = \frac{(\varepsilon + q)^2}{\varepsilon^2 + 1} \tag{5}$$

where $f(\varepsilon)$ denotes the normalized spectral line shape, $\varepsilon = \frac{E - E_r}{\Gamma/2}$ represents the reduced energy, E is the energy, E_r the resonant energy, Γ the resonance width, and q the Fano asymmetry parameter. The unique characteristics of Fano resonance make it exceptionally responsive to system changes, offering significant advantages in sensor and sound insulation technologies[238–241]. This asymmetric profile, resulting from constructive and destructive interference between discrete and continuum states, plays a vital role in improving sensitivity for a variety of applications[239,240,242].

6. Locally resonant sonic materials

Locally resonant materials are AMs featuring resonant structures with unique acoustic properties[243]. These materials have lattice constants much smaller than the sound wavelengths they interact with, allowing them to block specific frequencies of sound waves. This effect can also be created by embedding dense core materials, like lead, inside soft coatings such as silicone rubber. When sound waves hit these composites, the localised resonances can cause the material to reflect almost all the sound in certain frequency ranges[244].

Acoustic materials with local resonators show remarkable features due to their specialised inclusions designed to resonate at targeted frequencies. The effective mass density of these materials is defined as:

$$\rho_{eff}(\omega) = \rho\left(1 - \frac{\omega^2}{\omega_0^2}\right) \tag{6}$$

where: $\rho_{eff}(\omega)$ represents the effective density varying with frequency, ρ denotes the material's intrinsic density, ω stands for the angular frequency of the incoming wave, and ω_0 is the angular frequency at which the local resonators vibrate. Close to the resonance frequency ($\omega \approx \omega_0$), the effective density may turn negative, facilitating effects such as band gap formation and sound suppression, which are advantageous for uses such as noise reduction and vibration control[245–248]. This phenomenon of negative effective mass density characterises locally resonant acoustic metamaterials, granting them the ability to control sound waves in ways that ordinary materials cannot achieve[249–251].

7. Double open-ended resonators

Double open-ended resonators[8,27,40,252,253] could be represented as vacant passages or conduits permeable at both extremities and with a constant cross-section (Fig. 10f). The inlet of acoustic waves into these resonators triggers the air or any other entrapped medium to pulsate at certain distinct frequencies, which are the resonant frequencies associated with the geometrical characteristics of the resonator.

This latter phenomenon seems to be responsible for the position of the absorption coefficient peaks in acoustic metamaterials built with Hilbert or coiled geometry[8].

The potential applications for this type of resonator are broad and mainly around noise management. It is possible to modulate and tune frequencies maximising/minimising the acoustic absorption of a metamaterial by a careful design of the resonators' length and shapes.

Double open-ended resonators are defined by their capacity to sustain standing waves, with pressure nodes present in each extremity and pressure antinodes appearing centrally. The resonant frequencies for these systems are determined using the equation:

$$f_n = \frac{nv}{2L} \tag{7}$$

where: f_n signifies the n-th harmonic frequency, v is the speed of sound within the medium, L represents the resonator's length, and n is a positive integer (1, 2, 3, ...). These resonators play a vital role in numerous applications, such as acoustic filters and musical instruments, where they enhance specific harmonic frequencies, allowing improved sound quality and precise acoustic control[254,255].

8. Open-closed resonators

Open-closed resonators[10,58,252,256–260] provide a particular case of Fabry-Pérot resonance[68,198,233,234,252,253,261–263]. Open-closed resonators represent another variation of constant cross-section resonators used for the manipulation of acoustic waves. These resonators can be described as tubular constructs that bear a resemblance to their double open-ended resonators counterparts (Fig. 10f). There is however one critical distinction: one of their ends remains sealed.

The permeable end of the resonator is at the ingress of the sound waves, whilst the closed extremity establishes a fixed condition. This distinct arrangement alters the modalities of the oscillation of the air cavity or any other entrapped medium within the resonator, in response to the incoming sound waves.

These open-closed resonators display different resonant frequencies and diverse oscillation patterns when contrasted with double open-ended resonators. They are responsible for the position of the transmission loss peaks in specific parts of the frequency spectrum for Hilbert and coiled geometries[10,264].

The mathematical representation of their resonant frequencies is given by:

$$f_n = \frac{(2n-1)v}{4L} \tag{8}$$

where: f_n denotes the resonant frequency, n is a positive integer (1, 2, 3, ...), v indicates the speed of sound within the medium, and L corresponds to the resonator's length. These resonators operate at odd harmonics of the quarter wavelength, a feature essential for applications like noise reduction in mufflers and the optimisation of architectural acoustics, where the control of specific frequencies is pivotal[265,266].

9. Quarter-wave resonators

Quarter-wavelength resonators work through standing waves: they are tubes in which one end is closed and the other is open, while the length equals one-quarter of the resonant frequency wavelength for the operation it is designed to carry out. The consequence is a standing wave pattern of minimum air pressure at the open end, an antinode of maximum particle velocity at the open back, and vice versa at the closed end[267]. The resonant frequency, set by the tube length L, is $f = \frac{c}{4L}$, where c is the speed of sound[178]. Such resonators find wide use in musical instruments like clarinets and flutes in producing some definite pitch[268]. They are undoubtedly important in noise control, for instance, by making mufflers and silencers, achieving this end by matching the resonator's frequency to an unwanted frequency[269]. The same can apply in architectural acoustics to manage the acoustics of a room by the same principle: to cut down on reverberation and take charge of a particular frequency band[270].

10. Helmholtz resonators

The incorporation of Helmholtz resonators[67,271–276] in the architectural design of acoustic metamaterials allows the exploitation of their well-known narrow-band effect.

Each of these resonators can be calibrated to a particular frequency to absorb acoustic energy, effectively acting as a 'trap' for that specific frequency within the sound wave[277].

A system comprising multiple such resonators, with each resonator tuned to a distinct frequency, can provide an efficient noise reduction across a broad frequency bandwidth. The versatility of this solution is made possible by adjusting the volume, length and section of the Helmholtz resonator neck.

The positioning of coiled or fractal geometries inside the resonators also introduces an additional element of space efficiency. This design feature decreases the volume required for the spring component of the acoustic mechanism, thereby requiring less cavity volume to be used. A classic example of a Helmholtz resonator is the classic glass bottle, where the mass of air in the neck oscillates according to the spring action of the internal volume (Fig. 10g).

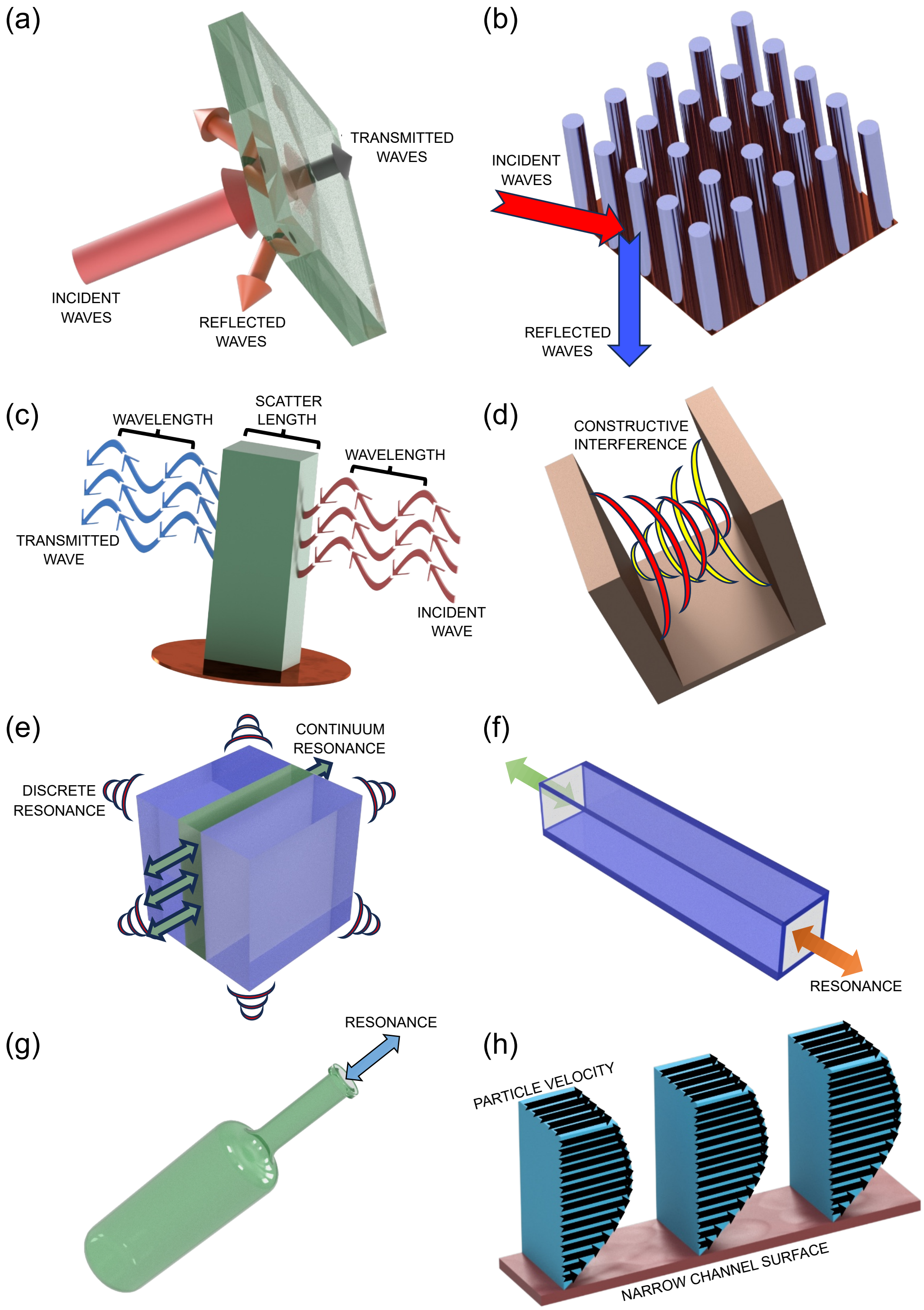

FIG. 10. Some of the main physical mechanisms underpinning the performance of acoustic metamaterials: Impedance between two media (a), Bragg scattering (b), Mie resonance (c), Fabry-Pérot resonance (d), Fano-like interference (e), double open-ended resonator (f), Helmholtz resonator (g), and thermoviscous losses (h). G. Comandini, *Hilbert Fractal Acoustic Metamaterials*, University of Bristol, 2024; licensed under a Creative Commons Attribution (CC BY) license[7].

The Helmholtz resonator is defined by its natural frequency, which is given by the equation:

$$f = \frac{v}{2\pi}\sqrt{\frac{A}{VL_{eff}}} \tag{9}$$

where: f denotes the resonant frequency (Hz), v represents the speed of sound in air (m/s), A is the neck's cross-sectional area (m^2), V is the cavity's volume (m^3), and L_{eff} signifies the neck's effective length, accounting for end corrections (m). The Helmholtz resonator serves as an efficient sound absorber in its resonance, which is advantageous for noise control and sound attenuation in multiple settings[278–281]. Its configuration enables it to function similar to a mass-spring system, where the air mass in the neck and the cavity compliance produce resonance capable of effectively suppressing specific sound frequencies[282–284].

11. Thermoviscous losses

Thermoviscous losses represent a special energy dissipation mechanism occurring within fluid systems, such as air or water. These losses occur near the boundary or borders with the material substrate, affecting the transmission of acoustic waves. As sound waves traverse a medium, the pressure and particle velocity oscillates, triggering viscothermal effects due to the near-zero particle velocity on the surface of the channel (Fig. 10h). The interplay between these effects culminates in energy dissipation.

When used in acoustic metamaterials, thermoviscous losses acquire significant importance in the design process of systems at scales where such losses become substantial.

Thermoviscous losses are especially critical in three main cases; perforated and microperforated panels[285], acoustic foam[286], and narrow channels inside acoustic metamaterial geometries[8].

Typically, thermoviscous losses[287] take place at the microscale, where dimensional features of the metamaterials are comparable with the thickness of the boundary layer in which the thermoviscous effects occur. This becomes particularly critical when designing metamaterials for applications in ultrasound or other high-frequency domains, where these losses must be accounted for to achieve optimum sound energy transmission.

As the sound wave advances, these losses become evident as attenuation or a reduction of the acoustic energy of the wave, thus impeding the effectiveness of the acoustic metamaterial. This behavior is highly significant if the objective of the metamaterial is to optimise the sonic energy transmission. However, the transmission of the acoustic wave, for applications like acoustic absorbers can be enhanced by thermoviscous losses. In such cases, the losses can be engineered to augment the absorption of sound energy, thereby mitigating noise and increase the magnitude of the transmission loss provided by the metamaterial.

The attenuation coefficient, represented as α, measures the energy dissipation caused by viscous friction and thermal conduction within confined spaces or boundary layers. It is expressed by the formula:

$$\alpha = \frac{2\rho v^3 \omega^2}{2}\left(\eta + \left(\frac{\gamma - 1}{\gamma}\right)\kappa c_p\right) \tag{10}$$

where: α denotes the attenuation coefficient (Np/m), ω is the angular frequency (rad/s), ρ refers to the density (kg/m^3), v indicates the speed of sound (m/s), η is the dynamic viscosity (Pas), γ is the ratio of heat capacities (c_p/c_v), κ is the thermal conductivity (W/mK), c_p signifies the specific heat at constant pressure (J/kgK), and c_v is the specific heat at constant volume (J/kgK). Grasping these variables is essential for the development of materials and structures optimised for sound absorption, including acoustic liners and microperforated panels, as they dictate energy dissipation and acoustic performance in numerous applications[288].

12. Control of acoustic waves with membranes

Membrane-type acoustic metamaterials (MAMs) are innovative materials that use lightweight[289], flexible membranes, sometimes enhanced with strategically placed rigid masses[290–292]. These enhancements help the membranes interact with the acoustic field, making them effective in influencing sound waves[293–295]. The design of these masses-considering their size, weight, and position-is crucial in creating specific resonances that can block or reflect sound waves.

The core idea behind MAMs is to utilize the resonance created by these masses to interfere with and significantly reduce sound transmission[293]. When sound waves hit the membrane, the attached masses cause it to vibrate in a manner that cancels out certain frequencies[183]. This is particularly effective for low-frequency sounds, which are typically harder to manage. By tweaking the properties of the masses and the tension of the membrane, specific frequencies can be targeted[292,296].

There are two primary ways to position these membranes relative to incoming sound waves: normal incidence[293], where the membrane faces the wave head-on, and grazing incidence[297,298], where the membrane is parallel to the wave.

For instance, increasing the tension in the membrane can shift its resonance frequency, allowing it to target different sound frequencies[293]. Theoretical models have been developed to predict the behaviour of these metamaterials[295], and experiments have consistently shown that MAMs can achieve significant transmission loss at specific frequencies.

A different approach involves active membranes[170], such as in the case of loudspeakers[299,300]. Here, the membrane's coil can be paired with either a passive or active shunt to enhance control.

Shunts play an important role in manipulating sound waves to achieve desired acoustic effects. By adjusting the impedance characteristics of the shunt[301], the interaction between the loudspeaker and the metamaterial can be fine-tuned, ensuring efficient energy transfer and improved acoustic properties like resonance and bandwidth. Shunts can also be designed to shape the frequency response of the loudspeaker-metamaterial system [302], creating bandgaps where sound is not transmitted or enhancing specific frequency ranges.

Moreover, active shunts enable dynamic adaptation of the system's acoustic properties in real-time [143]. This feature allows for the development of reconfigurable metamaterials that can adjust their acoustic characteristics based on the environment or specific requirements, providing a high level of versatility.

One of the most notable advantages of MAMs is their ability to provide high sound insulation without adding significant weight or thickness, unlike traditional soundproofing materials. This quality makes them particularly attractive for use in the aerospace and automotive industries, where reducing weight is crucial. Integrating shunts with MAMs further enhances their capabilities, offering more precise control over sound attenuation and the potential for real-time adjustments to the acoustic environment [303].

Membrane-type metamaterials are composed of thin flexible membranes with attached masses, demonstrating resonance at lower frequencies. The resonant frequency f can be expressed as:

$$f = \frac{1}{2\pi}\sqrt{\frac{k_{eff}}{m_{eff}}} \tag{11}$$

where k_{eff} signifies the effective stiffness (N/m), and m_{eff} represents the effective mass (kg). Resonance within the system results in a negative effective modulus, facilitating better sound insulation and vibration suppression. This negative modulus implies that the metamaterial effectively blocks or mitigates low-frequency sound waves, making it highly advantageous for applications such as vibration mitigation and soundproofing[303–306].

13. Topological acoustics and phononic edge states

The field of topological acoustics is rapidly evolving, with a focus on the crafting of metamaterials that exhibit resilient edge states resistant to backscatter caused by defects or irregularities. This phenomenon is analogous to the quantum Hall effect in electronic systems, where sound waves are guided unidirectionally by breaking time-reversal symmetry using techniques such as angular momentum biasing or circulating fluids[307]. The Chern number C, derived from the Berry curvature $\Omega(k)$ in the Brillouin zone, provides the mathematical framework describing these topological edge states[307]. Advances in this domain have introduced cutting-edge concepts such as Floquet engineering and topological semi-metal phases, expanding the potential of acoustic metamaterials[307]. These innovations hold immense promise for applications such as sound isolation and waveguiding, ensuring performance integrity even amidst environmental fluctuations[308]. The principal mathematical expression for characterizing these states employs the Chern number C, given by:

$$C = \frac{1}{2\pi}\int_{BZ}\Omega(k)\,d^2k \tag{12}$$

where $\Omega(k)$ signifies the Berry curvature and k denotes the wave vector, with the integral computed over the Brillouin zone (BZ). This formulation underscores the topological features of edge states, enabling unidirectional wave transmission immune to backscattering. These characteristics are especially beneficial for the creation of robust acoustic circuits and protected waveguides, which retain their functionality despite structural defects or environmental challenges[307–309].

14. Parity-time (PT) symmetry and non-Hermitian acoustics

Parity-time (PT) symmetry in acoustics pertains to systems where a balance between gain and loss results in extraordinary phenomena like exceptional points (EPs), where eigenvalues merge[310,311]. The scattering characteristics of PT-symmetric acoustic systems exhibit notable effects, such as unidirectional transparency and asymmetric reflection, made possible by precisely engineered materials with complex parameters. However, achieving such materials often necessitates active devices, as passive materials alone struggle to provide the required gain and loss profiles. A PT-symmetric medium is defined by $\kappa(r) = \kappa^*(-r)$ and $\rho(r) = \rho(-r)$, where ρ represents the mass density, and κ denotes the complex bulk modulus[312]. Recent progress in PT-symmetric acoustics has revealed applications such as asymmetric cloaking and improved sensor capabilities[310,313]. Research into these systems has expanded to diverse configurations, including piezoelectric composites and metamaterials, often integrating active components to achieve PT symmetry. This versatility highlights the potential of PT symmetry in controlling acoustic waves[314,315]. These discoveries have significant implications, proposing innovative approaches for the design of acoustic devices that take advantage of the distinctive characteristics of non-Hermitian systems, although their implementation often depends on active devices[226,316].

15. Generalized Snell's law

Generalized Snell's law in acoustics enables the modulation of wavefronts through spatially varying phase gradients created by metasurfaces. The relationship governing this phenomenon is given as:

$$k_t \sin\theta_t - k_i \sin\theta_i = \frac{d\Phi}{dx} \tag{13}$$

where k_i and k_t denote the wave numbers in the media of incidence and transmission, respectively, and θ_i and θ_t correspond to their respective angles. The term $\frac{d\Phi}{dx}$ represents the phase gradient introduced by the metasurface[317–319]. This approach allows for accurate manipulation of the acoustic wavefronts, paving the way for advanced technologies such as acoustic lenses and stealth devices[320,321]. Recent investigations underscore the ability of metasurfaces to realise non-standard refraction and reflection, showcasing their utility in diverse acoustic scenarios[322,323].

D. Machine Learning-Based Design Approaches in Acoustic Metamaterials

The incorporation of advanced techniques like machine learning (ML) and genetic algorithms in the development of acoustic metamaterials marks a notable improvement over conventional strategies, which often depend on human intuition combined with iterative simulations. These advanced methods allow the exploration of intricate design spaces, aiding in the discovery of unconventional configurations that can achieve enhanced acoustic performance. For example, ML algorithms expedite the design process by optimising unit cell geometries based on insights from predefined simulations, thereby fostering the creation of innovative structures[324,325]. Genetic algorithms similarly contribute by emulating natural selection to identify ideal design parameters, offering a versatile alternative to traditional trial-and-error techniques[326,327]. Furthermore, these intelligent methods are particularly advantageous in the creation of adaptive and multifunctional acoustic metamaterials that can dynamically respond to changing environmental conditions[328,329]. By generating effective initial configurations, these techniques complement conventional design methods, streamlined the process, and promoted innovation[325,330]. The transition to intelligent design methodologies not only improves the capabilities of acoustic metamaterials but also expands their potential applications, setting the stage for future progress in the field[324,331].

E. Comparative Analysis

Investigating acoustic phenomena uncovers a nuanced interplay between mechanisms, properties, and applications that range from basic to advanced principles. Core effects such as mismatches in acoustic impedance and Helmholtz resonators play crucial roles in sound insulation and noise suppression[332–334]. Cutting-edge topics, including topological acoustics and Parity-Time (PT) symmetry in non-Hermitian systems, extend the boundaries of acoustic control, facilitating directional wave travel and band gap optimisation organised[335,336].

Table I describes the fundamental acoustic phenomena associated with wave propagation, resonance, impedance, and band gap creation. It provides an organised overview of the mechanisms, properties, applications, geometries, and materials, serving as a foundational reference for principles of noise suppression and sound management. Expanding on these basics, Table II presents advanced acoustic control phenomena made possible through metamaterials. It showcases intricate designs and engineered interactions, allowing precise wave control for innovations such as acoustic cloaking, sound concentration, and advanced sensing applications.

TABLE I. Summary of fundamental acoustic phenomena, detailing mechanisms, properties, applications, geometries, and materials involved. This table focuses on essential principles related to sound wave propagation, impedance, resonance effects, and band gap formation, relevant to noise control and sound insulation.

Phenomenon	Mechanism	Properties	Applications	Geometries	Materials
Acoustic impedance	Sound waves interact with materials; impedance mismatches cause reflections[337,338]	Medium's density, and bulk modulus[339]	Ultrasound imaging; non-destructive testing[340,341]	Layered structures, transducers for impedance matching[342,343]	Biological tissues, engineered composites[344,345]
Bragg scattering	Constructive interference of waves scattered from periodic inhomogeneities[346–348]	Band gaps where sound cannot propagate[346–348]	Noise reduction and sound insulation[222,349]	Often cylindrical or fractal arrangements of scatterers[350]	Composites with high impedance contrasts, such as polymers or metals[347,351]
Mie resonance	Scattering of sound waves by resonant structures[352,353]	Ability to achieve negative effective mass density and bulk modulus[211,354]	Sound absorption, noise control, and sub-wavelength imaging, particularly in underwater environments[355–357]	Various geometries, such as spherical and cylindrical resonators[330,358]	Dielectrics, polymers, and composites, which are chosen for their specific acoustic properties and resonance characteristics[352].
Fabry-Pérot resonance	Excitation of resonant modes within the metamaterial structure[359–361]	Interference of waves reflecting between two boundaries, leading to enhanced transmission and absorption properties[359–361]	Medical diagnostics and noise control[362,363]	Layered structures and arrays of resonators[253,262 252]	Rubber-coated spheres or anisotropic materials[211,364,365]
Fano-like interference	Interaction between discrete and continuum states, leading to asymmetric resonance profiles[34,366]	Enhanced sensitivity and directionality in sensing applications[366,367]	Noise control and sound insulation[40,368]	Coupled Helmholtz resonators and periodic structures[369,370]	Ordinary materials including 3D printed photosensitive resin[371,372]
Locally resonant sonic materials	Integration of resonators within a host medium, allowing for the creation of negative effective mass density and bulk modulus[245,373,374]	Enhanced sound absorption and transmission loss[375–377]	Sound insulation, acoustic cloaking, and energy harvesting[376–378]	Various forms, including periodic arrays of resonators, sonic crystals, and composite structures that incorporate materials like rubber and metal[374,379,380]	Elastomers, metals, and piezoelectric components[245,380,381]
Double open-ended resonators	Resonance[251,382,383]	Negative mass density and the ability to create band gaps[251,382,383]	sound absorption, noise reduction, and acoustic cloaking[383,384]	Resonators can take various forms, such as cylindrical or planar structures[384]	Lightweight polymers or metals[251,383]
Open-closed resonators	Interaction between open and closed geometries to manipulate sound waves[385,386].	Enhanced sound absorption and tunable frequency responses[385,386]	Noise reduction and biomedical sensing[385,386]	Helmholtz resonators or variations of cylindrical and spherical shapes[385].	Traditional polymers to advanced composites[385,386]
Quarter-wave resonators	Resonance condition[387,388]	Bandgaps for noise reduction and energy harvesting[389 390].	Noise control systems, and energy harvesting devices[391]	Various geometries, such as cylindrical and conical shapes[389,392,393]	From metals to polymers[389,392,393]

TABLE II. Overview of advanced acoustic control phenomena enabled by metamaterials. This table highlights mechanisms, properties, applications, geometries, and materials, emphasizing engineered interactions and complex structural designs used for precise wave manipulation in applications such as acoustic cloaking, sound focusing, and advanced sensing technologies.

Phenomenon	Mechanism	Properties	Applications	Geometries	Materials
Topological acoustics and phononic edge states	Interplay of geometric and topological features in metamaterials, leading to the emergence of edge states that are resilient to disorder and defects[394,395]	Unidirectional wave propagation and the ability to localise sound at the edges of the material[396–398]	Soundproofing, acoustic sensing, and the development of advanced communication systems[399–401]	Honeycomb and kagome lattices, are employed to facilitate the desired topological characteristics, while materials like piezoelectric fibers and 3D-printed structures[402–404]	Piezoelectric fibers and 3D-printed structures are utilized to enhance performance[402–404]
Parity-Time (PT) symmetry and non-Hermitian acoustics	PT symmetry arises from the balance of gain and loss in a system, allowing for real eigenvalues even in non-Hermitian contexts, as established by Bender and Boettcher[405–407]	Unidirectional wave propagation and exceptional points[316,408], negative refraction and self-collimation[409]	From acoustic imaging to advanced communication systems[313,314]	Complex arrangements of resonators and metamaterials designed to exploit PT symmetry[315,410]	Piezoelectric composites and other engineered structures that facilitate gain-loss dynamics essential for maintaining PT symmetry[314,411]
Generalized Snell Law	Design of metasurfaces that create tailored phase shifts, which dictate the direction of wave propagation[323,412,413]	Negative refraction and extraordinary transmission[414–416]	Acoustic cloaking, beam steering, and enhanced imaging[415,417]	From simple planar structures to complex 3D configurations[418–421]	Subwavelength resonators and phase-gradient structures[412,414,422]
Thermoviscous losses	Interaction of sound waves with the viscous and thermal boundary layers at the surfaces of the materials[423]	Affecting the acoustic properties of metamaterials, such as sound absorption and transmission loss[423]	Noise control and architectural acoustics[358,424]	Slits and resonators, which are designed to maximise the interaction with sound waves while minimising reflections[425,426]	Polymers and composites that exhibit favorable viscous properties, enhancing the damping characteristics[427,428]
Control of acoustic waves with membranes	Thin membranes that resonate at specific frequencies, allowing for effective sound attenuation and wave manipulation[174,304,429]	Negative effective mass density and bulk modulus, achieving phenomena such as sound insulation and cloaking[212,430,431]	Noise reduction, sound absorption, and energy harvesting[147,400,432]	Flat panels and complex resonator arrays, which enhance their acoustic performance[433–435]	Polymers and composites that provide the necessary flexibility and resonance characteristics, enabling tunability and adaptability in various acoustic environments[436,437]
Helmholtz resonators	Principle of resonance, where the resonant frequency is determined by the geometry of the cavity and neck dimensions[438,439]	Effective sound absorption capabilities[333,400,440]	Architectural acoustics, automotive noise reduction, and biomedical devices, where they serve as passive absorbers or active noise control elements[441,442]	Multi-neck designs and coiled configurations, enhance their performance by broadening the absorption spectrum[443,444]	Porous substrates and composites that optimize acoustic performance while maintaining structural integrity[191,445]

III. CLASSIFICATION AND AIMS

In the open literature, terms like "zigzag", "coiled", "maze", and "labyrinthine", are frequently applied to acoustic metamaterial geometries, often creating ambiguity due to their interchangeable use (Table III). We propose here a possible classification based on the internal geometrical configuration of these metamaterials. The classification is based on how the acoustic wave navigates within the metamaterial basic periodic unit. The multichannel configuration (Fig. 11*a*) exemplifies structures that allow multiple paths of the propagating wave due to the intricacy of the internal metamaterial architecture. Maze or labyrinthine geometries (Fig. 1*l*) are excellent examples of these multichannel configurations because they enable both constructive and destructive wave interference. The single-channel configuration (Fig. 11*b*) represents a category of metamaterial in which the acoustic wave travels along a forced path inside the meta atom. Typical structures of this type are zigzag or coiled (Fig. 1*b*), which offer a unique trajectory for wave propagation. To further refine the classification, we also identify an additional "dead-end" category (Fig. 11*c*), applicable to both single and multichannel configurations. This subclass describes configurations where the acoustic paths terminate prematurely, as observed in the coiled channels of acoustic antennas. The proposed classification (Fig. 11) offers a simplified approach to categorise acoustic metamaterials, providing a clear distinction between metamaterial architectures based on the trajectory that an acoustic wave undertakes within each configuration.

A. Strengths and Weaknesses of the Proposed Classification Method

The proposed classification approach, which organises acoustic metamaterials based on the number of internal channels, provides a clear and straightforward method for understanding and categorising structural designs. This method is particularly advantageous for visualising the internal architecture of metamaterials and quickly identifying design patterns that might be suitable for specific sound manipulation applications. It effectively captures the diversity of geometries, ranging from simple coiled channels to complex, labyrinthine structures, that contribute to sound control through mechanisms like space-coiling, resonance enhancement, or wave redirection[446].

1. Strengths

- **Simplicity and Accessibility**: This classification is easy to understand and does not require extensive analysis of complex physical properties. It allows for a quick assessment of structural designs, making it particularly useful during the early phases of metamaterial development.

- **Versatility in Design**: The approach accommodates a wide variety of structural configurations, including fractal, coiled, and hierarchical designs, thereby offering flexibility for exploring innovative configurations that may not fit neatly into more restrictive classification schemes[184].

2. Weaknesses

- **Limited Predictive Capability**: The method primarily focuses on geometric characteristics and does not inherently provide insights into how these structures will interact with acoustic waves across different frequencies. This lack of a direct link between structural design and acoustic performance can limit its utility for predicting the precise behaviour of metamaterials, such as sound absorption peaks or bandwidths[402,446].

- **Oversimplification**: By concentrating solely on the internal channel count, the method may overlook other critical aspects, such as material composition, resonance behaviours, or dynamic tunability, which are essential for understanding and optimising acoustic properties in specific applications[184,399].

B. Pathway for Integration with Existing Classification Approaches

To address these limitations, it is beneficial to consider integrating the proposed geometric classification with existing frameworks that focus on physical and functional properties. Such integration can enhance the utility of the classification in the following ways:

1. Integration with resonance-based methods

Resonance-based classifications categorise acoustic metamaterials according to their interaction with sound waves at specific frequencies, often focusing on local resonance phenomena that create unique sound manipulation effects, such as negative mass density or impedance matching[184,446]. By integrating our geometric approach, we can first use the internal channel count to identify potential designs and then refine these designs by analysing their resonance behaviours. This combined method allows researchers to predict how internal structures will affect sound propagation, leading to more precise control over acoustic properties.

Example: Coiled structures identified through geometric classification can be further analyzed to determine their resonance frequencies. This additional step can help optimize these designs to achieve effective sound absorption at specific low frequencies, which is crucial for applications like noise reduction in industrial environments[399].

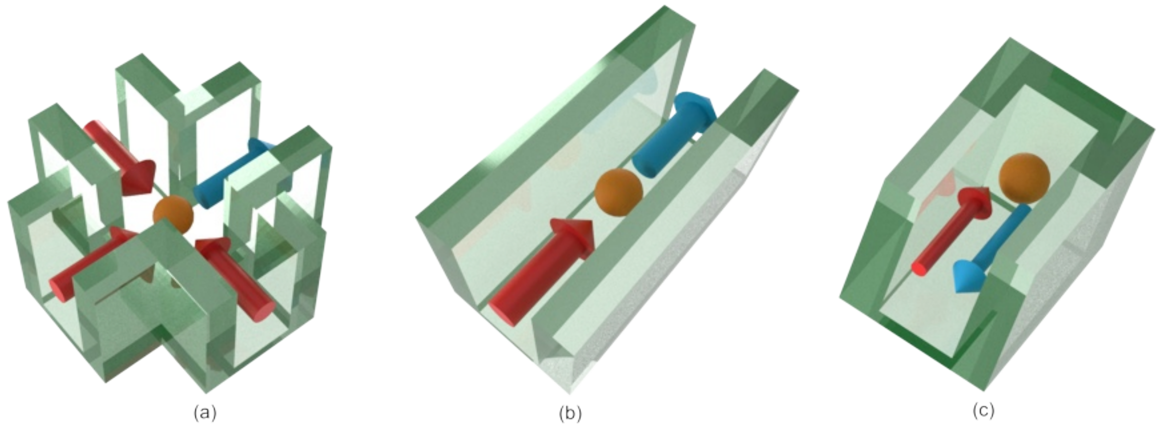

FIG. 11. Schematic representation of the proposed geometrical classification for acoustic metamaterials: (a) multichannel, (b) single channel, and (c) dead-end. Every 1D, 2D, or 3D geometry can be incorporated in either (a) or (b) alone or plus (c). The red arrow represents the wave entering a generic point of the metamaterial's path. The blue arrow stands for the existing wave. G. Comandini, *Hilbert Fractal Acoustic Metamaterials*, University of Bristol, 2024; licensed under a Creative Commons Attribution (CC BY) license[7].

2. Integration with topological and functional classifications

Topological methods classify metamaterials based on unique waveguiding features and topologically protected states that prevent backscattering and ensure robust sound transmission, even in the presence of defects[402]. By combining our classification, which focuses on internal channel architecture, with a topological approach, it is possible to identify and design metamaterials that not only fit a certain geometric category but also exhibit desirable topological behaviors, such as unidirectional waveguiding or tunability.

Example: A metamaterial initially categorized by its geometric design can be assessed for topological properties to see if its structure supports edge states. If so, the design can be further modified to enhance these properties, leading to robust, multifunctional devices useful for applications like acoustic sensing or waveguiding[447].

3. Incorporating hybrid structural-physical approaches

Hybrid classification systems combine structural design with physical parameters, such as effective bulk modulus, mass density, and impedance. Integrating our geometric classification into this framework can offer a multi-layered approach where internal structures serve as the baseline for categorization, and physical parameters refine this categorization based on performance requirements[399,447]. This can lead to a more holistic understanding of how structural features influence acoustic performance, enabling designers to target specific acoustic outcomes, such as broadband absorption or focused sound wave manipulation.

C. Types of Acoustic Metamaterials

Acoustic metamaterials (AMs) are engineered to regulate the propagation of sound waves using principles such as resonance, Bragg diffraction, and impedance discontinuity. These materials serve a wide range of purposes, including reducing noise in building designs and altering sound in consumer products such as hearing aids and noise cancelling devices[354,488]. Their ability to generate band-gap-specific frequency ranges where sound waves are heavily dampened facilitates efficient sound control, making them indispensable in sectors such as medical imaging and noise pollution mitigation[354,362]. Recent innovations emphasise the enhancement of the functionality of acoustic metamaterials by incorporating features such as adjustable resonances and auxetic geometries, which exhibit unique mechanical characteristics[174,375]. For example, the creation of broadband sound absorbers and tunable filters underscores the adaptability of these materials to customised acoustic settings, thus enhancing their utility in the real world[253,433]. Furthermore, investigations into locally resonant structures have prepared the ground for effective low-frequency sound absorption, a critical aspect for applications in urban noise control and industrial environments[325,355].

Fig. 1 shows the baseline geometrical shapes employed in acoustic metamaterials. Most of these configurations can be described as two-dimensional structures, which can be extruded into a third dimension without alteration to their initial *2D* shape. This property holds true for all configurations, excluding the helicoidal (Fig. 1g), the cochlear (Fig. 1i), and the Kelvin cell (Fig. 1k).
Another useful pattern is the one that utilises coiled and tapered fingers-like (Fig. 1*b*) channels[40,489,490]. This configuration is also used for acoustic sensors, where the peculiar geometry can be tailored to pick and amplify specific frequencies in a noisy environment.
Maze geometries (Fig. 1*l*) of acoustic metamaterials in-

TABLE III. Papers related to the four metamaterial geometries.

Geometry	Reference #
Labyrinthine	21,42,46,56,70,104,111,112,124,217,256,257,263,286,448–465
Coiled	27,58,62,73,80,85,104,106,134,198,252,258–260,263,466–480
Zigzag	32,40,131,217,262,456,481–483
Maze	86,470,484–487

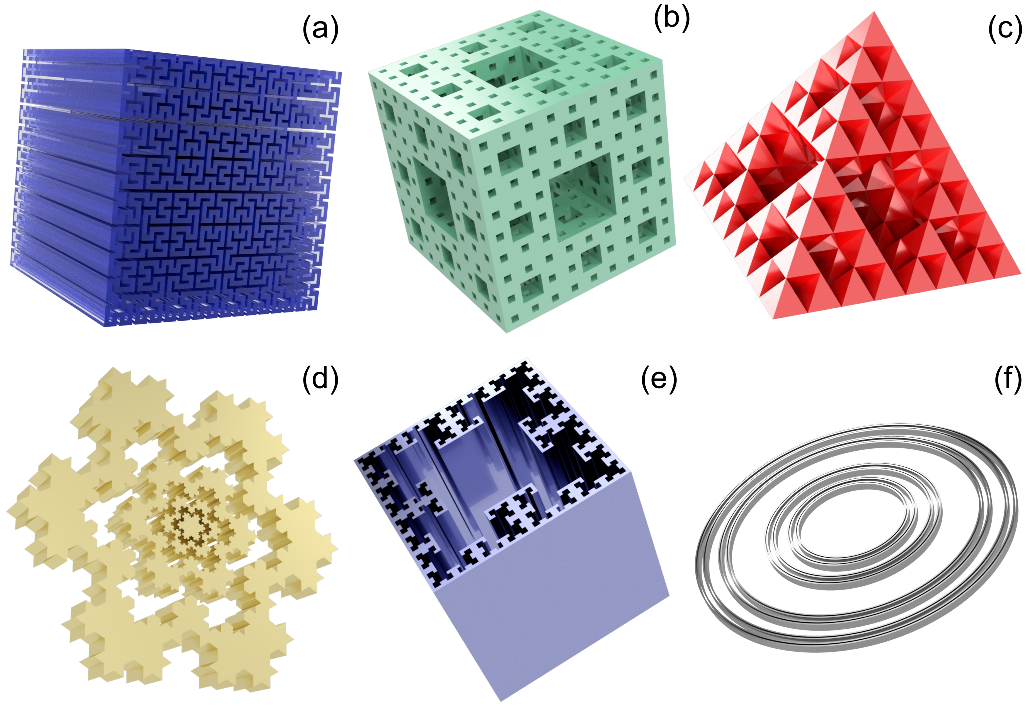

FIG. 12. Fifth order Hilbert fractal (a). Menger sponge, third order (b). Sierpinsky pyramid, third order (c). Koch fractal fourth order (d). T-shape fractal, third order (e). Cantor lens, third order (f). G. Comandini, *Hilbert Fractal Acoustic Metamaterials*, University of Bristol, 2024; licensed under a Creative Commons Attribution (CC BY) license[7].

volve the use of a labyrinth-like pattern that creates pathways and barriers to manipulate sound waves. This design principle allows for the creation of complex acoustic landscapes, which can be used to shape the propagation of sound waves[106,124,479,483,491–493] with designed reflective and refractive angles, focusing[1,27,45,106,469,478] (Fig. 9) or tunneling[106,494–496].
Bio-inspired[455] hierarchical assembly geometries of acoustic metamaterials imitate the structure found in biological systems. Examples include the spider web (Fig. 1*j*) geometry[69,305,461,497–502] and honeycomb (Fig. 1*f*) structures[503–513] that use hexagonal cells arranged in repeating patterns. These bio-inspired designs offer unique acoustic properties and can be used to create a wide range of AMs with tailored properties, like low-frequency sound and vibration control for the spider geometry and broadband hierarchical sound absorption at high temperatures for honeycomb.

Chiral lattice (Fig. 1*c*) geometry[514–521] in AMs utilises a lattice structure with chirality, resulting in asymmetric arrangements of unit cells. This design principle allows for creating of complex structures that can be used, such as sound-diffusing metasurfaces that allow non-specular scattering.
Antichiral lattices (Fig. 1*d*) geometry[522,523] in AMs are structures with an opposite chirality compared to their mirror image. For instance, the use of I-shaped anti-chiral units[524] to build AMs has been reported. This design principle allows for the creation of complex, multi-scale structures for enhanced broadband sound insulation in the lower part of the acoustic spectrum.
Auxetic lattice (Fig. 1*e*) geometry[522,525–528] in acoustic metamaterials make use of structures that exhibit a negative Poisson ratio behaviour. Some researchers have constructed curved shells with 3D re-entrant auxetic cellular metamaterials [77]. In contrast, other researchers have exploited the auxetic behaviour of these structures by applying external loads or other inputs to modify their acoustic performances[525,526]. This unique property allows the design of acoustic metamaterials with potentially high tunable characteristics.

D. Bio-Inspired and Hierarchical Acoustic Metamaterials

The increasing focus on bio-inspired and hierarchical acoustic metamaterials is largely due to their ability to mimic intricate natural geometries, thus improving the wave control capabilities. Natural structures such as tree branches and moth wings[529–531] present hierarchical configurations that allow better management of wave propagation, as highlighted in recent research[49,532]. These structures frequently incorporate self-similar or varied unit cell arrangements, which facilitate adjustable wave interaction properties, demonstrating improved sound absorption and filtering over diverse frequency ranges[533–535]. Hierarchical metamaterials embed smaller components within larger ones, enhancing energy dissipation while simultaneously managing both low- and high-frequency waves[502,536]. This nesting strategy has been shown to significantly enhance the functionality of phononic crystals, leading to the creation of versatile metamaterials that address both structural and acoustic requirements[49,537]. Incorporating bio-inspired elements into metamaterials not only strengthens their mechanical characteristics but also establishes the foundation for novel applications in noise control and energy dissipation[538,539].

1. *Fractals*

One of the most captivating categories among these configurations involves the use of self-similar structures at various scales. Fractal geometries can be subdivided into two macro-categories: space-filling (*SF*) and not-space-filling (*nSF*). *SF* tend to fill a confined space completely, with a polygonal line that theoretically can reach every point in the area or volume. At the same time, *nSF* cannot be contained in a *2D* or *3D* enclosed space if the number of iterations increases[540]. These geometries offer unique acoustic properties in terms of acoustic absorption and transmission loss, for instance, making them useful in various applications, like barriers in transformer noise reduction[541].

Fractal-inspired[18,106,456,468,542–544] or recursive structures, also known as pseudo-fractal geometry, are used in AMs to create patterns that mimic fractal properties. These structures exhibit self-similarity at different scales and include designs such as hexagonal or triangular lattices[456,498,542,545,546], hierarchical lattices[498,542,547], and self-similar beam lattices[456,542]. Moreover, it has been experimentally shown that the number of ninety-degree angles in a *2D* fractal or coiled structure does not influence the acoustic output in terms of acoustic absorption and transmission loss if the total length of the cavity patterns is the same. Thus, Fig. 1*a* and Fig. 1*b* contain metamaterials architectures that have the same absorption and transmission performance if the length and section of the polygonal shape is the same[8,264]. A notable example is the utilisation of Hilbert fractals[1,8,10,12,18,210,261,541,548,549], which are characterized by intricate self-similarity patterns inspired by the Hilbert curve (Fig. 1*a*). The hierarchical nature of the Hilbert fractal design offers flexibility in tuning the acoustic response across a wide range of frequencies, thereby enhancing acoustic properties such as sound absorption[8] and transmission loss[10].

In addition to the Hilbert fractal (Fig. 12a), the Menger fractal[13,17,22,483], also known as the Menger sponge (Fig. 12b), has been employed in the design of acoustic metamaterials. The unique structural properties of the Menger fractal, particularly its self-similarity at different scales, are exploited to control, manipulate, and block sound waves. The Menger fractal geometry provides a lightweight solution, allowing air passage due to the high porosity. It has also shown a remarkable tunnelling effect.

The Sierpinski fractal (Fig. 12c), also referred to as the Sierpinski triangle or pyramid, is a self-similar structure widely implemented in acoustic metamaterials[9,15,16,543,550–554]. This fractal is characterised by its recursive triangular patterns, which significantly influence sound wave propagation due to its repeating geometry. Its distinctive properties allow for the formation of band gaps; in addition, this geometry is used to enhance sound scattering in architectural acoustics, both inside buildings and on facades, to optimise sound wave diffraction in urban environments. Moreover, using this pattern in barriers between streets and residential areas can be an effective noise mitigation tool. The Koch fractal also referred to as the Koch snowflake (Fig. 12d), is a mathematical curve that can be applied to a segment or a polygonal shape perimeter[19,510,555]. It is defined by a recursive process that incrementally enhances the number of sides, and its sophisticated design is leveraged in the construction of acoustic metamaterials to boost properties such as wave scattering[19]. In addition to promoting wave scattering, this fractal can also modulate acoustic wave speed, create bandgaps, and steer the wavefront in a waveguide plate by modifying the fractal order.

The T-fractal (Fig. 12e), represents a potential fractal pattern that manifests the letter *T* at different scales and orientations within a *2D* space[556]. It could also be constructed using other alphabet letters or shapes, thereby providing bandgap capabilities and a spectrum of acoustic effects that remain largely unexplored.

Finally, the polyadic Cantor fractal (Fig. 12f), a variant of the conventional Cantor set, has been utilised in the design of acoustic metamaterials[14,557,558]. This fractal is derived from a process that iteratively excises portions from a line segment, mirroring the construction methodology of the Cantor set. Its primary applications are in ultrasonic imaging and, lately, low-frequency porosity absorbers.

2. *Other geometries*

Apart from fractal and fractal-inspired curves[18,456,468,542], recursive geometries have been shown to induce a phenomenon referred to as negative density[559], bulk modulus[560], or both[560], which is rare in the natural world[529]. This unnatural set of physical properties extends their utility to various applications encompassing noise reduction[253,484,497], sound focusing[27,28], and even acoustic cloaking[100,102,103,272,561,562]. The application of materials in recursive geometries can be illustrated using cylinders[563,564] or other extruded *2D* shapes, like the c-shape[565]; arranged in a well-defined square, hexagonal or Kagome[456] patterns. The effect of such geometric configurations will offer an overall density and bulk modulus different from the single scatter, forming the series (Fig. 10b).

Another interesting example entails the deployment of membranes along a 1D dimension, at a specified fixed interval from each other, with or without an additional mass incorporated within the membrane in different positions[294,566]. This configuration further enhances the versatility of acoustic metamaterials, even with just a monodimensional repeated pattern that can, generate zero reflection[566].

Recent scholarly endeavours have begun exploring the potential application of Kelvin cells[215,567] in developing acoustic metamaterials, yielding promising results. A Kelvin cell is a tetrakaidecahedron (Fig. 1*k*), essentially a polyhedron with 14 faces, comprising six squares and eight hexagons. This distinctive property of the Kelvin cell enables it to create a 3D space-filling tessellation, which makes it helpful in obtaining band gaps at designed frequencies.

Other geometrical configurations used to make AMs, are the spiral[33,104,253,515], and the helix[28,66,568], as shown in Fig. 1h and Fig. 1g. AMs that use spiral geometries can mainly develop their shape in a 2D plane. Spiral structures (Fig. 1*h*), can be arranged in a variety of configurations. The possibility of incorporating patterns that exemplify this versatility as Archimedean spirals[57,569] or logarithmic spirals[570] to make waveguides, each with unique properties, like slowing down, guiding, and confining the wave propagation.

Helix AMs add another dimension to the design possibilities in this rapidly advancing field. These metamaterials are characterised by incorporating helical structures (Fig. 1*g*) into their design, arranged in a periodic or variable pattern of the helix coils. The uniqueness of the helix, with its continuous curve winding about a central axis, can generate, for instance, phase shifting[568] of the acoustic wave, and consequent passive noise cancellation.

3. Possible combinations

The construction of acoustic metamaterials entails a strategic integration of specific geometries and acoustic technologies. The breadth and diversity of design approaches employed in developing these materials provide a wide spectrum of potential combinations. An illustrative strategy for the development of AMs can be concentrated into six primary elements, each reflecting the combination of different geometries and technologies. The first approach involves using mixed internal geometries or a singular one in combination with perforated or micro-perforated panels (Fig. 13*a*) internally or on top[49,198,460,473,489,497,548,571–579] (the perforations can be usually circular or rectangular). This method enhances the material's ability to damp certain frequencies through thermoviscous losses.

In general, microperforations (Fig. 13*a*) are used to damp high frequencies; meanwhile, the internal geometries (coiled, zigzag, maze, labyrinthine or fractal, as exemplified in Fig. 13*d*) act towards the spectrum's low-frequency range. This specific union can produce a broadband effect regarding acoustic losses if compared to the effect of the single "pieces" alone.

The second approach incorporates mixed geometries or a single one, with one or more Helmholtz resonators[39,56,273–275,475,485,580–583]. Helmholtz resonators (Fig. 13*c*) are structures designed to resonate at specific frequencies, thereby absorbing sound at these frequencies and reducing noise. Sound absorption can be maximised by integrating more than one resonator within the AMs design, enabling a more broadband absorption of the acoustic energy.

The next approach mixes membranes (Fig. 13*f*) and Helmholtz resonators (Fig. 13*c*), providing exceptional control over sound waves. By combining Helmholtz resonators with membranes-sometimes weighted with added mass-these materials can significantly shift the frequency range at which they operate[584–587]. This combination is particularly effective at lowering the frequency range, allowing the metamaterial to trap lower-frequency sounds more effectively. Additionally, this design approach broadens the range of frequencies the metamaterial can manage for a variety of applications, like mufflers[586,588–590] or ventilated structures[591]. It is possible to fine-tune these materials to suit specific needs, such as noise reduction and sound isolation by tweaking the properties of the membranes and the size of the resonators[592].

In the fourth approach, porous materials, such as acoustic foam like melamine (Fig. 13*b*), are combined with a specific geometry that takes care of the low-frequency range[286,449,454,459,583]. In this combination, the porous material, dampens sound wave propagation, reducing reflected sound and facilitating noise control through their double action separated by the Biot limit[454]. Under the Biot limit, the solid part of the foam will contribute to the metamaterials effect in the middle-frequency range. On the other hand, over the Biot limit, the air inside the pores, with their thermoviscous action, will contrast the middle-high frequency range.

The fifth approach merges one or more of our geometries with one or more piezoelectric patches[65,66,68,69]. Piezoelectric materials generate an electric charge in response to applied mechanical strain stress. By embedding piezoelectric patches (Fig. 13*e*) within the design of AMs, it becomes possible to control sound wave propagation and harvest electric energy from the sound waves. This approach creates multifunctional acoustic metamaterials that can serve dual roles; sound control and energy harvesting.

The last approach combines some of the aforementioned four methods[593,594], offering a comprehensive solution for constructing acoustic metamaterials. This strategy provides higher flexibility regarding covered frequency but with a consequent securely higher complexity and manufacturing cost.

E. Elastic Metamaterials for Solids

Elastic metamaterials are engineered to control mechanical waves, including stress waves and vibrations, within solid media. These distinctive characteristics enable applications ranging from seismic protection to vibration mitigation, which are vital for bolstering structural durability during phenomena such as earthquakes and dynamic loads in machinery and frameworks. Advances in fabrication technologies, especially 3D printing, have allowed the development of intricate elastic metamaterials with customised mechanical properties, improving their utility in real-world scenarios[595–597]. For example, research has illustrated the utility of such materials in forming seismic metamaterials capable of transforming harmful seismic waves into less destructive forms, offering groundbreaking approaches to earthquake resilience[598,599]. Moreover, incorporating locally resonant structures within elastic metamaterials has demonstrated significant potential to control low-frequency waves, a critical aspect of effective vibration isolation[600,601]. In conclusion, ongoing advances in elastic metamaterials continue to broaden their applications in diverse engineering domains.

IV. FABRICATION

The fabrication of acoustic metamaterials involves a range of technologies, each with its own unique strengths and capabilities. This section offers a detailed, though not exhaustive, overview of the main methods used to create acoustic metamaterials (AMs). We also look at the types of machinery involved and their specifications, particularly regarding precision and accuracy. This is especially important for the geometry of surfaces, such as rugosity, which can play a major role in energy dissipation through thermoviscous losses. Additionally, the methods and their tolerances are closely tied to the frequencies being studied with the manufactured samples. For example, at higher frequencies, it's crucial to minimise imperfections in the manufacturing process due to the shorter wavelengths involved.
For example, if the targeted frequency range is 1 kHz, using photolithography to produce metamaterials with operational wavelengths close to 34 cm would be excessive, given the precision requirements of the machining process. Conversely, small imperfections at reduced wavelengths for ultrasound applications can significantly affect the response of the metamaterials. The techniques considered in this work are classified as additive and subtractive manufacturing methods and are ordered from the least to the most precise.

A. Additive Manufacturing

Fused deposition modelling (*FDM*) is often used in fabricating acoustic metamaterials. *FDM* operates by extruding a thermoplastic filament layer by layer to construct a tridimensional object, with the advantage of a wide range of filament materials with varying properties, including *PLA*, one of the cheapest but reliable options for relatively fast prototyping. For example, the machine "*FORTUS 400mc*" has a building volume of 406.4 mm x 355.6 mm x 406.4 mm, with a printing tolerance of $\pm$ 0.127 mm, and a possible layer height between 0.127 mm and 0.3302 mm[602].
PolyJet[70] makes use of inkjet printing principles to create three-dimensional objects, making it a versatile *3D* printing process for fabricating acoustic metamaterials with complex geometries. Polyjet printing works similarly to 2D inkjet printing. The process, deposits layers of curable photopolymer resin onto the printer's building area rather than propelling ink droplets into a paper surface. According to the manufacturer *Stratasys* , the machine *Objet500*[603], has a building volume of 490 mm x 390 mm x 200 mm, with an accuracy of $\pm$ 0.1 mm if the highest dimension of the printed object is below 100 mm. Otherwise, if the highest dimension of the printed object is bigger than 100 mm, the accuracy drops from $\pm$ 0.1 mm to $\pm$ 0.2 mm.
Powder bed fusion technology (PBF) is an alternate method of additive manufacturing. To begin, the powder bed fusion printing process, a thin (around 0.1 *mm*) layer of it, is applied to the construction platform. Following that, a laser merges the primary stratum, or the design sliced sectional design. A roller is then used to distribute successive layers of dust over the previous layer, incorporating additional layers. This sequence is repeated until the entire prototype is formed. The loose and non-merged powder remains in place throughout the process but is removed during the subsequent cleaning phase. For instance, according to the manufacturer "*Wematter*", the machine *Wematter Gravity SLS 3D printing system*[604], has a building volume of 300 mm x 300 mm x 300 mm, with a precision of $\pm$ 0.1 mm.
Direct Ink Writing (DIW) is a relatively new layer-by-layer 3D printing technology that uses a small nozzle to distribute a pressure-driven viscoelastic ink, resulting in detailed structures. This process normally consists of three steps: first, creating 3D models with CAD software, then designing a 3D route for the nozzle with slicing software to create a G-code, and finally, a controlled ink release. DIW is distinguished by its extensive flexibility for customising the inks, allowing for the exact creation of 3D objects from the microscopic scale to the bigger ones. The precision and resolution of the printed object are heavily influenced by critical determinants such as nozzle diameter and printing speed, and it can print soft materials such as hydrogel to thermoset polymers. The x-y plane layer resolution ranges from $\pm$ 0.1 mm to $\pm$ 1.2 mm, and the z-axis resolution ranges from $\pm$ 0.1 mm to $\pm$ 0.4 mm, with the smallest potential feature size being around 0.5 mm[605].
Digital Light Processing (DLP) is typically considered to be faster than Stereolithography. This is because SLA uses a technology in which the laser cures the resin point by point; meanwhile, DLP uses a projector screen to expose a complete horizontal slice (layer) at once, allowing for simultaneous curing of all locations inside the slice. Thus, the time necessary to harden a single layer is lower than SLA. Compared to stereolithography, the DLP printing quality is slightly worse but faster than SLA; this is due to the possibility of specular or reflection effects that can make the polymerisation of the layers less precise. According to the manufacturer *FlashForge*, the machine *Hunter 3D Printer*[606], has a building volume of 120 mm x 67.5 mm x 150 mm, with a layer resolution between

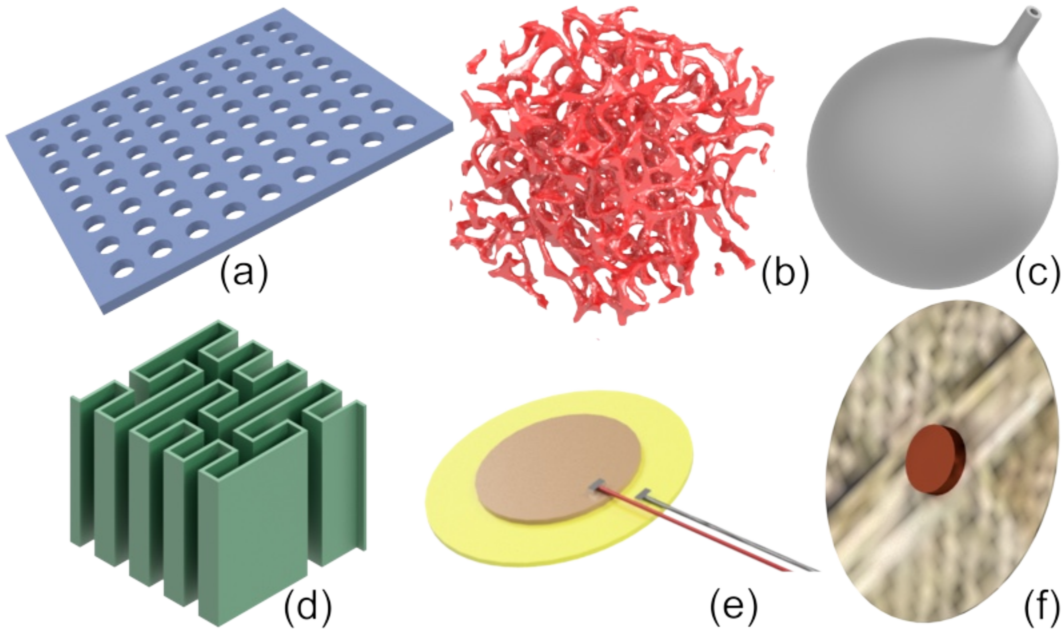

FIG. 13. Main components forming acoustic metamaterials: perforated and microperforated panels (a), acoustic foams (b), Helmholtz resonators (c), Coiled or fractal or maze geometries (d), piezoelectric patches (e), membranes with or without masses (f). G. Comandini, *Hilbert Fractal Acoustic Metamaterials*, University of Bristol, 2024; licensed under a Creative Commons Attribution (CC BY) license[7].

0.025 mm and 0.02 mm, and a print accuracy of ± 0.05 mm.
Stereolithography (SLA)[475], an additive manufacturing technique, has been instrumental in creating three-dimensional objects through a process of photopolymerisation. This technique involves selectively solidifying a liquid photopolymer resin point by point using a light source, such as a laser, to form the desired *3D* shape. For instance, according to the manufacturer "*3D Systems*", the machine *Projet 7000 HD*[607], has a building volume of 380 mm x 380 mm x 250 mm, with accuracy between ± 0.025 mm and 0.05 mm for every 25.4 mm of printed element.
Due to the dimensions of the typical wavelengths in acoustic metamaterials, techniques like Electron Beam Lithography, Ion Beam Lithography and X-ray lithography are not considered. Those techniques, due to their high cost, nanometric precision and accuracy, are rather used for optical metamaterials.
Multimaterial printing opens up exciting possibilities to design metamaterials that make use coupled structural vibration effects due the use of different materials. Techniques like PolyJet printing, which works like an inkjet but with materials, can blend different photopolymers, giving parts with different mechanical and acoustic properties.

Directed Energy Deposition (DED) methods [608], such as Laser Engineering Net Shaping [609] (LENS), allow for the simultaneous use of multiple powders, creating structures with potentially customised acoustic traits. Advanced Fused Deposition Modeling [437,610] (FDM) printers with one [611], or multiple extruders can produce parts with different stiffness and density [612], crucial for acoustic performance. While Binder Jetting has typically been a single-material process [613], new advancements allow it to use multiple powders or add secondary materials afterward, resulting in complex acoustic behaviours [614,615]. Lastly, technologies like Digital Light Processing (DLP) and multi-material Stereolithography (SLA) can switch between or combine different resins, crafting detailed structures like piezoelectric microphones [616], or an ultrasonic sensor equipped with three-dimensional printed holographic elements [617]. These multimaterial methods make it possible to fine-tune how parts handle vibrations, leading to better performance in many applications [618].

B. Subtractive Manufacturing

Subtractive manufacturing processes, such as laser cutting and water jet cutting, or classical machining, have also found applications in producing AMs. Water jet cutting employs a high-pressure jet of water (around 4000 *bar* for instance), mixed with abrasive particles, to cut through various materials. The accuracy for a straight cut of 1 m is, for instance, ± 0.1 mm for the machine *Mach 100*[603] of the company *Flow*[619], until ± 0.02 mm for a straight cut of 30 *cm* for the *NanoJet* machine from the same company[620].
On the other hand, laser cutting makes use of a high-power laser beam to cut or engrave materials, creating intricate patterns and structures. One downside is the possible difficulty in assembling precisely *3D* AMs structures using laser-cut *2D* slices[264]. It is worth noticing that if the pattern to laser-cut has relatively small recursive geometries, like in the case of fractals, particular care needs to be paid towards overheating of the material during the cutting session[264]. Moreover,

it is helpful to consider that the *X-Y* resolution is a function of the material, material thickness, and cutting speed[621]. For instance, the cut accuracy is ± 0.015 mm for the machine *Speedy 400 flexx*[603] of the company *Trotec*[622].

CNC milling machines can produce AMs by machining solid blocks or sheets of materials with desired patterns or structures[623]. A 5-axis CNC machine for instance has five planes of motion: sideways (*X-axis*), vertically (*Y-axis*), back and forth (*Z-axis*), and two additional axes for worktable rotation and tilt. Its primary advantage is enhanced productivity and efficiency when producing complex forms using continuous milling. The five-axis movement produces more precise and smooth parts, minimising manual tool changes and saving time. The versatility of this machine enables a vast range of components and forms, highlighting its adaptability across diverse metamaterial complex shapes. According to the manufacturer *Bridgeport* , the machine *VMC 600*[624], has a building volume of 600 mm x 410 mm x 520 mm, with an accuracy of ± 0.005 mm[625].

Electrical Discharge Machining (EDM) uses heat energy to carve accurate, complicated shapes in electrically conductive materials, which standard processes such as CNC milling may not be able to accomplish because of the material toughness. This distortion-free technology, which does not make physical contact with the workpiece, enables the production of complex shapes, produces a high-quality finish, and ensures remarkable precision, making it particularly useful for small-scale manufacturing. Even tough materials like inconels and tungsten carbide can be used for EDM. However, the slower material removal rate increases production time and costs, and the extreme heat utilised can change the material's metallurgy. According to the manufacturer *Agie*, the machine *Agiecut classic 2*[624], has a building volume of 750 mm x 550 mm x 250 mm, with an accuracy of ± 0.006 mm.

Photolithography is a micromanufacturing technique used to create intricate structures on a 2*D* substrate. Photolithography is an intricate micromanufacturing procedure, it involves subjecting a polymer surface to ultraviolet (*UV*) light to eliminate the areas that are not covered by the design mask. This masking process on the two-dimensional polymer surface is akin to the function of a photo negative. Areas covered by the mask are protected from *UV* light exposure. As a result, there is no curving or deformation of the geometric pattern beneath these masked regions. For instance, this technique has been used in AMs to enable active broadband tunability[626] and create ultrasonic transducers[627]. For instance, the machine *SLX 3 e1* from the company *Micronic*[628] can ensure a minimum line width of 400 *nm*, with an accuracy of ± 30 *nm* for an area of 150 *mm* x 150 *mm*.

C. Nanoscale to Macro-scale Fabrication Techniques in Acoustic Metamaterials

The advancement of acoustic metamaterials (AMs) depends significantly on sophisticated fabrication methods that offer precise control over microstructural features while remaining scalable for practical use. Techniques at ultrafine scales, such as electron-beam lithography (EBL) and focused ion beam lithography (FIB), enable detailed patterning with nanometre accuracy, which is vital for influencing sound waves at subwavelength dimensions[629]. However, these approaches often face challenges in scalability and expense, restricting their application mainly to experimental environments[630]. On the other hand, macroscale production methods, including large-scale additive manufacturing processes such as fused deposition modelling (FDM) and powder bed fusion (PBF), are crucial in creating AMs intended for practical use, such as noise barriers and construction materials[211]. These techniques allow the incorporation of sound-diffusing and sound-absorbing components into larger systems, improving their functional applicability[631]. The combination of multiscale fabrication strategies, such as Direct Ink Writing (DIW) and Multi-Material Jetting, offers a promising pathway to develop hierarchical acoustic metamaterials that merge nanoscale accuracy with macroscale designs[146]. This multiscale capability can tackle technical issues in the field, especially for applications requiring wide frequency attenuation and durability under environmental conditions[632]. Despite these progressions, the scaling of AMs remains challenging due to material and process limitations, highlighting the need for further exploration into the integration of top-down lithographic techniques with scalable 3D printing methods[163].

D. Emerging Manufacturing Technologies and Their Impact on Acoustic Metamaterial Performance

Advancements in modern manufacturing techniques, especially multi-material additive manufacturing (AM), have markedly improved the acoustic properties of metamaterials. This approach enables the precise arrangement of materials with distinct mechanical properties, facilitating the development of customised material gradients that enhance both vibration damping and sound absorption[211,633,634]. These capabilities allow for the design of metamaterials optimised for targeted acoustic uses, enhancing structural integrity and enabling greater control over acoustic attributes[400,635]. Topology optimisation has become a vital technique in designing intricate geometries that maximise acoustic efficiency while reducing material consumption. By strategically distributing materials, engineers can create lightweight structures capable of accurately manipulating sound waves, leading to improved impedance matching and sound attenuation[325,636]. Moreover, integrating machine learning into the design process accelerates the iteration and optimisation of metamaterials, enabling predictions of acoustic behaviours across extensive frequency ranges[324,637]. Advanced manufacturing techniques featuring real-time monitoring and adaptive controls significantly enhance the precision and reproducibility of acoustic metamaterials. Materials with intelligent properties that adapt to environmental changes smooth the way for novel applications in adaptive noise mitigation and energy harvesting[175,326,638]. The choice of fabrication technique for acoustic metamaterials is pivotal in optimising their functional characteristics.

Additive manufacturing, particularly multi-material printing, enables the fabrication of complex gradients that enhance sound absorption over broader frequency ranges, expanding their utility[174,639,640]. On the other hand, subtractive techniques such as CNC milling and Electrical Discharge Machining (EDM) deliver the accuracy required for high-frequency applications, where slight imperfections can significantly alter acoustic behaviour[161,175]. Hybrid manufacturing approaches, which combine additive and subtractive techniques, provide a balanced solution, achieving both scalability and the precise microstructural details necessary for particular acoustic properties[211,641]. Additionally, integrating machine learning into these processes enables real-time adjustments and predictive modelling, boosting the adaptability and reproducibility of acoustic metamaterials[394,642]. This integration supports the creation of multifunctional metamaterials designed for noise control and energy absorption, facilitating their implementation across various settings[638,643,644].
Additive manufacturing methods, including 3D printing and multi-material printing[645,646], enable the production of complex structures that effectively minimise unwanted resonances and enhance broadband absorption. These techniques offer precise control over geometry and material distribution, which is vital for optimising acoustic performance in devices such as transducers and metamaterials[647,648]. For instance, polymeric cellular structures created through additive manufacturing have shown significant advantages in acoustic absorption due to their custom-designed microstructural attributes[647]. Conversely, subtractive methods like CNC milling enhance surface quality and dimensional precision, which is critical for reducing wave scattering and achieving optimal impedance matching. The high accuracy of CNC milling ensures smooth, uniform surfaces on acoustic devices, improving sound wave transmission and minimising reflections at material interfaces[649,650]. Nanoscale fabrication methods, such as nanoscale lithography, refine microstructural features, improving frequency selectivity and resonance performance. These techniques are essential for applications like noise suppression, where controlling specific frequencies is critical[164,651]. The integration of various materials and manufacturing methods further enhances performance; for example, polymers used in additive manufacturing allow for the flexible tuning of metamaterial properties, making them ideal for lightweight acoustic control applications[652,653].

E. Optimization of Experimental Methodologies for Real-World Applications

Techniques for measuring acoustics are fundamental in defining the properties of acoustic metamaterials within controlled settings. Commonly used configurations include reverberation chambers, impedance tubes, and anechoic chambers. Reverberation chambers generate a diffuse sound field, allowing evaluation of the sound absorption and scattering properties of materials in a controlled environment, which is critical for analysing their acoustic performance[654]. In contrast, impedance tubes are used to determine the acoustic impedance and absorption coefficients of materials, shedding light on sound-surface interactions[655]. Anechoic chambers are uniquely designed to suppress reflections, allowing precise measurements of sound propagation and material characteristics without interference from echoes or external noise[656]. These approaches are indispensable for advancing the research of acoustic metamaterials, ensuring accurate and consistent measurements that support the creation of materials with custom acoustic properties.
In contrast, impedance tubes offer a quicker and more economical means to assess acoustic characteristics, although they may lack the precision necessary to capture intricate wave behaviours in some metamaterials[657]. This contrast emphasises the need to carefully select measurement methods based on the particular demands of the research or application, striking a balance between the desire for accuracy and the constraints of time and budget.
Recent advances in optimisation are shaping acoustic measurement methods. Automated systems and real-time data processing are becoming standard in experimental setups, speeding up data analysis, and minimising the costs associated with repetitive testing[658]. Machine learning algorithms are also being used to improve the interpretation of complex datasets, enabling faster insight derivation[659]. In addition, adaptive systems that adjust measurement frequency ranges based on initial results are gaining traction, significantly increasing measurement efficiency in industrial contexts[660]. These advances streamline the testing process and enhance the reliability and precision of the results, driving forward the practical implementation of acoustic metamaterials.
Emerging research highlights how innovative measurement methods address practical limitations. For example, 3D printed prototypes have proven effective in assessing acoustic properties quickly, allowing quicker iterations in design and performance analysis[661]. This technique accelerates development while offering crucial insight into the acoustic behaviours of novel materials and structures. Furthermore, combining diverse measurement methods has provided a holistic understanding of acoustic properties, helping researchers choose techniques that optimise precision, scalability, and resource efficiency[662]. Such examples underscore the importance of flexibility in measurement approaches as researchers tackle the challenges posed by acoustic metamaterials and their wide-ranging applications.

V. MATERIALS AND FREQUENCIES

A. Materials

The section provides an overview of the materials used to produce acoustic metamaterials, with an emphasis on those most frequently employed in research-based applications. The selection of these materials varies significantly based on the intended application; specifically, the materials can range from rigid to flexible, particularly in scenarios involving structural-acoustic coupling.
Photosensitive resins, or photopolymers[1], are liquid polymers

that solidify when exposed to a specific wavelength of light, typically ultraviolet light. They are commonly used in stereolithography[475] or digital light processing 3D printing technologies. These resins offer sufficient precision for acoustic applications and can produce intricate structures with fine details, making them ideal for creating complex geometries.

Metals such as copper[663], brass[14], and aluminium[564] have also been used to create AM if we consider multifunctionality. Copper's excellent electrical conductivity and high thermal conductivity make it desirable for AMs applications. Brass and aluminium, due to their relatively high density (compared to polymers), stiffness and stability over time, are valuable for manipulating sound waves. Thin composite plates, using steel and rubber[664], have also been used due to their insulation power against a wide range of frequencies, exploiting their resistance to substantial underwater pressure.

Polylactic acid[264] (PLA), a biodegradable thermoplastic polymer, is commonly used in 3D printing[665] and various applications. PLA is one of the most typical materials used for fast prototyping, because of its relatively low cost and good printability. Similarly, other thermoplastic polymers such as polyethylene terephthalate[666] (PET), acrylonitrile butadiene styrene[667] (ABS), acrylonitrile styrene acrylate[575] (ASA), and polymethyl methacrylate[114] (PMMA) have been used in certain scenarios due to their unique properties, for instance, PMMA can be used to build waveguides, meanwhile, the others polymers can be selected for their respective mechanical properties like stiffness, impact and heat resistance.

Another material widely used in AMs prototyping is epoxy resin[482]. This type of thermosetting polymer, undergoes a chemical reaction when combined with a hardener to form a strong and rigid material. This material has been explored for use in acoustic metamaterials due to its strength and rigidity.

Polydimethylsiloxane[668] (PDMS) and thermoplastic polyurethane[669] (TPU) are flexible and versatile materials that can be utilised to create deformable structures. Their flexibility and elasticity enable the creation of AMs that can adapt to different acoustic environments.

Composite structures can be created by combining metal honeycomb frameworks with ethylene vinyl acetate (EVA) copolymer films[504]. The metal honeycomb frameworks provide structural support, a high strength-to-weight ratio, and sound transmission control, while EVA copolymer films[670] offer flexibility, damping properties, and additional acoustic properties.

Materials such as aluminium nitride[671] (AlN), silicon dioxide[672] (SiO_2), barium titanate[673] ($BaTiO_3$), and lithium niobate[674] ($LiNbO_3$) have been used for applications that require converting mechanical energy to electrical.

Natural materials like wood have been tested as well to produce AMs. Due to the low density and workability, cylindrical wood[675] scatterers have been used in 2D waveguide prototypes without finding substantial differences in terms of acoustic output compared to other materials like iron or aluminium, but are interesting in terms of manufacturing costs due to the relatively easy workability.

Melamine foam[286], known for its high porosity and interconnected open-cell structures, is another material used in acoustic metamaterials. It contributes to sound attenuation and absorption through multiple reflections, diffusion, and conversions of sound energy into thermal energy.

Metal fibres[46], made of various materials such as steel, aluminium, or copper, provide stiffness, structural integrity, and heat resistance; meanwhile, at the same time, the porous matrix contributes to sound control and can be tailored to specific acoustic requirements and applications, like inside mufflers.

Polyurethane foam[193], with an open-cell structure, can be moulded, cut, or shaped into various forms, allowing flexibility in the design and manufacturing process, especially used in anechoic chambers, perimeters of *2D* waveguides, and impedance tubes.

Flexibility can be granted by nonwoven materials[454] made by entangling fibres together (without weaving or knitting), resulting in a porous and flexible structure. These can be manufactured from various fibres, such as polyester and polypropylene, or natural fibres, like cotton or wool. Their porous structure makes them particularly suitable for sound absorption applications.

Lastly, polyvinyl chloride[676] (PVC) foam can be used as a material to create AMs, providing sound absorption and transmission control properties. PVC offers advantages such as flexibility and lightweight, making it a suitable material for AMs prototyping.

In conclusion, the choice of the material depends on the specific requirements for the application (if prototype or not, for instance), including the desired acoustic properties, fabrication method, and environmental and operational considerations. The materials discussed in this review offer a wide range of possibilities for designing and fabricating acoustic metamaterials, each with unique and sometimes similar advantages and challenges.

B. Frequencies Involved

The exploration of acoustic metamaterials encompasses a wide array of frequencies, each with distinct properties and potential applications. At the lower end of the spectrum, we find infrasound frequencies, typically below 20 Hz, which are not detectable by the human ear. Despite being imperceptible, these frequencies play a significant role in both natural events, such as earthquakes, and human-induced activities, including specific industrial operations.

Noise manifesting at low frequencies conventionally bracketed within 20 Hz to 600 Hz, originates from various sources. These may encompass the deep grumble produced by lorry engines, auditory manifestations of distant meteorological phenomena such as thunderstorms, or the persistent hum generated by sizable air conditioning apparatus. Normally, these sound waves with long wavelengths can traverse physical barriers like walls in a relatively easier manner, if compared to their high-frequency counterparts. This exacerbates potential noise pollution issues. Due to the low-frequency spectra involved, stopping them with a thin layer of traditional acoustic materials is difficult. This is one of the most researched subtopics of AMs for sound insulation[1,253,261,449,453,471,497,524,574,576,677]. The goal is to induce sound blocking with a reasonable thin layer of material[63,198,234,274,459,461,463,473,484,574,577,667,678,679].

Sounds falling within the medium frequency range between approximately 600 Hz to 2 kHz has different sources. These can include conversational exchanges conducted within typical vocal ranges, the operational noise emanating from domestic electrical devices like a vacuum cleaner, or the audible hustle and bustle associated with heavy traffic on populous thoroughfares. Moreover, middle frequencies play a crucial role in facilitating intelligible speech. Thus, the contribution of AMs can potentially be linked to the combined use of foams plus coiled structures to mitigate and modulate sound energy[49,55,57,217,257,460,485,548,579,582].

High-frequency noise encompasses the spectrum from 2 kHz upwards to 20 kHz. Representative sources include the high-pitched hiss discharged by a pressure cooker under strain, the piercing emission from a blown whistle or the acute shriek of a distressed child. Owing to their comparatively shorter wavelength, these types of sound are often more effectively attenuated or absorbed by conventional acoustic materials. For this frequency range, traditional acoustic technologies like acoustic foams having open cells and Helmholtz resonators are also efficient[449,469,579].

Lastly, ultrasounds are sound waves with frequencies exceeding the upper limit of human audibility, typically above 20 kHz. Previous studies have discussed the generation of ultrasound within the 20 kHz to 240 kHz frequency interval. Ultrasounds are widely used in medical imaging and industrial testing because they can penetrate materials and tissues, exposing their internal features or defects[14,45,57,70,114,680].

VI. ACOUSTIC CHAMBERS, AND MEASURED QUANTITIES

Laboratory tests are essential to evaluate the effects of acoustic metamaterials before developing real-world applications. We report here on the fundamental techniques used in experimental acoustics, categorized by the measured quantities and specific applications of the metamaterials.

Interestingly, most acoustic metamaterials proposed in the literature have not been validated experimentally or are tested only in very controlled settings, like 1D ducts with normal incidence. A few studies explore grazing incidence or flow conditions, but these are not frequent. Additionally, most validations are performed under monomodal configurations- i.e., scenarios that only consider simple geometries and specific angles like 0° and 90°. This means very few acoustic metamaterials have been tested under complex, real-world setups that resemble industrial applications.

There is a clear need for experimental setups that can handle more complicated configurations. This includes the 2D apparatus mentioned later in this study, which is designed to test AMs in conditions that are much closer to what you would find in real-life industrial settings. By using such advanced testing devices, we can ensure that AMs are not just theoretically sound but also practically viable in a variety of real-world applications.

A. Reverberation Chamber

The reverberation chamber[681], or reverberation room, aims to generate a homogeneous sound field. It is designed so that sound waves can reflect uniformly off the encompassing surfaces, including walls, ceilings, and floors[682]. This construct's primary objective is to facilitate quantifying the absorption coefficient and the reverberation time of various AMs from several angles of incidence of the acoustic waves[485]. For instance, in architectural acoustics, metamaterials are tested to measure the absorbing acoustic capability to limit the echo inside structures. Another significant measure that can be obtained is the diffusion coefficient, which assesses the evenness of sound distribution within an enclosure. This is particularly crucial in designing spaces such as concert halls and recording studios, where a balanced sound field is paramount for an optimal acoustic experience.

B. Impedance Tube

An experimental apparatus commonly used to determine the characteristics and effectiveness of acoustic metamaterials is the Kundt tube equipped with generally two [683], or four microphones [684]. A speaker is placed on one side of the tube. Recently, the three-microphone technique has been gaining popularity due to its advantages in complexity and cost reduction [685].

The two-microphone configuration can extract the acoustic impedance, which is a measure of resistance to sound wave propagation in a medium, and the absorption coefficient, which indicates a percentage of acoustic energy absorbed when the wave hits the acoustic metamaterial sample. Moreover, the reflection coefficient indicates how strong is the impedance mismatch between air and AMs.

The three-microphone method, specifically the three-microphone two-load method, as highlighted in the report "Complement to standard method for measuring normal incidence sound transmission loss with three microphones," offers a significant modification to the ASTM E2611-09 standard. It proposes a setup that involves fewer transfer function measurements and one less microphone, thereby simplifying the experimental procedure and potentially reducing costs. This method has been validated on both symmetrical homogeneous and non-symmetrical non-homogeneous specimens. For symmetrical specimens, the process can be further simplified to a three-microphone one-load method.

The four-microphone setup allows us to estimate mainly the transmission loss and the transmission coefficient. With the transmission loss, we quantify the number of decibels that specific AMs can cut. On the other hand, the transmission coefficient specifies the portion of acoustic energy passing through the generic sample, in a specific frequency interval. The measurements taken with four microphone configurations are generally more time-consuming than the two microphone ones since it is necessary to perform a double set of measurements for each sample to get transmission loss and transmission coefficient.

C. 2D Waveguide

A two-dimensional waveguide [286] is a structure that extends primarily across two planes and consists of an anechoic foam encircling a two-dimensional plate, a wave generator, and one or more microphones. Several values are typically measured in these setups, including transmission and reflection coefficients, which provide information about the amount of incident acoustic waves that are either reflected or transmitted by the metamaterial. Stop bands are also important to consider as they represent frequency ranges where sound propagation is heavily reduced or completely blocked. Other values like sound pressure level and pressure field can give data on sound intensity after interacting with the metamaterial. At the same time, measurements of the phase and amplitude of the acoustic wave can provide insights into the wavefront shaping capabilities of the metamaterial. 2D waveguides are especially important to measure effects related to the bending (Fig. 14) of the wavefront [134], which can happen with different angles, and cloaking effects, where a total or partial lack of reflection of the acoustic waves can be observed.

(Insert Fig. 14 here)

D. Anechoic Chamber

Anechoic chambers[686], or semi-anechoic chambers, are specially designed rooms that minimise sound wave reflection, resulting in an environment with minimal echo and reverberation. These chambers are often used for various acoustic measurements, including those related to acoustic metamaterials. In an anechoic chamber, we can perform several measurements. For instance, we can measure sound pressure and sound intensity[687], and moreover, the transmission loss, as shown in the work of Wang, *et al*[688], and Wu, *et al*[689]. Plus, it can also obtain near and far field measurements of ultrasonic wave beams, generated by AMs[680].
Acoustic metamaterials can revolutionize the way we build anechoic rooms. Normally, these rooms require a lot of space filled with foam wedges to absorb sound. However, metamaterials can do the same job without taking up as much room. They can absorb sound effectively, with an absorption coefficient higher than 0.85 for frequencies above 100 Hz. This makes them a great alternative to traditional methods, as shown in a study by Yang et al. (2023)[690].

VII. POSSIBLE ACTIVE ACOUSTIC METAMATERIALS STRATEGIES

Electroacoustic resonators, comprising a combination of loudspeakers and microphones, are employed for noise reduction in enclosed spaces. Traditionally, these resonators utilise a linear control model, resulting in predictable responses to sound variations. However, recent research indicates the potential to shift to a nonlinear control approach by employing a model-inversion technique. This technique adjusts the loudspeaker's electrical current based on sound pressure measurements, allowing for a more dynamic response[691]. A state-space representation model and a control algorithm to achieve a Duffing-like nonlinear response, which has proven to be particularly effective at noise reduction[167]. The findings suggest that this advanced nonlinear control technique could lead to more efficient noise reduction devices with broader applications across various domains, including buildings, vehicles, and industrial environments.

Moreover, it is possible to create new cutting-edge acoustic devices such as high-performance lenses, cloaks, and absorbers. These innovations adopt designs from electromagnetic metamaterials, but with the added benefit of the slower propagation speed of acoustic waves, enabling more precise control and enhanced stability [186]. For example, the dynamic tunability of AMs makes them ideal for applications like unidirectional sound transmission and acoustic diodes, thanks to their mechanical robustness and the ability to adjust properties electronically [144]. Moreover, the capability to change the properties of these materials on the fly, without altering their physical structure, allows for versatile functions such as sharper imaging through nonlinear harmonic responses [176].

The potential applications of these materials are extensive. They include sound insulation, acoustic cloaking, wavefront engineering, and noise reduction across various fields like underwater acoustics, medical ultrasound, and architectural acoustics [166]. Despite the progress, practical challenges such as achieving real-time control and maintaining stability across a wide frequency range persist. Nevertheless, research has shown that active acoustic metamaterial cells, which can be controlled in real-time, offer significant advantages over their passive counterparts, setting the stage for next-generation acoustic devices [692].

Additionally, the development of non-reciprocal acoustic metamaterials using nonlinear electronic circuits offers a compact and efficient solution for applications that require unidirectional sound propagation. This includes noise mitigation in aircraft fuselages and underwater vehicles, where controlling the direction of sound is crucial [143]. Experimental prototypes and theoretical models continue to validate these designs' robustness and efficiency, suggesting a promising future for active control strategies in advanced acoustic applications [693].

Recent advancements in acoustics have underscored the potential of innovative plasma-based technologies for sound control, as evidenced by two pivotal studies. The first study, titled "Ultrabroadband sound control with deep-subwavelength plasmacoustic metalayers", explores the utilization of plasmacoustic metalayers for comprehensive sound control across a wide frequency range[694]. These metalayers, consisting of small layers of air plasma, achieve perfect sound absorption and tunable acoustic reflection from several Hz to the kHz range. This approach effectively overcomes the limitations of traditional noise absorption techniques, such as porous materials and acoustic resonators, which typically underperform below 1 kHz and are inherently narrowband. The technology offers promising applications in noise control, audio engineering, room acoustics, imaging, and metamaterial design.

Complementing this, a second study introduces the creation of a plasma electroacoustic actuator bu using corona discharge to generate sound[695]. This actuator provides a compact and efficient solution for active noise control. The design features two metallic electrodes separated by an air gap, with one electrode comprising thin wires and the other a coarse grid. Upon the application of high voltage, the system produces positive ions that interact with air particles, functioning as a dipolar acoustic source with minimal inertia. The theoretical and experimental analysis demonstrates the actuator's capability to significantly reduce noise across a wide frequency spectrum. Together, these studies underscore the transformative potential of plasma-based technologies in advancing sound control methodologies

Integrating active control mechanisms in acoustic metamaterials marks a significant advancement in terms of acoustic engineering. By overcoming the limitations of passive designs, these tunable metamaterials provide a versatile and effective means to manipulate acoustic waves, potentially transforming various acoustic technologies and applications [696]. However, further research is necessary to address current challenges and fully harness these innovative materials' potential for practical use [697].

A. Challenges

Active acoustic metamaterials offer enhanced control and tunability over passive counterparts but present significant disadvantages that must be considered for specific applications. The primary drawbacks include increased complexity and cost due to the integration of external control mechanisms, sensors, actuators, and power supplies[698]. These elements lead to higher production and maintenance expenses and increased energy consumption, necessitating a continuous power supply, which can be problematic in power-constrained environments. Additionally, these materials face issues with battery life, reliability, and stability under varying conditions, as well as susceptibility to wear and tear, demanding regular maintenance[399]. The complexity of control systems, involving sophisticated algorithms and real-time processing, adds further challenges, including potential latency and response time delays. The risk of malfunction due to numerous electronic and mechanical components, along with environmental constraints and electromagnetic interference, further limits their applicability. Finally, the design and fabrication of active elements require advanced techniques, posing additional hurdles. These factors collectively present substantial challenges that need careful consideration against the benefits of active acoustic metamaterials for their intended applications. However, it is essential to recognize the significant advantages that active acoustic metamaterials bring to the table. Unlike passive systems, they can achieve low-frequency absorption in limited spaces and offer real-time tunability. This adaptive capability means they can adjust to changing conditions, which passive systems simply can't match. Yes, they are more complex and expensive, which explains why they aren't widespread, but in some specialized cases, they can be game-changers.

Another important issue to address is their frequency range performance. Active acoustic metamaterials typically perform well only over a limited frequency range, especially at low frequencies. When they do manage to cover low frequencies, it's often at the cost of a very narrow bandwidth due to resonance or requiring a lot of space. This is a significant limitation that needs to be discussed more prominently.

It's also worth noting that the benefits of active control aren't limited to piezoelectric materials. Electroactive transducers, like loudspeakers, can achieve similar effects. In practical applications, energy from the system is often dissipated into an electric circuit to optimize target impedance, similar to what is done with distributed cells. This highlights the versatility and potential of active acoustic metamaterials beyond just piezoelectric systems.

B. Technological Approaches for Active and Tunable Acoustic Metamaterials

Active acoustic metamaterials mark a substantial improvement over their passive counterparts, offering dynamic capabilities for sound control, including noise suppression, adaptable acoustic devices, and on-the-fly sound adjustment. These materials incorporate active elements to respond to environmental variations, improving their functionality in fields such as medical technology and the automotive sector[699,700].
Modern design strategies emphasise the integration of microactuators and piezoelectric components to instantly modify acoustic properties[212,700]. Advanced materials such as shape memory alloys and magnetorheological materials further enhance adjustability through external stimuli[155,212]. Additive manufacturing methods, especially multimaterial 3D printing, enable the construction of intricate designs that were previously unattainable by conventional approaches[400,700].
In engineering contexts, active metamaterials surpass passive solutions in soundproofing and adaptive noise barriers by actively tuning acoustic properties for optimal performance[157,177]. However, issues such as energy consumption and the complexity of embedding active components persist[212,700]. Future advancements might use machine learning tools to refine design settings for greater adaptability[155,700].
Traditional electromechanical devices, including loudspeakers, play a key role in active acoustic metamaterials by efficiently transforming electrical inputs into mechanical vibrations, allowing precise control of sound waves for applications such as noise reduction and adaptive acoustic

environments[701]. Cutting-edge innovations in lightweight designs, such as membrane-based loudspeakers, leverage thin membranes to reduce weight and size, improving portability[276]. Furthermore, plasma-based acoustic sources provide ultralight and efficient options that could revolutionise optimised active metamaterial configurations[702]. Incorporating multiple distributed sensors and actuators poses considerable challenges in managing signal processing. The handling of associated data requires rapid and adaptive algorithms capable of real-time adjustments to fluctuating environmental conditions[703,704]. Using sophisticated signal processing methods, particularly those enhanced by machine learning, can greatly enhance computational performance and flexibility, critical for the advancement of active and tunable acoustic metamaterials[150].

VIII. ISSUES

Passive acoustic metamaterials are an emerging field that promises to revolutionise acoustics and noise control technologies. However, several complex challenges in this exciting and dynamic field of study should be addressed to enable the real-world implementation of AMs. These challenges span multiple domains, ranging from design constraints to manufacturing complications and inherent physical limitations. A significant concern in the domain of acoustic metamaterials is the broadband behaviour and tunability issue. Most AMs are designed to operate efficiently within a targeted frequency range, which essentially limits their application in scenarios requiring broadband noise reduction from the low to the high-frequency range. Moreover, some applications require acoustic tailorability, like in the case of biomedical applications where ultrasonic beam precision is fundamental. Thus, designing acoustic metamaterials with adaptable tunability and broadband behaviour may require both theoretical advances and innovative material design.

The potential for energy harvesting in acoustic metamaterials is a tantalising prospect but poses unique challenges. The amount of energy that can be harvested from sound waves is relatively small compared to the amount of sonic energy hitting a generic piezoelectric metamaterial. This requires the development of metamaterials with the ability to harvest a higher amount of energy efficiently, exploiting, for instance, resonance phenomena. Currently, the integration of AMs, with piezoelectric patches is a good starting point, exhibiting promising performances for the future in terms of acoustic energy exploitation.

The directionality problem also poses a significant obstacle in developing acoustic metamaterials. Unlike electromagnetic waves, sound waves spread out in all directions when they encounter a medium. This omnidirectional characteristic of sound poses challenges in designing metamaterials that can precisely guide sound propagation in a specific direction. The need for directionality is imperative in many applications, such as medical imaging and acoustic antennas.

Another challenge faced is the lack of ready-to-use design equations for acoustic metamaterials, which allow engineers to design and use this relatively new technology more efficiently. Furthermore, the manufacturing difficulties and associated costs also pose substantial challenges in developing acoustic metamaterials. These materials often involve the use of unconventional materials and intricate geometric designs that are not easy to produce using standard techniques. Furthermore, the processes involved are often time-consuming and resource-intensive, making the production of AMs potentially too expensive. High production costs and manufacturing complications may limit the widespread adoption of these materials unless new and more effective solutions are found to streamline production on an industrial scale.

Multifunctionality, or lack thereof, is another pressing issue in acoustic metamaterials. While these materials demonstrate remarkable properties such as a negative refractive index or super absorption, their single-function nature may limit their applicability. There is a potential growing demand for metamaterials with multiple functionalities, such as simultaneous sound absorption and energy harvesting or sound absorption with airflow and/or heat resistance. The challenge lies in the design of such multifunctional materials, which must strike a balance between competing design requirements and material properties.

Finally, the thickness of acoustic metamaterials also constitutes a significant impediment to their applicability. The thickness of these materials often needs to be proportional to the wavelength of sound for effective operation, which results in a bulky apparatus for low-frequency sound waves. These size constraints may limit the use of acoustic metamaterials in space-sensitive applications. However, the attempt to miniaturise acoustic metamaterials is complex, requiring a careful balance between reducing size and maintaining performance. It involves theoretical considerations and experimental campaigns. These structures can significantly reduce the thickness of the material while maintaining its ability to control sound propagation. Fig. 15, accompanied by Table IV, which provides explanatory details, and Table V, showcase a variety of representative works published on the subject of layer or metamaterial thickness. In Fig. 15, on the y-axis, a series of coefficients C, when multiplied by the wavelength, determine the necessary thickness of the AM for the geometry used. In Table V, we have the AMs layer thickness, independent from the wavelength, as in Fig. 15. Here, the thickness layer is displayed directly in millimetres (Table V). Interestingly, it is worth noting that the five examples involving the use of fractal geometries ([1,453,548,577,582]), which are discussed in the context of acoustic performance, require a comparatively thinner metamaterial layer compared to the other ones. The other internal geometries reported include the coiled, helicoidal, maze, and honeycomb configurations. Among these, fractal geometry appears to be one of the most effective solutions for the internal structure of the metamaterial layer. However, searching

for multifunctional acoustic metamaterials inspires and challenges interdisciplinary collaborations, combining acoustics, materials science and engineering. Because of that, multidisciplinary knowledge is needed to address multiphysics challenges.

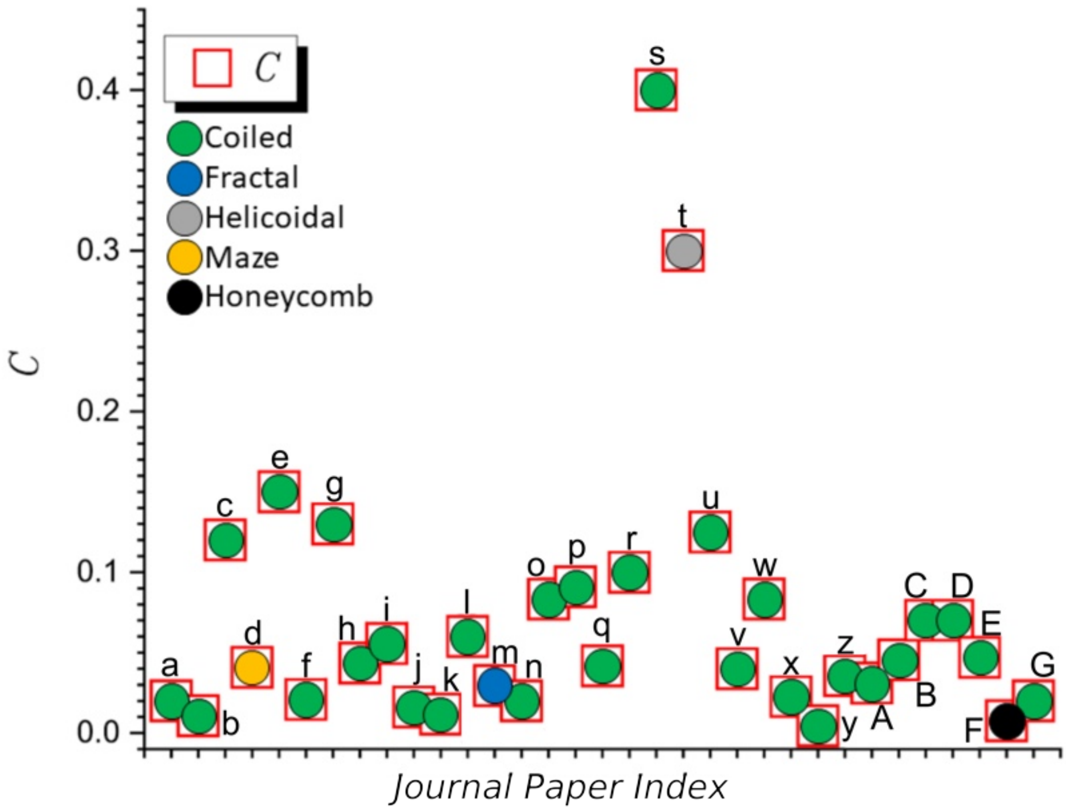

FIG. 15. The coefficient C multiplied by the wavelength λ provides the thickness of acoustic metamaterial types described in open literature (see Table IV for the corresponding research papers). The colored circles indicate the type of internal geometry of the metamaterials. The x-axis represents the journal paper number from which the data were extracted. This arrangement highlights (on the y-axes) the thickness of each metamaterial layer as a function of the frequency of the incident acoustic wave. The figure demonstrates how various internal geometries correlate with different frequencies, affecting the effectiveness of the metamaterial. Table IV lists the corresponding research papers and geometries. G. Comandini, *Hilbert Fractal Acoustic Metamaterials*, University of Bristol, 2024; licensed under a Creative Commons Attribution (CC BY) license[7].

TABLE IV. Table corresponding to Fig. 15. The top row displays the letters representing various thicknesses of the acoustic metamaterial, while the bottom row indicates the research papers identified by the corresponding letters in the top row.

a	b	c	d	e	f	g	h	i	j	k	l	m	n	o	p	q	r	s	t	u	v	w	x	y	z	A	B	C	D	E	F	G
464	463	41	667	482	578	460	475	582	57	473	40	453	471	580	548	489	469	124	55	258	257	576	571	148	451	574	449	448	705	706	707	708

A. Structural Challenges and Hot Topics in Acoustic Metamaterials

Acoustic metamaterials encounter various structural difficulties that influence their multifunctional capabilities, geometric constraints, and fabrication challenges. A primary concern is directional control, where the omnidirectional nature of sound waves complicates their use in domains such as medical imaging and spatial audio systems[709]. Furthermore, these materials are often optimised for specific frequency ranges, limiting their effectiveness in low-frequency applications such as underwater acoustics, as their design typically sacrifices bandwidth to achieve reduced spatial dimensions[211,400,538].
In addition, elaborate structures needed for precise sound manipulation pose significant challenges for manufacturing and scalability. The reliance on advanced fabrication methods, such as additive manufacturing, to achieve the necessary structural accuracy makes production complex and expensive, limiting widespread application[644]. However, advances in multifunctional metamaterials are promising, especially in the integration of sound absorption, energy harvesting, and thermal insulation, which have great potential for use in aerospace and industrial machinery[147,710].

B. Future Directions

Future work in the field of advanced material innovation should emphasise utilising the development of intelligent and adaptive materials capable of adjusting their prop-

erties in real-time to adapt to changing environmental conditions. These materials can utilise machine learning for customisable designs, expanding their use in various domains, including acoustic metamaterials, which benefit from precise production methods such as multi-material 3D printing and nanoscale lithography[163,711]. Furthermore, studying topological and nonreciprocal metamaterials is imperative, as these materials enable reliable sound manipulation and directional wave propagation, critical for use in complex settings[712,713].
Collaboration between disciplines is essential to progress in these areas, merging knowledge from materials science, engineering, and artificial intelligence to improve material capabilities and utility[324,714–716]. The promising role of smart materials in cutting-edge applications, such as monitoring of structural integrity and energy-efficient systems, highlights the importance of continued investigation and innovation within this rapidly evolving field[717,718].

IX. CONCLUSIONS

This comprehensive review has summarised various discoveries and insights into acoustic metamaterials, providing an overview of the materials and manufacturing methodologies underpinning this field. Moreover, the smart blending of various geometric configurations in the creation of hybrid metamaterials further illustrates the complexity and potential of this area.

The synthesis of this literature review points out that the performance of acoustic metamaterials is greatly enhanced by employing intricate fractal formations and different geometric configurations. This recognised variety has necessitated a new classification system, complementary to the existing ones, focused on the quantity and variety of channels inherent in the geometry of metamaterials. Further exploration of combining various geometric configurations to synthesise more intricate or hybrid acoustic metamaterials revealed interesting design intersections, such as combining geometries with and without acoustic apparatuses, such as acoustic foams or resonators. Furthermore, this study also describes the materials and machines used in manufacturing, underlining achievable precision and applications.

The principal test rigs and testing rooms used in research with the relative measurable quantities to get their characterisation and performance evaluation are outlined for the acoustic measurements.

However, acoustic metamaterials present many opportunities but are not without challenges. This review identified complexities that may hinder their successful application, including their broadband behaviour, tuneability, and directionality for the wave entering and leaving the metamaterial cell, plus energy harvesting efficiency and multi-functionality. A critical challenge is that acoustic metamaterials often exhibit effects in a relatively narrow bandwidth spectrum, which poses difficulties in fine-tuning or translating the same wanted metamaterial effects to other frequencies. Furthermore, the directionality angle of an acoustic wave entering the metamaterial cell can significantly alter the effectiveness of the AMs.

TABLE V. Thickness in mm of the acoustic metamaterial layers, independent from λ.

Thickness	72	50	36	40	30	20	60	113	13	43.5	28	80	80
Reference #	579	198	574	234	217	577	259	256	1	575	573	253	719

Achieving accuracy in directing the acoustic wavefront at a predetermined angle can also be problematic. Furthermore, the thickness of the metamaterial layer can have a significant impact on phenomena such as sound attenuation, particularly within thin metamaterial layers. This effect arises from the direct correlation between the volume occupied by the metamaterial and the frequency spectra that are affected. Although this challenge might be addressed with the use of active acoustic metamaterials, precise tuning remains critical for broadband performance.

Another challenge lies in the limited energy harvesting of acoustic metamaterials, even when resonance phenomena are strategically employed to enhance the collected vibrations. A further consideration is a move towards multifunctionality in AMs, to solve more than one issue within the same metamaterial layer, for instance, vibroacoustic solutions for industrial machinery.

Finally, clarifying the differences between acoustic and elastic metamaterials is essential for advancing research and development in wave manipulation technologies, ensuring that each type is effectively utilized in its specific application domain.

ACKNOWLEDGEMENTS

G.C. acknowledges the support of UK EPSRC through the EPSRC Centre for Doctoral Training in Advanced Composites for Innovation and Science [EP/L016028/1], and Charles P. Macleod for the technical assistance. F.S. and G.C. acknowledge the support of ERC-2020-AdG-NEUROMETA (No. 101020715). M.O. acknowledges the support of EIPHI (ANR-17-EURE-0002). V.T. acknowledges funding from the EPSRC (EP/R01650X/1).

AUTHOR DECLARATIONS

The authors declare no competing interests.

AUTHOR CONTRIBUTIONS

Gianni Comandini: Conceptualization (lead); Data curation (lead); Formal analysis (lead); Investigation (lead); Visualization (lead); Writing - original draft (lead); Review & editing (equal). **Morvan Ouisse**: Review & editing (equal); Supervision (supporting); Conceptualization (supporting). **Valeska P. Ting**: Review & editing (equal); Supervision (supporting); Conceptualization (supporting). **Fabrizio Scarpa**: Funding acquisition (lead); Review & editing (lead); Conceptualization (equal); Supervision (lead).

DATA AVAILABILITY

Data available on request from the authors

[1]G. Y. Song, Q. Cheng, B. Huang, H. Y. Dong, and T. J. Cui, "Broadband fractal acoustic metamaterials for low-frequency sound attenuation," Applied Physics Letters **109** (2016).
[2]S. Qi, M. Oudich, Y. Li, and B. Assouar, "Acoustic energy harvesting based on a planar acoustic metamaterial," Applied Physics Letters **108** (2016).
[3]H. Gao, Z. Gu, S. Liang, T. Liu, J. Zhu, and Z. Su, "Enhancing ultrasound transmission and focusing through a stiff plate with inversely optimized auxiliary meta-lens," Applied Physics Letters **120**, 111701 (2022).
[4]F. Ma, M. Huang, Y. Xu, and J. H. Wu, "Bi-layer plate-type acoustic metamaterials with willis coupling," Journal of Applied Physics **123**, 035104 (2018).
[5]L. Chisari, L. Bonoldi, and G. Memoli, "Metamaterial solutions for noise management in hospital settings," The Journal of the Acoustical Society of America **148**, 2754–2754 (2020).
[6]J. Dandsena, K. Mohapatra, A. Satapathy, and D. Jena, "Noise control of outdoor unit of split type air-conditioner using periodic scatterers made with array of helmholtz resonators," Applied Acoustics **179**, 108054 (2021).
[7]G. Comandini, *Hilbert Fractal Acoustic Metamaterials*, Ph.D. thesis, University of Bristol (2024).
[8]G. Comandini, C. Khodr, V. Ting, M. Azarpeyvand, and F. Scarpa, "Sound absorption in hilbert fractal and coiled acoustic metamaterials," Applied Physics Letters **120**, 061902 (2022).
[9]A. Alippi, A. Bettucci, F. Craciun, F. Farrelly, E. Molinari, and A. Petri, "Acoustic modes in 2-dimensional self-similar composite plates," in *1993 Proceedings IEEE Ultrasonics Symposium* (IEEE, 1993) pp. 533–536.
[10]G. Comandini, M. Ouisse, V. P. Ting, and F. Scarpa, "Acoustic transmission loss in hilbert fractal metamaterials," Scientific Reports **13**, 19058 (2023).
[11]X.-J. Liu and Y.-H. Fan, "Band structure characteristics of t-square fractal phononic crystals," Chinese Physics B **22**, 036101 (2013).
[12]X. Man, Z. Luo, J. Liu, and B. Xia, "Hilbert fractal acoustic metamaterials with negative mass density and bulk modulus on subwavelength scale," Materials & design **180**, 107911 (2019).
[13]B. Kushwaha, K. Dwivedi, R. S. Ambekar, V. Pal, D. P. Jena, D. R. Mahapatra, and C. S. Tiwary, "Mechanical and acoustic behavior of 3d-printed hierarchical mathematical fractal menger sponge," Advanced Engineering Materials **23**, 2001471 (2021).
[14]D. Tarrazó-Serrano, S. Castiñeira-Ibáñez, P. Candelas, J. M. Fuster, and C. Rubio, "Numerical simulation and laboratory measurements on the influence of fractal dimension on the acoustic beam modulation of a polyadic cantor fractal lenses," Applied Acoustics **148**, 119–122 (2019).
[15]S. Castiñeira-Ibáñez, V. Romero-García, J. V. Sánchez-Pérez, and L. Garcia-Raffi, "Overlapping of acoustic bandgaps using fractal geometries," Europhysics Letters **92**, 24007 (2010).
[16]S. Castiñeira-Ibáñez, C. Rubio, J. Redondo, and J. V. Sánchez-Pérez, "Quantitative characterization of bandgap properties of sets of isolated acoustic scatterers arranged using fractal geometries," Applied Physics Express **7**, 042201 (2014).
[17]T. Kawabe, T. Miyazaki, D. Oka, S. Koyanagi, and A. Hinokidani, "Sound absorption by menger sponge fractal," The Journal of the Acoustical Society of America **125**, 2830–2833 (2009).
[18]X. Man, T. Liu, B. Xia, Z. Luo, L. Xie, and J. Liu, "Space-coiling fractal metamaterial with multi-bandgaps on subwavelength scale," Journal of Sound and Vibration **423**, 322–339 (2018).
[19]Z. Qian, "Wave scattering on a fractal surface," The Journal of the Acoustical Society of America **107**, 260–262 (2000).
[20]B. B. Mandelbrot and B. B. Mandelbrot, *The fractal geometry of nature*, Vol. 1 (WH freeman New York, 1982).
[21]Y. Xie, A. Konneker, B.-I. Popa, and S. A. Cummer, "Tapered labyrinthine acoustic metamaterials for broadband impedance matching," Applied Physics Letters **103**, 201906 (2013).
[22]Y. Liu, W. Xu, M. Chen, D. Pei, T. Yang, H. Jiang, and Y. Wang, "Menger fractal structure with negative refraction and sound tunnelling properties," Materials Research Express **6**, 116211 (2019).
[23]G. Ma, M. Yang, S. Xiao, Z. Yang, and P. Sheng, "Acoustic metasurface with hybrid resonances," Nature materials **13**, 873–878 (2014).
[24]N. Aközbek, N. Mattiucci, M. Bloemer, M. Sanghadasa, and G. D'Aguanno, "Manipulating the extraordinary acoustic transmission through metamaterial-based acoustic band gap structures," Applied Physics Letters **104**, 161906 (2014).
[25]Y. Lei, J. H. Wu, Z. Huang, L. Wang, and Y. Huang, "Broadband directional resonant tunneling emission enhancement via acoustic anisotropic metamaterials," Applied Acoustics **200**, 109050 (2022).
[26]X. Yu, Z. Lu, T. Liu, L. Cheng, J. Zhu, and F. Cui, "Sound transmission through a periodic acoustic metamaterial grating," Journal of Sound and Vibration **449**, 140–156 (2019).
[27]Y. Li, B. Liang, X. Tao, X.-f. Zhu, X.-y. Zou, and J.-c. Cheng, "Acoustic focusing by coiling up space," Applied Physics Letters **101**, 233508 (2012).
[28]W. Li, F. Meng, and X. Huang, "Coding metalens with helical-structured units for acoustic focusing and splitting," Applied Physics Letters **117**, 021901 (2020).
[29]G. Liao, Z. Wang, C. Luan, J. Liu, X. Yao, and J. Fu, "Broadband controllable acoustic focusing and asymmetric focusing by acoustic metamaterials," Smart Materials and Structures **30**, 045021 (2021).
[30]W. Wang, Y. Xie, A. Konneker, B.-I. Popa, and S. A. Cummer, "Design and demonstration of broadband thin planar diffractive acoustic lenses," Applied Physics Letters **105**, 101904 (2014).
[31]J. Prat-Camps, G. Christopoulos, J. Hardwick, and S. Subramanian, "A manually reconfigurable reflective spatial sound modulator for ultrasonic waves in air," Advanced Materials Technologies **5**, 2000041 (2020).
[32]Y. Lei, J. H. Wu, L. Wang, Y. Huang, S. Yang, and J. Niu, "Acoustic emission enhancement and self-centering effect via an extreme anisotropic metamaterial," Applied Physics Express **16**, 057002 (2023).
[33]L. Xiang, L. Jian, and H. Xinjing, "Acoustic magnifying lens based on compact non-dispersive spiral metamaterial array," in *Quantitative Nondestructive Evaluation*, Vol. 85529 (American Society of Mechanical Engineers, 2021) p. V001T11A010.
[34]R. Ghaffarivardavagh, J. Nikolajczyk, S. Anderson, and X. Zhang, "Ultra-open acoustic metamaterial silencer based on fano-like interference," Physical Review B **99**, 024302 (2019).
[35]A. Melnikov, M. Maeder, N. Friedrich, Y. Pozhanka, A. Wollmann, M. Scheffler, S. Oberst, D. Powell, and S. Marburg, "Acoustic metamaterial capsule for reduction of stage machinery noise," The Journal of the Acoustical Society of America **147**, 1491–1503 (2020).
[36]J. Chen, Y. Zhang, Y. Yu, Y. Zhai, H. Nguyen, S. Tracy, X. Zhou, and G. Huang, "Broadband acoustic attenuation in microperforated meta-shells with ventilation," Applied Physics Letters **122** (2023).
[37]S.-H. Kim and S.-H. Lee, "Air transparent soundproof window," AIP Advances **4**, 117123 (2014).
[38]C. Yang, T. Zhong, J. Li, S. You, S. Yang, H. Zhang, and Z. Zheng, "Extended tube acoustic metamaterial: Its modeling and application to a kitchen hood," Applied Acoustics **185**, 108398 (2022).
[39]S. Kumar, T. B. Xiang, and H. P. Lee, "Ventilated acoustic metamaterial window panels for simultaneous noise shielding and air circulation," Applied Acoustics **159**, 107088 (2020).
[40]X. Li, H. Zhang, H. Tian, Y. Huang, and L. Wang, "Frequency-tunable sound insulation via a reconfigurable and ventilated acoustic metamaterial," Journal of Physics D: Applied Physics **55**, 495108 (2022).
[41]J. He, Z. Zhou, C. Zhang, Y. Zheng, Y. Li, Y. Li, X. Jiang, and D. Ta, "Ultrasparse and omnidirectional acoustic ventilated meta-barrier," Applied Physics Letters **120** (2022).
[42]J. Du, Y. Luo, X. Zhao, X. Sun, Y. Song, and X. Hu, "Bilayer ventilated labyrinthine metasurfaces with high sound absorption and tunable bandwidth," Scientific Reports **11**, 5829 (2021).
[43]H. Nguyen, Q. Wu, X. Xu, H. Chen, S. Tracy, and G. Huang, "Broadband acoustic silencer with ventilation based on slit-type helmholtz resonators," Applied Physics Letters **117**, 134103 (2020).
[44]Y.-x. Gao, Z.-w. Li, B. Liang, J. Yang, and J.-c. Cheng, "Improving sound absorption via coupling modulation of resonance energy leakage and loss in ventilated metamaterials," Applied Physics Letters **120**, 261701 (2022).
[45]K. Li, B. Liang, J. Yang, J. Yang, and J.-c. Cheng, "Broadband transmission-type coding metamaterial for wavefront manipulation for airborne sound," Applied Physics Express **11**, 077301 (2018).

[46]W. Zhang, X. Liu, and F. Xin, "Normal incidence sound absorption of an acoustic labyrinthine metal-fibers-based porous metamaterial at high temperature," International Journal of Mechanical Sciences **237**, 107821 (2023).

[47]S. Ning, Z. Yan, D. Chu, H. Jiang, Z. Liu, and Z. Zhuang, "Ultralow-frequency tunable acoustic metamaterials through tuning gauge pressure and gas temperature," Extreme Mechanics Letters **44**, 101218 (2021).

[48]B. Xia, N. Chen, L. Xie, Y. Qin, and D. Yu, "Temperature-controlled tunable acoustic metamaterial with active band gap and negative bulk modulus," Applied Acoustics **112**, 1–9 (2016).

[49]Z. Li, Z. Wang, Z. Guo, X. Wang, and X. Liang, "Ultra-broadband sound absorption of a hierarchical acoustic metamaterial at high temperatures," Applied Physics Letters **118**, 161903 (2021).

[50]D.-Y. Kim and J.-G. Ih, "Wideband reduction of in-duct noise using acoustic metamaterial with serially connected resonators made with mpp and cavities," Applied Physics Letters **116**, 251904 (2020).

[51]Z. Zhang, M. Abom, H. Boden, M. Karlsson, and D. Katoshevski, "Particle number reduction in automotive exhausts using acoustic metamaterials," SAE International Journal of Engines **10**, 1566–1572 (2017).

[52]Y. A. Knysh and G. Xanthopoulou, "New metamaterials with combined subnano-and mesoscale topology for high-efficiency catalytic combustion chambers of innovative gas turbine engines," in *IOP Conference Series: Materials Science and Engineering*, Vol. 302 (IOP Publishing, 2018) p. 012071.

[53]M. Kheybari and S. Ebrahimi-Nejad, "Locally resonant stop band acoustic metamaterial muffler with tuned resonance frequency range," Materials Research Express **6**, 025802 (2018).

[54]Y. Song, J. Wen, H. Tian, X. Lu, Z. Li, and L. Feng, "Vibration and sound properties of metamaterial sandwich panels with periodically attached resonators: Simulation and experiment study," Journal of Sound and Vibration **489**, 115644 (2020).

[55]Y. Tang, B. Liang, and S. Lin, "Broadband ventilated meta-barrier based on the synergy of mode superposition and consecutive fano resonances," The Journal of the Acoustical Society of America **152**, 2412–2418 (2022).

[56]S. Kumar, C. W. Shan, J. W. Aow, and H. P. Lee, "Mitigating the toilet flush noise: A psychometric analysis of noise assessment and design of labyrinthine acoustic meta-absorber for noise mitigation," The Journal of the Acoustical Society of America **150**, 3747–3762 (2021).

[57]M. Boccaccio, G. P. M. Fierro, F. Bucciarelli, and M. Meo, "Multi-tonal subwavelength metamaterial for absorption and amplification of acoustic and ultrasonic waves," Engineering Research Express **3**, 025024 (2021).

[58]R. Ghaffarivardavagh, J. Nikolajczyk, R. Glynn Holt, S. Anderson, and X. Zhang, "Horn-like space-coiling metamaterials toward simultaneous phase and amplitude modulation," Nature communications **9**, 1349 (2018).

[59]Y. Ohara, T. Oshiumi, H. Nakajima, K. Yamanaka, X. Wu, T. Uchimoto, T. Takagi, T. Tsuji, and T. Mihara, "Ultrasonic phased array with surface acoustic wave for imaging cracks," AIP Advances **7**, 065214 (2017).

[60]C. Shen, Y. Xie, N. Sui, W. Wang, S. A. Cummer, and Y. Jing, "Broadband acoustic hyperbolic metamaterial," Physical review letters **115**, 254301 (2015).

[61]C. Lu, R. Yu, Q. Ma, K. Wang, J. Wang, and D. Wu, "Grin metamaterial generalized luneburg lens for ultra-long acoustic jet," Applied Physics Letters **118**, 144103 (2021).

[62]H. Zou, Z. Xu, Y. Hu, Q. Du, and P. Peng, "Reflected continuously tunable acoustic metasurface with rotatable space coiling-up structure," Physics Letters A **426**, 127891 (2022).

[63]C. Zhou, B. Yuan, Y. Cheng, and X. Liu, "Precise rainbow trapping for low-frequency acoustic waves with micro mie resonance-based structures," Applied Physics Letters **108**, 063501 (2016).

[64]A. Kumar and W. Arnold, "High resolution in non-destructive testing: A review," Journal of Applied Physics **132**, 100901 (2022).

[65]Z. Zhang, Q. Li, M. Oudich, Y. Pan, and Y. Li, "Experimental demonstration of enhanced acoustic energy harvesting with a subwavelength metamaterial plate," New Journal of Physics **22**, 123019 (2020).

[66]M. Yuan, Z. Cao, J. Luo, and Z. Pang, "Helix structure for low frequency acoustic energy harvesting," Review of Scientific Instruments **89**, 055002 (2018).

[67]K. Ma, T. Tan, Z. Yan, F. Liu, W.-H. Liao, and W. Zhang, "Metamaterial and helmholtz coupled resonator for high-density acoustic energy harvesting," Nano Energy **82**, 105693 (2021).

[68]K. H. Sun, J. E. Kim, J. Kim, and K. Song, "Sound energy harvesting using a doubly coiled-up acoustic metamaterial cavity," Smart Materials and Structures **26**, 075011 (2017).

[69]F.-H. Bao, X.-Q. Wu, X. Zhou, Q.-D. Wu, X.-S. Zhang, and J.-F. Bao, "Spider web-like phononic crystals for piezoelectric mems resonators to reduce acoustic energy dissipation," Micromachines **10**, 626 (2019).

[70]S. Bansal, C. Choi, J. Hardwick, B. Bagchi, M. K. Tiwari, and S. Subramanian, "Transmissive labyrinthine acoustic metamaterial-based holography for extraordinary energy harvesting," Advanced Engineering Materials **25**, 2201117 (2023).

[71]M. Rupin, G. Lerosey, J. de Rosny, and F. Lemoult, "Mimicking the cochlea with an active acoustic metamaterial," New Journal of Physics **21**, 093012 (2019).

[72]F. Ma, J. H. Wu, M. Huang, G. Fu, and C. Bai, "Cochlear bionic acoustic metamaterials," Applied Physics Letters **105**, 213702 (2014).

[73]X. Ni, Y. Wu, Z.-G. Chen, L.-Y. Zheng, Y.-L. Xu, P. Nayar, X.-P. Liu, M.-H. Lu, and Y.-F. Chen, "Acoustic rainbow trapping by coiling up space," Scientific reports **4**, 7038 (2014).

[74]H. Tang, S. Zhang, Y. Tian, T. Kang, C. Zhou, S. Yang, Y. Liu, X. Liu, Q. Chen, H. Xiao, *et al.*, "Bioinspired soft elastic metamaterials for reconstruction of natural hearing," Advanced Science , 2207273 (2023).

[75]L. Zhao and S. Zhou, "Compact acoustic rainbow trapping in a bioinspired spiral array of graded locally resonant metamaterials," Sensors **19**, 788 (2019).

[76]V. F. Dal Poggetto, F. Bosia, D. Urban, P. H. Beoletto, J. Torgersen, N. M. Pugno, and A. S. Gliozzi, "Cochlea-inspired tonotopic resonators," Materials & Design **227**, 111712 (2023).

[77]M. Ghafouri, M. Ghassabi, and R. Talebitooti, "Acoustic sound propagation of a doubly curved shell with 3d re-entrant auxetic cellular metamaterials," Waves in Random and Complex Media , 1–19 (2022).

[78]C. Casarini, J. F. Windmill, and J. C. Jackson, "3d printed small-scale acoustic metamaterials based on helmholtz resonators with tuned overtones," in *2017 IEEE SENSORS* (IEEE, 2017) pp. 1–3.

[79]J. Zhang, Y. Cheng, and X. Liu, "Tunable directional subwavelength acoustic antenna based on mie resonance," Scientific reports **8**, 1–8 (2018).

[80]T. Jiang, Q. He, and Z.-K. Peng, "Proposal for the realization of a single-detector acoustic camera using a space-coiling anisotropic metamaterial," Physical Review Applied **11**, 034013 (2019).

[81]M. Dubois, C. Shi, X. Zhu, Y. Wang, and X. Zhang, "Observation of acoustic dirac-like cone and double zero refractive index," Nature communications **8**, 14871 (2017).

[82]P. Zhang, T. Li, J. Zhu, X. Zhu, S. Yang, Y. Wang, X. Yin, and X. Zhang, "Generation of acoustic self-bending and bottle beams by phase engineering," Nature communications **5**, 4316 (2014).

[83]J. Li, L. Fok, X. Yin, G. Bartal, and X. Zhang, "Experimental demonstration of an acoustic magnifying hyperlens," Nature materials **8**, 931–934 (2009).

[84]J. Christensen and F. J. G. de Abajo, "Anisotropic metamaterials for full control of acoustic waves," Physical review letters **108**, 124301 (2012).

[85]X. Jia, M. Hong, and M. Yan, "Inclined space-coiling metamaterials for highly efficient sound energy transmission at various incident angles," Journal of Applied Physics **127**, 194901 (2020).

[86]T. Zhang, E. Bok, M. Tomoda, O. Matsuda, J. Guo, X. Liu, and O. B. Wright, "Compact acoustic metamaterial based on the 3d mie resonance of a maze ball with an octahedral structure," Applied Physics Letters **120**, 161701 (2022).

[87]C. Ma, S. Gao, Y. Cheng, and X. Liu, "Acoustic metamaterial antennas for combined highly directive-sensitive detection," Applied Physics Letters **115**, 053501 (2019).

[88]Y. Zhao, H. Y. Dong, S. Zhao, S. Min, J. Cheng, B. Li, F. Chi, and S. Liu, "Design of broadband impedance-matching bessel lens with acoustic metamaterials," Journal of Applied Physics **126**, 065103 (2019).

[89]A. Liu, X. Zhou, G. Huang, and G. Hu, "Super-resolution imaging by resonant tunneling in anisotropic acoustic metamaterials," The Journal of the Acoustical Society of America **132**, 2800–2806 (2012).

[90]Y.-F. Zhu, X.-Y. Zou, B. Liang, and J.-C. Cheng, "Acoustic one-way open tunnel by using metasurface," Applied Physics Letters **107** (2015).

[91]C. Shi, M. Dubois, Y. Wang, and X. Zhang, "High-speed acoustic communication by multiplexing orbital angular momentum," Proceedings of the National Academy of Sciences **114**, 7250–7253 (2017).

[92] A. Weissler, H. W. Cooper, and S. Snyder, "Chemical effect of ultrasonic waves: oxidation of potassium iodide solution by carbon tetrachloride," Journal of the American Chemical society **72**, 1769–1775 (1950).

[93] M. Doosti, R. Kargar, and M. Sayadi, "Water treatment using ultrasonic assistance: A review," Proceedings of the international academy of ecology and environmental sciences **2**, 96 (2012).

[94] J. W. Kim, H. J. Kong, Y. H. Kim, and K. I. Kang, "A pattern of cell death induced by 40 khz ultrasound in yeast cell model," The Journal of the Acoustical Society of Korea **36**, 172–178 (2017).

[95] M. Park, J. Lee, J.-R. Lee, Y. Cho, and Y. H. Kim, "Optimize ultrasound condition for water treatment by coiled-up space metamaterial," in *Proceedings of Meetings on Acoustics ICU*, Vol. 38 (Acoustical Society of America, 2019) p. 045010.

[96] H.-T. Zhou, S.-W. Fan, X.-S. Li, W.-X. Fu, Y.-F. Wang, and Y.-S. Wang, "Tunable arc-shaped acoustic metasurface carpet cloak," Smart Materials and Structures **29**, 065016 (2020).

[97] H. Esfahlani, S. Karkar, H. Lissek, and J. R. Mosig, "Acoustic carpet cloak based on an ultrathin metasurface," Physical Review B **94**, 014302 (2016).

[98] Y. Yang, H. Wang, F. Yu, Z. Xu, and H. Chen, "A metasurface carpet cloak for electromagnetic, acoustic and water waves," Scientific reports **6**, 20219 (2016).

[99] S. Zhai, H. Chen, C. Ding, L. Li, F. Shen, C. Luo, and X. Zhao, "Ultrathin skin cloaks with metasurfaces for audible sound," Journal of Physics D: Applied Physics **49**, 225302 (2016).

[100] R. Yang, X. Zhang, and G. Wang, "A hybrid acoustic cloaking based on binary splitting metasurfaces and near-zero-index metamaterials," Applied Physics Letters **120**, 021603 (2022).

[101] G. Wu, Y. Ke, L. Zhang, and M. Tao, "Acoustic manipulation of fractal metamaterials with negative properties and near-zero densities," Applied Physics Express **15**, 014002 (2021).

[102] H. Chen and C. T. Chan, "Acoustic cloaking in three dimensions using acoustic metamaterials," Applied physics letters **91**, 183518 (2007).

[103] W. Zhao, H. Chu, Z. Tao, and Z. H. Hang, "Acoustic transmissive cloaking using zero-index materials and metasurfaces," Applied Physics Express **12**, 054004 (2019).

[104] C. Liu, B. Xia, and D. Yu, "The spiral-labyrinthine acoustic metamaterial by coiling up space," Physics Letters A **381**, 3112–3118 (2017).

[105] B.-I. Popa, L. Zigoneanu, and S. A. Cummer, "Experimental acoustic ground cloak in air," Physical review letters **106**, 253901 (2011).

[106] L. Xiang, G. Wang, and C. Zhu, "Controlling sound transmission by space-coiling fractal acoustic metamaterials with broadband on the subwavelength scale," Applied Acoustics **188**, 108585 (2022).

[107] M. Zaremanesh and A. Bahrami, "Multilayer acoustic invisibility cloak based on composite lattice," Scientific Reports **12**, 16096 (2022).

[108] J. Jing Yang, M. Huang, G. Hui Cai, R. Sheng Xie, and J. Yang, "Design of acoustic metamaterial devices based on inverse method," Journal of Vibration and Acoustics **135** (2013).

[109] A. Silva, F. Monticone, G. Castaldi, V. Galdi, A. Alù, and N. Engheta, "Performing mathematical operations with metamaterials," Science **343**, 160–163 (2014).

[110] T. Zhang, Y. Cheng, B.-G. Yuan, J.-Z. Guo, and X.-J. Liu, "Compact transformable acoustic logic gates for broadband complex boolean operations based on density-near-zero metamaterials," Applied Physics Letters **108**, 183508 (2016).

[111] S.-Y. Zuo, Q. Wei, Y. Cheng, and X.-J. Liu, "Mathematical operations for acoustic signals based on layered labyrinthine metasurfaces," Applied Physics Letters **110**, 011904 (2017).

[112] S. Zuo, Q. Wei, Y. Tian, Y. Cheng, and X. Liu, "Acoustic analog computing system based on labyrinthine metasurfaces," Scientific reports **8**, 10103 (2018).

[113] S. Polychronopoulos and G. Memoli, "Acoustic levitation with optimized reflective metamaterials," Scientific reports **10**, 4254 (2020).

[114] Z. Xu, L. Qin, W. Xu, S. Fang, and J. Wang, "Design approach of perforated labyrinth-based acoustic metasurface for selective acoustic levitation manipulation," Scientific Reports **11**, 7619 (2021).

[115] G. Memoli, M. Caleap, M. Asakawa, D. R. Sahoo, B. W. Drinkwater, and S. Subramanian, "Metamaterial bricks and quantization of meta-surfaces," Nature communications **8**, 14608 (2017).

[116] M. A. Norasikin, D. Martinez Plasencia, S. Polychronopoulos, G. Memoli, Y. Tokuda, and S. Subramanian, "Soundbender: dynamic acoustic control behind obstacles," in *proceedings of the 31st annual ACM symposium on user interface software and technology* (2018) pp. 247–259.

[117] M. A. Andrade, A. L. Bernassau, and J. C. Adamowski, "Acoustic levitation of a large solid sphere," Applied Physics Letters **109** (2016).

[118] W. Xie, C. Cao, Y. Lü, Z. Hong, and B. Wei, "Acoustic method for levitation of small living animals," Applied Physics Letters **89**, 214102 (2006).

[119] A. Marzo, S. A. Seah, B. W. Drinkwater, D. R. Sahoo, B. Long, and S. Subramanian, "Holographic acoustic elements for manipulation of levitated objects," Nature communications **6**, 8661 (2015).

[120] R. H. Morris, E. R. Dye, P. Docker, and M. I. Newton, "Beyond the langevin horn: Transducer arrays for the acoustic levitation of liquid drops," Physics of Fluids **31** (2019).

[121] P. D'Antonio, J. Madison, and T. J. Cox, "Review of the perception of diffusive surfaces in architectural spaces," The Journal of the Acoustical Society of America **142**, 2499–2499 (2017).

[122] D. Bradley, E. O. Snow, K. A. Riegel, Z. D. Nasipak, and A. S. Terenzi, "Numerical prediction of sound scattering from surfaces with fractal geometry: A preliminary investigation," in *Proceedings of Meetings on Acoustics*, Vol. 12 (Acoustical Society of America, 2011) p. 015010.

[123] C. J. Naify, J. S. Rogers, M. D. Guild, C. A. Rohde, and G. J. Orris, "Evaluation of the resolution of a metamaterial acoustic leaky wave antenna," The Journal of the Acoustical Society of America **139**, 3251–3258 (2016).

[124] C. Ren, "Compact acoustic antenna design using labyrinthine metamaterials," Applied Physics A **119**, 461–465 (2015).

[125] S. Gao, Y. Li, C. Ma, Y. Cheng, and X. Liu, "Emitting long-distance spiral airborne sound using low-profile planar acoustic antenna," Nature Communications **12**, 2006 (2021).

[126] O. Petrella, S. Ameduri, V. Quaranta, G. Betta, and M. Laracca, "An experimental setup for the calibration of acoustic antenna," IEEE Transactions on Instrumentation and Measurement **63**, 1014–1021 (2014).

[127] Y. Chen, H. Liu, M. Reilly, H. Bae, and M. Yu, "Enhanced acoustic sensing through wave compression and pressure amplification in anisotropic metamaterials," Nature communications **5**, 5247 (2014).

[128] T. Chen, D. Yu, B. Wu, and B. Xia, "Weak signals detection by acoustic metamaterials-based sensor," IEEE Sensors Journal **21**, 16815–16825 (2021).

[129] H. Xinjing, Y. Yutian, M. Jinyu, L. Jian, and R. Xiaobo, "An acoustic metamaterial-based sensor capable of multiband filtering and amplification," IEEE Sensors Journal **20**, 4413–4419 (2019).

[130] Y. Xie, T.-H. Tsai, A. Konneker, B.-I. Popa, D. J. Brady, and S. A. Cummer, "Single-sensor multispeaker listening with acoustic metamaterials," Proceedings of the National Academy of Sciences **112**, 10595–10598 (2015).

[131] H.-W. Wu, J.-Q. Quan, Y.-Q. Yin, and Z.-Q. Sheng, "Rainbow trapping of spoof acoustic surface waves in a defective closed surface," Journal of Physics D: Applied Physics **53**, 455101 (2020).

[132] M. Molerón and C. Daraio, "Acoustic metamaterial for subwavelength edge detection," Nature communications **6**, 8037 (2015).

[133] T. Yang, B. Xiao, Y. Feng, D. Pei, Y. Liu, M. Chen, H. Jiang, Z. Zheng, and Y. Wang, "Acoustic edge mode in spiral-based metamaterials at subwavelength scale," Results in Physics **42**, 106008 (2022).

[134] Z. Liang and J. Li, "Extreme acoustic metamaterial by coiling up space," Physical review letters **108**, 114301 (2012).

[135] C. Liu, C. Ma, X. Li, J. Luo, N. X. Fang, and Y. Lai, "Wide-angle broadband nonreflecting acoustic metamaterial fence," Physical Review Applied **13**, 054012 (2020).

[136] Y.-F. Chen, Z.-G. Chen, H. Ge, C. He, X. Li, M.-H. Lu, X.-C. Sun, S.-Y. Yu, and X. Zhang, "Various topological phases and their abnormal effects of topological acoustic metamaterials," Interdisciplinary Materials **2**, 179–230 (2023).

[137] Y. Li *et al.*, "Realization of controllable acoustic acceleration beams via flexible active surfaces," Journal of Physics D: Applied Physics **53**, 215001 (2020).

[138] X. Liu, X. Cai, Q. Guo, and J. Yang, "Robust nonreciprocal acoustic propagation in a compact acoustic circulator empowered by natural convection," New Journal of Physics **21**, 053001 (2019).

[139] P. J. Shah, D. A. Bas, I. Lisenkov, A. Matyushov, N. X. Sun, and M. R. Page, "Giant nonreciprocity of surface acoustic waves enabled by the magnetoelastic interaction," Science advances **6**, eabc5648 (2020).

[140] S. Karkar, E. De Bono, M. Collet, G. Matten, M. Ouisse, and E. Rivet, "Broadband nonreciprocal acoustic propagation using programmable boundary conditions: From analytical modeling to experimental implementation," Physical Review Applied **12**, 054033 (2019).

[141] F. Zangeneh-Nejad and R. Fleury, "Doppler-based acoustic gyrator," Applied Sciences **8**, 1083 (2018).

[142] X. Wang, W. Chen, and S. Li, "Multi-order asymmetric acoustic metamaterials with broad bandgaps at subwavelength scales," Materials **16**, 7587 (2023).

[143] A. Baz, "Active nonreciprocal acoustic metamaterials using a switching controller," The Journal of the Acoustical Society of America **143**, 1376–1384 (2018).

[144] B.-I. Popa and S. A. Cummer, "Non-reciprocal and highly nonlinear active acoustic metamaterials," Nature communications **5**, 3398 (2014).

[145] G. Liao, C. Luan, Z. Wang, J. Liu, X. Yao, and J. Fu, "Acoustic metamaterials: A review of theories, structures, fabrication approaches, and applications," Advanced Materials Technologies **6**, 2000787 (2021).

[146] H. Ahmed, R. Ahmed, M. M. Indaleeb, and S. Banerjee, "Multifunction acoustic modulation by a multi-mode acoustic metamaterial architecture," Journal of Physics Communications **2**, 115001 (2018).

[147] X. Zhang, H. Zhang, Z. Chen, and G. Wang, "Simultaneous realization of large sound insulation and efficient energy harvesting with acoustic metamaterial," Smart Materials and Structures **27**, 105018 (2018).

[148] Y. Li and B. M. Assouar, "Acoustic metasurface-based perfect absorber with deep subwavelength thickness," Applied Physics Letters **108** (2016).

[149] M. Yago, "Machine learning in solid mechanics: Application to acoustic metamaterial design," International Journal for Numerical Methods in Engineering **120**, 7476 (2024).

[150] A. Bacigalupo, G. Gnecco, M. Lepidi, and L. Gambarotta, "Machine-learning techniques for the optimal design of acoustic metamaterials," Journal of Optimization Theory and Applications **187**, 630–653 (2020).

[151] N. Akashi, M. Toma, and K. Kajikawa, "Design by neural network of concentric multilayered cylindrical metamaterials," Applied Physics Express **13**, 042003 (2020).

[152] A. Ural and Z. H. Kilimci, "The prediction of chiral metamaterial resonance using convolutional neural networks and conventional machine learning algorithms," International Journal of Computational and Experimental Science and Engineering **7**, 156–163 (2021).

[153] B. Yakupov and I. Smirnov, "Application of machine learning to predict the acoustic cavitation threshold of fluids," Fluids **8**, 168 (2023).

[154] H. Tian, X. Xiang, K. He, C. Liu, S. Hou, S. Wang, Y. Huang, X. Wu, and W. Wen, "Automatically adaptive ventilated metamaterial absorber for environment with varying noises," Advanced Materials Technologies **6**, 2100668 (2021).

[155] F. Mir, D. Mandal, and S. Banerjee, "Metamaterials for acoustic noise filtering and energy harvesting," Sensors **23**, 4227 (2023).

[156] E. Dong, P. Cao, J. Zhang, S. Zhang, N. X. Fang, and Y. Zhang, "Underwater acoustic metamaterials," National Science Review **10**, nwac246 (2023).

[157] S. Kumar and H. P. Lee, "The present and future role of acoustic metamaterials for architectural and urban noise mitigations," in *Acoustics*, Vol. 1 (MDPI, 2019) pp. 590–607.

[158] B. Yazıcı and Z. S. Gül, "Biomimetic metamaterial design simulation and evaluation for building acoustics by impedance measurements," Journal of Testing and Evaluation **49**, 3183–3203 (2021).

[159] J. Kennedy, L. Flanagan, L. Dowling, G. Bennett, H. Rice, and D. Trimble, "The influence of additive manufacturing processes on the performance of a periodic acoustic metamaterial," International Journal of Polymer Science **2019**, 7029143 (2019).

[160] J. C. Baena, C. Wang, Y. Fu, I. I. Kabir, A. C. Y. Yuen, Z. Peng, and G. H. Yeoh, "A new fabrication method of designed metamaterial based on a 3d-printed structure for underwater sound absorption applications," Applied Acoustics **203**, 109221 (2023).

[161] A. Melnikov, S. Köble, S. Schweiger, Y. K. Chiang, S. Marburg, and D. A. Powell, "Microacoustic metagratings at ultra-high frequencies fabricated by two-photon lithography," Advanced Science **9**, 2200990 (2022).

[162] S. S. Shah, D. Singh, J. S. Saini, and N. Garg, "Sound absorption advancements: exploring 3d printing in the development of tetrakaidecahedron cell-based acoustic metamaterials," Rapid Prototyping Journal **30**, 609–619 (2024).

[163] A. Gardiner, P. Daly, R. Domingo-Roca, J. F. Windmill, A. Feeney, and J. C. Jackson-Camargo, "Additive manufacture of small-scale metamaterial structures for acoustic and ultrasonic applications," Micromachines **12**, 634 (2021).

[164] J. Dong *et al.*, "Bioinspired metagel with broadband tunable impedance matching," Science Advances **6**, abb3641 (2020).

[165] Y.-F. Wang, Y.-Z. Wang, B. Wu, W. Chen, and Y.-S. Wang, "Tunable and active phononic crystals and metamaterials," Applied Mechanics Reviews **72**, 040801 (2020).

[166] S. Chen, Y. Fan, Q. Fu, H. Wu, Y. Jin, J. Zheng, and F. Zhang, "A review of tunable acoustic metamaterials," Applied Sciences **8**, 1480 (2018).

[167] E. De Bono, M. Morell, M. Collet, E. Gourdon, A. T. Savadkoohi, M. Ouisse, and C.-H. Lamarque, "Model-inversion control to enforce tunable duffing-like acoustical response on an electroacoustic resonator at low excitation levels," Journal of Sound and Vibration **570**, 118070 (2024).

[168] K. Koutserimpas *et al.*, "Active acoustic resonators with reconfigurable resonance frequency, absorption, and bandwidth," Physical Review Applied **12**, 054064 (2019).

[169] B. I. Popa, "New perspectives for active acoustic metamaterials," The Journal of the Acoustical Society of America **151**, 1234–1245 (2022).

[170] F. Langfeldt and J. Cheer, "Controlling the effective surface mass density of membrane-type acoustic metamaterials using dynamic actuators," The Journal of the Acoustical Society of America **153**, 961–961 (2023).

[171] M. Morell, E. Gourdon, M. Collet, A. T. Savadkoohi, E. De Bono, and C.-H. Lamarque, "Towards digitally programmed nonlinear electroacoustic resonators for low amplitude sound pressure levels: Modeling and experiments," Journal of Sound and Vibration **584**, 118437 (2024).

[172] T. Yang, Z.-G. Song, E. Clerkin, Y.-W. Zhang, J.-H. Sun, Y.-S. Su, L.-Q. Chen, and P. Hagedorn, "A programmable nonlinear acoustic metamaterial," AIP Advances **7** (2017).

[173] A. Zabihi, C. Ellouzi, and C. Shen, "Tunable, reconfigurable, and programmable acoustic metasurfaces: A review," Frontiers in Materials **10**, 1132585 (2023).

[174] S. Kumar and H. P. Lee, "Recent advances in acoustic metamaterials for simultaneous sound attenuation and air ventilation performances," Crystals **10**, 686 (2020).

[175] K. H. Lee, K. Yu, H. Al Ba ' ba'a, A. Xin, Z. Feng, and Q. Wang, "Sharkskin-inspired magnetoactive reconfigurable acoustic metamaterials," Research (2020).

[176] B.-I. Popa, D. Shinde, A. Konneker, and S. A. Cummer, "Active acoustic metamaterials reconfigurable in real time," Physical Review B **91**, 220303 (2015).

[177] C. Zhao, X. Zhang, P. Wang, N. Wei, M. Geng, Q. Hui, Q. Yu, K. Qiao, and T. Lu, "Optimized modular design of acoustic metamaterials: targeted noise attenuation," Annalen der Physik **535**, 2300063 (2023).

[178] I. L. Vér and L. L. Beranek, *Noise and vibration control engineering: principles and applications* (John Wiley & Sons, 2005).

[179] F. Asdrubali, S. Schiavoni, and K. Horoshenkov, "A review of sustainable materials for acoustic applications," Building Acoustics **19**, 283–311 (2012).

[180] K. Attenborough, "Acoustical characteristics of porous materials," Physics reports **82**, 179–227 (1982).

[181] M. Delany and E. Bazley, "Acoustical properties of fibrous absorbent materials," Applied acoustics **3**, 105–116 (1970).

[182] M. R. Kidner and C. H. Hansen, "A comparison and review of theories of the acoustics of porous materials," International Journal of Acoustics and Vibration **13**, 112–119 (2008).

[183] S. A. Cummer, J. Christensen, and A. Alù, "Controlling sound with acoustic metamaterials," Nature Reviews Materials **1**, 1–13 (2016).

[184] J. Li, X. Wen, and P. Sheng, "Acoustic metamaterials," Journal of Applied Physics **129**, 171103 (2021).

[185] Y. Wu, M. Yang, and P. Sheng, "Perspective: Acoustic metamaterials in transition," Journal of Applied Physics **123**, 090901 (2018).

[186] B.-I. Popa, L. Zigoneanu, and S. A. Cummer, "Tunable active acoustic metamaterials," Physical Review B **88**, 024303 (2013).

[187]M. Kadic, G. W. Milton, M. van Hecke, and M. Wegener, "3d metamaterials," Nature Reviews Physics **1**, 198–210 (2019).
[188]M. Howe, "On the helmholtz resonator," Journal of Sound and Vibration **45**, 427–440 (1976).
[189]P. Tang and W. Sirignano, "Theory of a generalized helmholtz resonator," Journal of Sound and Vibration **26**, 247–262 (1973).
[190]A. Benouhiba, P. Rougeot, N. Andreff, K. Rabenorosoa, and M. Ouisse, "Origami-based auxetic tunable helmholtz resonator for noise control," Smart Materials and Structures **30**, 035029 (2021).
[191]A. Abbad, N. Atalla, M. Ouisse, and O. Doutres, "Numerical and experimental investigations on the acoustic performances of membraned helmholtz resonators embedded in a porous matrix," Journal of Sound and Vibration **459**, 114873 (2019).
[192]A. Benouhiba, M. Ouisse, K. Rabenorosoa, and N. Andreff, "Investigations on an adaptive helmholtz resonator concept," in *Euro-Mediterranean Conference on Structural Dynamics and Vibroacoustics* (2020).
[193]J. Ning, G. Zhao, and X. He, "Non-acoustical parameters and sound absorption characteristics of porous polyurethane foams," Physics of Fluids **31**, 037106 (2019).
[194]C. Gaulon, J. Pierre, C. Derec, L. Jaouen, F.-X. Bécot, F. Chevillotte, F. Elias, W. Drenckhan, and V. Leroy, "Acoustic absorption of solid foams with thin membranes," Applied Physics Letters **112**, 261904 (2018).
[195]A. Abbad, K. Jaboviste, M. Ouisse, and N. Dauchez, "Acoustic performances of silicone foams for sound absorption," Journal of Cellular Plastics **54**, 651–670 (2018).
[196]D. Magliacano, M. Ouisse, S. De Rosa, F. Franco, and A. Khelif, "Computation of acoustic properties and design guidelines of periodic biot-modeled foams," Applied Acoustics **168**, 107428 (2020).
[197]O. Doutres, M. Ouisse, N. Atalla, and M. Ichchou, "Impact of the irregular microgeometry of polyurethane foam on the macroscopic acoustic behavior predicted by a unit-cell model," The Journal of the Acoustical Society of America **136**, 1666–1681 (2014).
[198]F. Wu, Y. Xiao, D. Yu, H. Zhao, Y. Wang, and J. Wen, "Low-frequency sound absorption of hybrid absorber based on micro-perforated panel and coiled-up channels," Applied Physics Letters **114** (2019).
[199]C. Wang and L. Huang, "On the acoustic properties of parallel arrangement of multiple micro-perforated panel absorbers with different cavity depths," The Journal of the Acoustical Society of America **130**, 208–218 (2011).
[200]C. Wang, L. Cheng, J. Pan, and G. Yu, "Sound absorption of a micro-perforated panel backed by an irregular-shaped cavity," The Journal of the Acoustical Society of America **127**, 238–246 (2010).
[201]M. Toyoda and D. Takahashi, "Sound transmission through a microperforated-panel structure with subdivided air cavities," The Journal of the Acoustical Society of America **124**, 3594–3603 (2008).
[202]X. Zhang and L. Cheng, "Acoustic impedance of micro-perforated panels in a grazing flow," The Journal of the Acoustical Society of America **145**, 2461–2469 (2019).
[203]G. Ma and P. Sheng, "Acoustic metamaterials: From local resonances to broad horizons," Science advances **2**, e1501595 (2016).
[204]M. Haberman and M. Guild, "Acoustic metamaterials," Physics Today **69**, 42–48 (2016).
[205]H. Zhang, R. Li, Y. Bao, X. Liu, and Y. Zhang, "Total acoustic transmission in a honeycomb network empowered by compact acoustic isolator," Scientific Reports **13** (2023), 10.1038/s41598-023-28097-y.
[206]H. Dai, T. Liu, B. Xia, and D. Yu, "Quasilossless acoustic transmission in an arbitrary pathway of a network," Physical Review B **95** (2017), 10.1103/physrevb.95.054109.
[207]Z. He, Y. Wang, and Y. Wang, "Sound transmission comparisons of active elastic wave metamaterial immersed in external mean flow," Acta Mechanica Solida Sinica **34**, 307–325 (2021).
[208]M. Mellmann and C. Zhang, "Tuning of vibration and wave propagation characteristics in pre-deformed periodic lattice frame structures," Pamm **19** (2019), 10.1002/pamm.201900291.
[209]E. Li, Z. He, G. Wang, and Y. Jong, "Fundamental study of mechanism of band gap in fluid and solid/fluid phononic crystals," Advances in Engineering Software **121**, 167–177 (2018).
[210]G. Y. Song, B. Huang, H. Y. Dong, Q. Cheng, and T. J. Cui, "Broadband focusing acoustic lens based on fractal metamaterials," Scientific reports **6**, 35929 (2016).
[211]E. Dong, P. Cao, J. Zhang, S. Zhang, and N. Fang, "Underwater acoustic metamaterials," National Science Review **10** (2022), 10.1093/nsr/nwac246.
[212]K. Yu, N. Fang, G. Huang, and Q. Wang, "Magnetoactive acoustic metamaterials," Advanced Materials **30** (2018), 10.1002/adma.201706348.
[213]S. Varanasi, J. Bolton, T. Siegmund, and R. Cipra, "The low frequency performance of metamaterial barriers based on cellular structures," Applied Acoustics **74**, 485–495 (2013).
[214]N. Jiménez, R. Picó, V. Sánchez-Morcillo, V. Romero-García, L. M. García-Raffi, and K. Staliunas, "Formation of high-order acoustic bessel beams by spiral diffraction gratings," Physical Review E **94**, 053004 (2016).
[215]H. Rice, J. Kennedy, P. Göransson, L. Dowling, and D. Trimble, "Design of a kelvin cell acoustic metamaterial," Journal of Sound and Vibration **472**, 115167 (2020).
[216]J. W. Jung, J. E. Kim, and J. W. Lee, "Acoustic metamaterial panel for both fluid passage and broadband soundproofing in the audible frequency range," Applied Physics Letters **112**, 041903 (2018).
[217]S. Kumar and H. P. Lee, "Labyrinthine acoustic metastructures enabling broadband sound absorption and ventilation," Applied Physics Letters **116** (2020).
[218]X. Meng, Y. Yi, Y. Meng, G. Lv, X. Jiang, Y. Wu, W. Yang, L. Pan, H. Xu, and W. Bu, "Self-enhanced acoustic impedance difference strategy for detecting the acidic tumor microenvironment," Acs Nano **16**, 4217–4227 (2022).
[219]L. Jiang, Y. Yang, R. Chen, G. Lu, R. Li, D. Li, M. Humayun, K. Shung, J. Zhu, Y. Chen, and Q. Zhou, "Flexible piezoelectric ultrasonic energy harvester array for bio-implantable wireless generator," Nano Energy **56**, 216–224 (2019).
[220]Y. Chen and L. Wang, "Periodic co-continuous acoustic metamaterials with overlapping locally resonant and bragg band gaps," Applied Physics Letters **105**, 191907 (2014).
[221]Y. Jin, E. Walker, T.-Y. Choi, A. Neogi, and A. Krokhin, "Simultaneous negative reflection and refraction and reverse-incident right-angle collimation of sound in a solid-fluid phononic crystal," The Journal of the Acoustical Society of America **151**, 2723–2731 (2022).
[222]K. Mohapatra and D. Jena, "Numerical and experimental methods to measure the acoustic performance of sonic crystal noise barrier," Building Acoustics **30**, 339–356 (2023).
[223]H. Tsuchiya, N. Lertsirisopon, J. Takada, and T. Kobayashi, "Effects of bragg scattering on ultra-wideband signal transmission from periodic surfaces," Ieice Transactions on Communications **E91-B**, 536–542 (2008).
[224]F. G. Mitri, "Generalized theory of resonance excitation by sound scattering from an elastic spherical shell in a nonviscous fluid," IEEE transactions on ultrasonics, ferroelectrics, and frequency control **59**, 1781–1790 (2012).
[225]H. Shen, J. Wen, M. P. Païdoussis, D. Yu, L. Cai, and X. Wen, "Parameter derivation for an acoustic cloak based on scattering theory and realization with tunable metamaterials," Modelling and Simulation in Materials Science and Engineering **21**, 065011 (2013).
[226]V. Achilleos, G. Theocharis, O. Richoux, and V. Pagneux, "Non-hermitian acoustic metamaterials: Role of exceptional points in sound absorption," Physical Review B **95**, 144303 (2017).
[227]A. G. Semenov, "Sound scattering laws for moving microinhomogeneous media," American Journal of Fluid Dynamics **2**, 42–54 (2012).
[228]S. Roy, A. Gogoi, and G. Ahmed, "Size dependent optical characterization of semiconductor particle: cds embedded in polymer matrix," Indian Journal of Physics **84**, 1405–1411 (2010).
[229]Y. Chen, Y. Chang, J. Huang, I. Chen, and C. Kuo, "Light scattering and enhanced photoactivities of electrospun titania nanofibers," The Journal of Physical Chemistry C **116**, 3857–3865 (2012).
[230]A. Bekshaev, K. Bliokh, and F. Nori, "Mie scattering and optical forces from evanescent fields: a complex-angle approach," Optics Express **21**, 7082 (2013).
[231]G. Xie and X. Wang, "Length correction model considering a right-angle bend of fabry–pérot sound absorbers," Journal of Applied Physics **131**, 115103 (2022).
[232]G. Ward, R. Lovelock, A. Murray, A. P. Hibbins, J. R. Sambles, and J. Smith, "Boundary-layer effects on acoustic transmission through narrow slit cavities," Physical review letters **115**, 044302 (2015).

[233]S. B. Gebrekidan, Y.-I. Hwang, H.-J. Kim, and S.-J. Song, "Broadband impedance matching using acoustic metamaterial with a helical hole," Applied Physics Letters **115**, 151901 (2019).
[234]Y. Shen, Y. Yang, X. Guo, Y. Shen, and D. Zhang, "Low-frequency anechoic metasurface based on coiled channel of gradient cross-section," Applied Physics Letters **114** (2019).
[235]Y. Zheng, J. Chen, J. Bai, Z. Li, X. Zhao, and X. Chen, "The manufacture and reliability analysis of the all-rigid fabry-perot resonator for fiber-optic acoustic sensors," Frontiers in Physics **11** (2023), 10.3389/fphy.2023.1172113.
[236]Y. Wong, S. Lorenzo, and O. Solgaard, "Design and fabrication of monolithic photonic crystal fiber acoustic sensor," Ieee Sensors Journal **18**, 7826–7832 (2018).
[237]C. Goffaux, J. Sánchez-Dehesa, A. L. Yeyati, P. Lambin, A. Khelif, J. Vasseur, and B. Djafari-Rouhani, "Evidence of fano-like interference phenomena in locally resonant materials," Physical review letters **88**, 225502 (2002).
[238]I. Quotane, E. Boudouti, and B. DjafariâĂŘRouhani, "Trapped-mode-induced fano resonance and acoustical transparency in a one-dimensional solid-fluid phononic crystal," Physical Review B **97** (2018), 10.1103/physrevb.97.024304.
[239]Z. Li, S. Cakmakyapan, B. Butun, C. Daskalaki, S. Tzortzakis, X. Yang, and E. Ozbay, "Fano resonances in thz metamaterials composed of continuous metallic wires and split ring resonators," Optics Express **22**, 26572–26584 (2014).
[240]A. Miroshnichenko, S. Flach, and Y. Kivshar, "Fano resonances in nanoscale structures," Reviews of Modern Physics **82**, 2257–2298 (2010).
[241]Q. Wang, Z. Ouyang, M. Lin, and Q. Liu, "Independently tunable fano resonances based on the coupled hetero-cavities in a plasmonic mim system," Materials **11**, 1675 (2018).
[242]L. Schwarz, H. Cartarius, W. Heiss, and J. Main, "Fano resonances in scattering: an alternative perspective," The European Physical Journal D **69** (2015), 10.1140/epjd/e2015-60202-9.
[243]S. Yves and A. Alù, "Extreme anisotropy and dispersion engineering in locally resonant acoustic metamaterials," The Journal of the Acoustical Society of America **150**, 2040–2045 (2021).
[244]Z. Liu, X. Zhang, Y. Mao, Y. Zhu, Z. Yang, C. T. Chan, and P. Sheng, "Locally resonant sonic materials," science **289**, 1734–1736 (2000).
[245]C. Guattari, P. Gori, R. Vollaro, L. Evangelisti, G. Battista, C. Basilicata, A. Toscano, and F. Bilotti, "Robustness of acoustic scattering cancellation to parameter variations," Sustainability **6**, 4416–4425 (2014).
[246]X. Xiao, Z. He, E. Li, and A. Cheng, "Design multi-stopband laminate acoustic metamaterials for structural-acoustic coupled system," Mechanical Systems and Signal Processing **115**, 418–433 (2019).
[247]H. Zeng, L. Chen, H. Chen, S. Zhai, C. Ding, and X. Zhao, "Flute-model acoustic metamaterials with simultaneously negative bulk modulus and mass density," Solid State Communications **173**, 14–18 (2013).
[248]M. Chen, D. Meng, H. Jiang, and Y. Wang, "Investigation on the band gap and negative properties of concentric ring acoustic metamaterial," Shock and Vibration **2018** (2018), 10.1155/2018/1369858.
[249]Y. Xu, J. Wu, Y. Cai, and F. Ma, "Investigation on dynamic effective parameters of perforated thin-plate acoustic metamaterials," Journal of Physics D Applied Physics **52**, 405301 (2019).
[250]M. Farhat, P.-Y. Chen, and H. Bağcı, "Localized acoustic surface modes," Applied Physics A **122**, 1–8 (2016).
[251]M. Yang, G. Ma, Z. Yang, and P. Sheng, "Coupled membranes with doubly negative mass density and bulk modulus," Physical Review Letters **110** (2013), 10.1103/physrevlett.110.134301.
[252]Y. Li, B. Liang, X.-y. Zou, and J.-c. Cheng, "Extraordinary acoustic transmission through ultrathin acoustic metamaterials by coiling up space," Applied Physics Letters **103**, 063509 (2013).
[253]H. Duan, F. Yang, X. Shen, Q. Yin, E. Wang, X. Zhang, X. Yang, C. Shen, and W. Peng, "Acoustic metamaterials for low-frequency noise reduction based on parallel connection of multiple spiral chambers," Materials **15**, 3882 (2022).
[254]J. Shin, I. Song, Y. Ai, S. Hwang, and J. Rieh, "Characterisation and analysis of harmonic emissions in nonlinear bulk acoustic wave resonators," Electronics Letters **49**, 1311–1312 (2013).
[255]J. Ma, M. Steer, and X. Jiang, "An acoustic filter based on layered structure," Applied Physics Letters **106** (2015), 10.1063/1.4915100.
[256]H. Chang, L. Liu, C. Zhang, and X. Hu, "Broadband high sound absorption from labyrinthine metasurfaces," Aip Advances **8** (2018).
[257]Y.-x. Gao, Y.-p. Lin, Y.-f. Zhu, B. Liang, J. Yang, J. Yang, and J.-c. Cheng, "Broadband thin sound absorber based on hybrid labyrinthine metastructures with optimally designed parameters," Scientific Reports **10**, 10705 (2020).
[258]Y. Zhu, K. Donda, S. Fan, L. Cao, and B. Assouar, "Broadband ultrathin acoustic metasurface absorber with coiled structure," Applied Physics Express **12**, 114002 (2019).
[259]S. Chen, Y. Fan, F. Yang, K. Sun, Q. Fu, J. Zheng, and F. Zhang, "Coiling-up space metasurface for high-efficient and wide-angle acoustic wavefront steering," Frontiers in Materials **8**, 790987 (2021).
[260]T. Chen, J. Jiao, and D. Yu, "Enhanced broadband acoustic sensing in gradient coiled metamaterials," Journal of Physics D: Applied Physics **54**, 085501 (2020).
[261]X.-f. Man, B.-z. Xia, Z. Luo, and J. Liu, "3d hilbert fractal acoustic metamaterials: low-frequency and multi-band sound insulation," Journal of Physics D: Applied Physics **52**, 195302 (2019).
[262]K. Song, S.-H. Lee, K. Kim, S. Hur, and J. Kim, "Emission enhancement of sound emitters using an acoustic metamaterial cavity," Scientific reports **4**, 4165 (2014).
[263]A. O. Krushynska, F. Bosia, and N. M. Pugno, "Labyrinthine acoustic metamaterials with space-coiling channels for low-frequency sound control," arXiv preprint arXiv:1712.06063 (2017).
[264]G. Comandini, T. Panzera, A. Celik, A. Gautam, F. Scarpa, M. Azarpeyvand, and V. Ting, "Hilbert fractal metamaterials for lightweight sound insulation," in *e-Forum Acusticum 2020* (2020) pp. 15–22.
[265]M. Creasy, "Impedance modelling of pipes," European Journal of Physics **37**, 025001 (2015).
[266]S. Sugiyanto, S. Kamal, J. Waluyo, and A. Widyaparaga, "Resonator influence simulation of designed close-open standing wave thermoacoustic engine," Advances in Science Technology and Engineering Systems Journal **4**, 300–305 (2019).
[267]F. Simon, "Long elastic open neck acoustic resonator for low frequency absorption," Journal of Sound and Vibration **421**, 1–16 (2018).
[268]E. Petersen, P. Guillemain, J. Kergomard, and T. Colinot, "The effect of the cutoff frequency on the sound production of a clarinet-like instrument," The Journal of the Acoustical Society of America **145**, 3784–3794 (2019).
[269]J. Li and H. Chang Gea, "Sound reduction of side-branch resonators: An energy-based theoretical perspective," AIP Advances **14** (2024).
[270]C. N. Brooks, *Architectural acoustics* (McFarland, 2015).
[271]J.-S. Chen, Y.-B. Chen, Y.-H. Cheng, and L.-C. Chou, "A sound absorption panel containing coiled helmholtz resonators," Physics Letters A **384**, 126887 (2020).
[272]W. Wang, X. Fang, N. Wang, Y. Li, and T. Hao, "Broadband acoustic double-zero-index cloaking with coupled helmholtz resonators," New Journal of Physics **24**, 083032 (2022).
[273]S.-H. Baek, J.-Y. Jang, K.-J. Song, and S.-H. Park, "Design of flat broadband sound insulation metamaterials by combining helmholtz resonator and fractal structure," Journal of Mechanical Science and Technology **35**, 2809–2817 (2021).
[274]H. Cui, Z. Hu, and H. Hu, "Research on the low-frequency sound absorption characteristics of coiled helmholtz cavity acoustic metamaterials," Advances in Mechanical Engineering **14**, 16878132221119996 (2022).
[275]Z. Zeng, M. Zhang, C. Li, L. Ren, P. Wang, J. Li, W. Yang, and Y. Pan, "Simulation study on characteristics of acoustic metamaterials based on mie and helmholtz resonance for low-frequency acoustic wave control," Journal of Physics D: Applied Physics **54**, 385501 (2021).
[276]A. Abbad, K. Rabenorosoa, M. Ouisse, and N. Atalla, "Adaptive helmholtz resonator based on electroactive polymers: modeling, characterization, and control," Smart Materials and Structures **27**, 105029 (2018).
[277]U. Ingard, "On the theory and design of acoustic resonators," The Journal of the acoustical society of America **25**, 1037–1061 (1953).
[278]E. Webster and C. Davies, "The use of helmholtz resonance for measuring the volume of liquids and solids," Sensors **10**, 10663–10672 (2010).
[279]S. Griffiths, B. Nennig, and S. Job, "Porogranular materials composed of elastic helmholtz resonators for acoustic wave absorption," The Journal of the Acoustical Society of America **141**, 254–264 (2017).
[280]M. Suchenek, "Model of the photoacoustic helmholtz resonator with conical-ended duct," International Journal of Thermophysics **35**, 2279–

2286 (2014).

[281]M. Chiu, "Noise elimination of a multi-tone broadband noise with hybrid helmholtz mufflers using a simulated annealing method," Archives of Acoustics **37**, 489–498 (2012).

[282]Z. Zhang, C. Ji, and Y. Win, "Case studies on aeroacoustics damping performances of coupled helmholtz resonators over low frequency ranges," Journal of Low Frequency Noise Vibration and Active Control **42**, 598–627 (2022).

[283]B. Crow, J. Cullen, W. McKenzie, V. Koju, and W. Robertson, "Experimental realization of extraordinary acoustic transmission using helmholtz resonators," Aip Advances **5** (2015), 10.1063/1.4908180.

[284]S. Bhagwat and M. Creasy, "Adjustable pipes and adaptive passive damping," European Journal of Physics **38**, 035003 (2017).

[285]V. Naderyan, R. Raspet, and C. Hickey, "Thermo-viscous acoustic modeling of perforated micro-electro-mechanical systems (mems)," The Journal of the Acoustical Society of America **148**, 2376–2385 (2020).

[286]G. Ji, Y. Fang, J. Zhou, and X. Huang, "Porous labyrinthine acoustic metamaterials with high transmission loss property," Journal of Applied Physics **125**, 215110 (2019).

[287]T. C. Kone, M. Lopez, S. Ghinet, T. Dupont, and R. Panneton, "Thermoviscous-acoustic metamaterials to damp acoustic modes in complex shape geometries at low frequencies," The Journal of the Acoustical Society of America **150**, 2272–2281 (2021).

[288]D. Khamis, "Viscous effects on the attenuation of a plane wave by an acoustic lining in shear flow," The Journal of the Acoustical Society of America **141**, 2408–2417 (2017).

[289]F. Ma, J. H. Wu, M. Huang, W. Zhang, and S. Zhang, "A purely flexible lightweight membrane-type acoustic metamaterial," Journal of Physics D: Applied Physics **48**, 175105 (2015).

[290]F. Langfeldt and W. Gleine, "Plate-type acoustic metamaterials with strip masses," The Journal of the Acoustical Society of America **149**, 3727–3738 (2021).

[291]Y. Aurégan, "Ultra-thin low frequency perfect sound absorber with high ratio of active area," Applied Physics Letters **113** (2018).

[292]S. Xiao, G. Ma, Y. Li, Z. Yang, and P. Sheng, "Active control of membrane-type acoustic metamaterial by electric field," Applied Physics Letters **106** (2015).

[293]T.-Y. Huang, C. Shen, and Y. Jing, "Membrane-and plate-type acoustic metamaterials," The Journal of the Acoustical Society of America **139**, 3240–3250 (2016).

[294]Z. Yang, J. Mei, M. Yang, N. Chan, and P. Sheng, "Membrane-type acoustic metamaterial with negative dynamic mass," Physical review letters **101**, 204301 (2008).

[295]Y. Chen, G. Huang, X. Zhou, G. Hu, and C.-T. Sun, "Analytical coupled vibroacoustic modeling of membrane-type acoustic metamaterials: Membrane model," The Journal of the Acoustical Society of America **136**, 969–979 (2014).

[296]F. Bongard, H. Lissek, and J. R. Mosig, "Acoustic transmission line metamaterial with negative/zero/positive refractive index," physical Review B **82**, 094306 (2010).

[297]M. E. D'Elia, T. Humbert, and Y. Aurégan, "Effect of flow on an array of helmholtz resonators: Is kevlar a "magic layer"?" The Journal of the Acoustical Society of America **148**, 3392–3396 (2020).

[298]R. Qu, J. Guo, Y. Fang, W. Yi, S. Zhong, and X. Zhang, "Sound reflection by periodic acoustic metasurface in sheared grazing flows," International Journal of Mechanical Sciences **239**, 107895 (2023).

[299]Y. Zhang, C. Wang, and L. Huang, "A tunable electromagnetic acoustic switch," Applied Physics Letters **116** (2020).

[300]E. De Bono, M. Collet, G. Matten, S. Karkar, H. Lissek, M. Ouisse, K. Billon, T. Laurence, and M. Volery, "Effect of time delay on the impedance control of a pressure-based, current-driven electroacoustic absorber," Journal of Sound and Vibration **537**, 117201 (2022).

[301]L. Gu, C. Zhao, K. Wang, S. Li, X. Wang, and Z. Huang, "Asymmetric sound absorption achieved by double-layer piezoelectric metamaterials with tunable shunt circuit," Applied Physics Letters **119** (2021).

[302]S. Alan, A. Allam, and A. Erturk, "Programmable mode conversion and bandgap formation for surface acoustic waves using piezoelectric metamaterials," Applied Physics Letters **115** (2019).

[303]Y. Liao, Y. Chen, G. Huang, and X. Zhou, "Broadband low-frequency sound isolation by lightweight adaptive metamaterials," Journal of applied physics **123** (2018).

[304]J. Li, X. Zhou, G. Huang, and G. Hu, "Acoustic metamaterials capable of both sound insulation and energy harvesting," Smart Materials and Structures **25**, 045013 (2016).

[305]H. Huang, E. Cao, M. Zhao, S. Alamri, and B. Li, "Spider web-inspired lightweight membrane-type acoustic metamaterials for broadband low-frequency sound isolation," Polymers **13**, 1146 (2021).

[306]R. Jiang, G. Shi, C. Huang, W. Zheng, and S. Li, "Acoustic insulation characteristics and optimal design of membrane-type metamaterials loaded with asymmetric mass blocks," Materials **16**, 1308 (2023).

[307]H. Xue, Y. Yang, and B. Zhang, "Topological acoustics," Nature Reviews Materials **7**, 974–990 (2022).

[308]S. Kuchibhatla, "Numerical demonstration of a topologically-protected electroacoustic transistor," Front. Acoust. **1** (2023), 10.3389/facou.2023.1251215.

[309]X. Zhang, M. Xiao, Y. Cheng, M. Lu, and J. Christensen, "Topological sound," Communications Physics **1** (2018), 10.1038/s42005-018-0094-4.

[310]C. Shi, M. Dubois, Y. Chen, L. Cheng, H. Ramezani, Y. Wang, and X. Zhang, "Accessing the exceptional points of parity-time symmetric acoustics," Nature Communications **7** (2016), 10.1038/ncomms11110.

[311]X. Zhu, H. Ramezani, C. Shi, J. Zhu, and X. Zhang, "pt-symmetric acoustics," The Journal of the Acoustical Society of America **137**, 2403–2403 (2015).

[312]X. Zhu, H. Ramezani, C. Shi, J. Zhu, and X. Zhang, "Pt-symmetric acoustics," Physical Review X **4**, 031042 (2014).

[313]H. Yang, X. Zhang, Y. Liu, Y. Yao, F. Wu, and D. Zhao, "Novel acoustic flat focusing based on the asymmetric response in parity-time-symmetric phononic crystals," Scientific Reports **9** (2019), 10.1038/s41598-019-46467-3.

[314]Y. Zhou, Z.-Z. Yang, Y.-Y. Peng, and X.-Y. Zou, "Parity–time symmetric acoustic system constructed by piezoelectric composite plates with active external circuits," Chinese Physics B **31**, 064304 (2022).

[315]X. Wang, X. Fang, D. Mao, Y. Jing, and Y. Li, "Extremely asymmetrical acoustic metasurface mirror at the exceptional point," Physical Review Letters **123** (2019), 10.1103/physrevlett.123.214302.

[316]J. Liu, X. Zhang, L. Wang, Y. Lai, and X. Liu, "Bidirectional acoustic negative refraction based on a pair of metasurfaces with both local and global pt-symmetries," Scientific Reports **10** (2020), 10.1038/s41598-020-67793-x.

[317]W. Wang, Y. Xie, B.-I. Popa, and S. A. Cummer, "Subwavelength diffractive acoustics and wavefront manipulation with a reflective acoustic metasurface," Journal of Applied Physics **120** (2016).

[318]Y. Li, B. Liang, Z.-m. Gu, X.-y. Zou, and J.-c. Cheng, "Reflected wavefront manipulation based on ultrathin planar acoustic metasurfaces," Scientific reports **3**, 2546 (2013).

[319]Y. Xie, W. Wang, H. Chen, A. Konneker, B.-I. Popa, and S. A. Cummer, "Wavefront modulation and subwavelength diffractive acoustics with an acoustic metasurface," Nature communications **5**, 5553 (2014).

[320]J. Zhang, Z. Lei Mei, W. Ru Zhang, F. Yang, and T. Jun Cui, "An ultrathin directional carpet cloak based on generalized snell's law," Applied Physics Letters **103** (2013).

[321]M. Stein, S. Keller, Y. Luo, and O. Ilic, "Shaping contactless radiation forces through anomalous acoustic scattering," Nature Communications **13** (2022), 10.1038/s41467-022-34207-7.

[322]S. Eslamzadeh, M. Ghaffari-Miab, and B. Abbasi-Arand, "Design of a broadband metamaterial-based acoustic lens using elaborated carpet cloak strategy," Applied Physics A **127**, 897 (2021).

[323]J. Qian, Y. Wang, S.-q. Yuan, H.-x. Sun, and X.-j. Liu, "Reflected acoustic wavefront manipulation by an ultrathin metasurface based on three-dimensional generalized snellâĂŹs law," Applied Physics Express **12**, 094001 (2019).

[324]J. Chen, J. Huang, M. An, P. Hu, Y. Xie, J. Wu, and Y. Chen, "Application of machine learning on the design of acoustic metamaterials and phonon crystals: A review," Smart Materials and Structures (2024).

[325]E. Wang, F. Yang, X. Shen, H. Duan, X. Zhang, Q. Yin, W. Peng, X. Yang, and Y. Liu, "Development and optimization of broadband acoustic metamaterial absorber based on parallelâĂŞconnection square helmholtz resonators," Materials **15**, 3417 (2022).

[326]Y. Zheng, H. Dai, J. Wu, C. Zhou, Z. Wang, R. Zhou, and W. Li, "Research progress and development trend of smart metamaterials," Frontiers

in Physics **10** (2022), 10.3389/fphy.2022.1069722.
[327] B. Huang, Q. Cheng, G. Song, and T. Cui, “Design of acoustic metamaterials using the covariance matrix adaptation evolutionary strategy,” Applied Physics Express **10**, 037301 (2017).
[328] H. Gao, X. Fang, Z. Gu, T. Liu, S. Liang, Y. Li, and J. Zhu, “Conformally mapped multifunctional acoustic metamaterial lens for spectral sound guiding and talbot effect,” Research **2019** (2019), 10.34133/2019/1748537.
[329] Y. Zhou, J. Chen, L. Liu, Z. Fan, and Y. Ma, “Magnetic-acoustic biphysical invisible coats for underwater objects,” NPG Asia Materials **12** (2020), 10.1038/s41427-020-0209-8.
[330] Z. Cai, S. Zhao, Z. Huang, Z. Liang, M. Su, Z. Zhang, Z. Zhao, and Y. Song, “Negative refraction acoustic lens based on elastic shell encapsulated bubbles,” Advanced Materials Technologies **7** (2022), 10.1002/admt.202101186.
[331] T.-W. Liu, C.-T. Chan, and R.-T. Wu, “Deep-learning-based acoustic metamaterial design for attenuating structure-borne noise in auditory frequency bands,” Materials **16**, 1879 (2023).
[332] F. Yang, S. Bi, X. Shen, Z. Li, X. Zhang, E. Wang, X. Yang, W. Peng, C. Huang, L. Peng, and G. Sun, “Adjustable sound absorber of multiple parallel-connection helmholtz resonators with tunable apertures prepared by low-force stereolithography of photopolymer resin,” Polymers **14**, 5434 (2022).
[333] C. Zanin, J. G. L. G. Alves, P. C. Gonçalves, J. A. G. Sánchez, and N. G. R. de Melo Filho, “A review of acoustic metamaterials applied to noise control in civil engineering,” Caderno Pedagógico **20**, 4537–4556 (2023).
[334] H. Lee, K. Lim, and H. Lee, “Environmental and sound divergence effects on the performance of rectangular sonic crystals with helmholtz resonators,” Journal of Vibration and Control **24**, 2483–2493 (2017).
[335] L. Huang, B. Jia, Y. Chiang, S. Huang, C. Shen, F. Deng, T. Yang, D. Powell, Y. Li, and A. Miroshnichenko, “Topological supercavity resonances in the finite system,” Advanced Science **9** (2022), 10.1002/advs.202200257.
[336] S. Wan, L. Cao, Y. Zhu, M. Oudich, and B. Assouar, “Nonreciprocal sound propagation via cascaded time-modulated slab resonators,” Physical Review Applied **16** (2021), 10.1103/physrevapplied.16.064061.
[337] V. Rennoll, I. McLane, A. Eisape, D. Grant, H. Hahn, M. Elhilali, and J. West, “Electrostatic acoustic sensor with an impedance-matched diaphragm characterized for body sound monitoring,” Acs Applied Bio Materials **6**, 3241–3256 (2023).
[338] M. Bakhtiari-Nejad, M. Hajj, and S. Shahab, “Dynamics of acoustic impedance matching layers in contactless ultrasonic power transfer systems,” Smart Materials and Structures **29**, 035037 (2020).
[339] J. Olivares, E. Wegmann, J. Capilla, E. Iborra, M. Clement, L. Vergara, and R. Aigner, “Sputtered sio 2 as low acoustic impedance material for bragg mirror fabrication in baw resonators,” *2009 IEEE International frequency control symposium joint with the 22nd European frequency and time forum*, , 316–321 (2009).
[340] V. Rathod, “A review of acoustic impedance matching techniques for piezoelectric sensors and transducers,” Sensors **20**, 4051 (2020).
[341] N. Hiremath, V. Kumar, N. Motahari, and D. Shukla, “An overview of acoustic impedance measurement techniques and future prospects,” Metrology **1**, 17–38 (2021).
[342] H. Shu, “Micromechanical piezoelectric micromachined ultrasonic transducer array package enhancement with integrated frontliners,” Journal of Micromechanics and Microengineering **34**, 075009 (2024).
[343] H. Tanaka, S. Machida, and M. Nanri, “Fabrication and evaluation of mut-type acoustic metamaterial for impedance matching,” IEEJ Transactions on Electrical and Electronic Engineering **19**, 586–594 (2024).
[344] Y. Ohashi, R. Murakami, H. Yamaguchi, Y. Yokota, and A. Yoshikawa, “Acoustic properties for ga–sn–zn liquid metal coupler with low melting point and high acoustic impedance,” Japanese Journal of Applied Physics **62**, SJ1006 (2023).
[345] R. Guillermic, M. Lanoy, A. Strybulevych, and J. Page, “A pdms-based broadband acoustic impedance matched material for underwater applications,” Ultrasonics **94**, 152–157 (2019).
[346] T. Lu, G. Gao, S. Ma, F. Jin, and T. Kim, “Acoustic band gaps in two-dimensional square arrays of semi-hollow circular cylinders,” Science in China Series E: Technological Sciences **52**, 303–312 (2009).
[347] C. Cai, Z. Wang, Y. Chu, G. Liu, and Z. Xu, “The phononic band gaps of bragg scattering and locally resonant pentamode metamaterials,” Journal of Physics D Applied Physics **50**, 415105 (2017).
[348] D. P. Jena and X. Qiu, “Sound transmission loss of porous materials in ducts with embedded periodic scatterers,” The Journal of the Acoustical Society of America **147**, 978–983 (2020).
[349] A. Shakouri, F. Xu, and Z. Fan, “Broadband acoustic energy confinement in hierarchical sonic crystals composed of rotated square inclusions,” Applied Physics Letters **111** (2017), 10.1063/1.4985230.
[350] R. Pourabolghasem, A. Khelif, S. Mohammadi, A. Eftekhar, and A. Adibi, “Physics of band-gap formation and its evolution in the pillar-based phononic crystal structures,” Journal of Applied Physics **116** (2014), 10.1063/1.4887115.
[351] B. Yuan, Y. Chen, M. Jiang, S. Tang, M. He, and M. Tu, “The interaction of resonance and bragg scattering effects for the locally resonant phononic crystal with alternating elastic and fluid matrices,” Archive of Mechanical Engineering **42**, 725–733 (2017).
[352] J. Zhang, K. Pan, and J. Qiu, “Mie-resonance-based metamaterials with perfect absorption in the terahertz frequency range,” physica status solidi (RRL)–Rapid Research Letters **15**, 2100031 (2021).
[353] X. Wang, H. Li, and J. Zhou, “Asymmetric transmission in a mie-based dielectric metamaterial with fano resonance,” Materials **12**, 1003 (2019).
[354] F. Casadei and K. Bertoldi, “Harnessing fluid-structure interactions to design self-regulating acoustic metamaterials,” Journal of Applied Physics **115**, 034907 (2014).
[355] T. Wang, G. Wang, R. Zhang, and M. Ke, “Low-frequency underwater sound absorption metamaterial,” Physica Scripta **97**, 125706 (2022).
[356] S. Laureti, D. Hutchins, L. Astolfi, R. Watson, P. Thomas, P. Burrascano, L. Nie, S. Freear, M. Askari, A. Clare, and M. Ricci, “Trapped air metamaterial concept for ultrasonic sub-wavelength imaging in water,” Scientific Reports **10** (2020), 10.1038/s41598-020-67454-z.
[357] K. Ma, T. Tan, F. Liu, L. Zhao, W. Liao, and W. Zhang, “Acoustic energy harvesting enhanced by locally resonant metamaterials,” Smart Materials and Structures **29**, 075025 (2020).
[358] H. Cui, C. Liu, and H. Hu, “Research on low-frequency noise control based on fractal coiled acoustic metamaterials,” Shock and Vibration **2022**, 1–14 (2022).
[359] M. Boccaccio, P. Rachiglia, G. Fierro, and M. Meo, “Deep-subwavelength-optimized holey-structured metamaterial lens for nonlinear air-coupled ultrasonic imaging,” Sensors **21**, 1170 (2021).
[360] L. Astolfi, D. Hutchins, P. Thomas, R. Watson, L. Nie, S. Freear, A. Clare, M. Ricci, and S. Laureti, “Holey-structured tungsten metamaterials for broadband ultrasonic sub-wavelength imaging in water,” The Journal of the Acoustical Society of America **150**, 74–81 (2021).
[361] X. Zhang, Z. He, and G. Wang, “Extraordinary sound transmission through geometrical mismatched channels based on near zero bulk modulus and fabry–pérot resonance,” Journal of Physics D: Applied Physics **52**, 055301 (2018).
[362] G. D’Aguanno, K. Q. Le, R. Trimm, A. Alù, N. Mattiucci, A. D. Mathias, N. Aközbek, and M. J. Bloemer, “Broadband metamaterial for nonresonant matching of acoustic waves,” Scientific Reports **2**, 340 (2012).
[363] Y. Lei, J. Wu, Z. Huang, and S. Yang, “Enhanced broadband monopole emission and acoustic energy harvesting via a dual anisotropic metamaterial,” Journal of Physics D Applied Physics **55**, 065301 (2021).
[364] L. Zhang, X. Guo, J. Tu, J. Cheng, J. Wu, and Z. Dong, “Acoustic focusing of sub-wavelength scale achieved by multiple fabry-perot resonance effect,” Journal of Applied Physics **115** (2014), 10.1063/1.4868629.
[365] X. Cai, J. Xiao, H. Zhang, Y. Zhang, G. Hu, and J. Yang, “Compact acoustic double negative metamaterial based on coexisting local resonances,” Applied Physics Letters **113** (2018), 10.1063/1.5052026.
[366] T. Lee, T. Nomura, X. Su, and H. Iizuka, “Fano-like acoustic resonance for subwavelength directional sensing: 0–360 degree measurement,” Advanced Science **7**, 1903101 (2020).
[367] W. Peng, S. Bi, X. Shen, X. Yang, F. Yang, and E. Wang, “Study on sound-insulation performance of an acoustic metamaterial of air-permeable multiple-parallel-connection folding chambers by acoustic finite element simulation,” Materials **16**, 4298 (2023).
[368] R. Dong, M. Sun, F. Mo, D. Mao, X. Wang, and Y. Li, “Recent advances in acoustic ventilation barriers,” Journal of Physics D Applied Physics **54**, 403002 (2021).
[369] W. Xu, L. Qin, and J. Wang, “Coupled helmholtz resonators with multiple resonant modes for fano-like interferences,” physica status solidi (a) **220**,

2200779 (2023).
[370] F. Lemoult, N. Kaina, M. Fink, and G. Lerosey, "Soda cans metamaterial: A subwavelength-scaled phononic crystal," Crystals **6**, 82 (2016).
[371] X. Zhang, C. Zhao, P. Wang, and R. Chen, "Combined acoustic metamaterial design based on multi-channel fano resonance effect," Journal of Applied Physics **136** (2024).
[372] H. Nguyen, Q. Wu, H. Chen, J. Chen, Y. Yu, S. Tracy, and G. Huang, "A fano-based acoustic metamaterial for ultra-broadband sound barriers," Proceedings of the Royal Society A **477**, 20210024 (2021).
[373] G. Theocharis, O. Richoux, V. R. García, A. Merkel, and V. Tournat, "Limits of slow sound propagation and transparency in lossy, locally resonant periodic structures," New Journal of Physics **16**, 093017 (2014).
[374] A. Elayouch, M. Addouche, M. Farhat, and A. Khelif, "Subwavelength sound screening by coupling space-coiled fabry-perot resonators," Epl (Europhysics Letters) **119**, 36001 (2017).
[375] F. Casadei, T. Delpero, A. Bergamini, P. Ermanni, and M. Ruzzene, "Piezoelectric resonator arrays for tunable acoustic waveguides and metamaterials," Journal of Applied Physics **112** (2012), 10.1063/1.4752468.
[376] A. Hall, E. Calius, G. Dodd, E. Wester, and K. Chan, "Development of locally resonant structures for sonic barriers," Building Acoustics **21**, 199–220 (2014).
[377] T. Cavalieri, A. Cebrecos, J.-P. Groby, C. Chaufour, and V. Romero-García, "Three-dimensional multiresonant lossy sonic crystal for broadband acoustic attenuation: Application to train noise reduction," Applied Acoustics **146**, 1–8 (2019).
[378] K. Matsushima, Y. Noguchi, and T. Yamada, "Omnidirectional acoustic cloaking against airborne sound realized by a locally resonant sonic material," Scientific Reports **12** (2022), 10.1038/s41598-022-20591-z.
[379] L. Lu, T. Yamamoto, M. Otomori, T. Yamada, K. Izui, and S. Nishiwaki, "Topology optimization of an acoustic metamaterial with negative bulk modulus using local resonance," Finite Elements in Analysis and Design **72**, 1–12 (2013).
[380] B. Yuan, "A parametric analysis on the sound absorbing performance of the locally resonant sonic material using a mass-damper-spring model," American Journal of Physics and Applications **4**, 124 (2016).
[381] W. Wang, L. Wu, L. Chen, and C. Liu, "Acoustic energy harvesting by piezoelectric curved beams in the cavity of a sonic crystal," Smart Materials and Structures **19**, 045016 (2010).
[382] P. Sheng, "Coupled membranes with doubly negative mass density and bulk modulus," The Journal of the Acoustical Society of America **134**, 4026–4026 (2013).
[383] M. Chen, W. Xu, Y. Liu, K. Yan, H. Jiang, and Y. Wang, "Band gap and double-negative properties of a star-structured sonic metamaterial," Applied Acoustics **139**, 235–242 (2018).
[384] G. Li, L. Wang, Y. Gao, and W. Sun, "Wave motion in double-resonator metamaterials," Engineering Research Express **1**, 025049 (2019).
[385] R. Hedayati, "Active acoustic metamaterial based on helmholtz resonators to absorb broadband low-frequency noise," Materials **17**, 962 (2024).
[386] Z. Zaky, "Periodic open and closed resonators as a biosensor using two computational methods," Scientific Reports **14** (2024), 10.1038/s41598-024-61987-3.
[387] H. Guo, Y. Wang, X. Wang, and C. Xu, "Investigation on acoustic energy harvesting based on quarter-wavelength resonator phononic crystals," Advances in Mechanical Engineering **10** (2018), 10.1177/1687814017748077.
[388] S. Lin, Y. Wu, H. Yen, W. Hsu, and Y. Cheng, "Noise reduction on centrifugal fan via the quarter-wave resonator," Applied Mechanics and Materials **764-765**, 319–323 (2015).
[389] A. Elayouch, M. Addouche, and A. Khelif, "Extensive tailorability of sound absorption using acoustic metamaterials," Journal of Applied Physics **124** (2018).
[390] K. Donda, Y. Zhu, S. Fan, L. Cao, Y. Li, and B. Assouar, "Extreme low-frequency ultrathin acoustic absorbing metasurface," Applied Physics Letters **115** (2019), 10.1063/1.5122704.
[391] X. Xiao, "Research on an optimized quarter-wavelength resonator-based triboelectric nanogenerator for efficient low-frequency acoustic energy harvesting," Nanomaterials **13**, 1676 (2023).
[392] M. Hariyanto, M. Mayantasari, and F. Robiandi, "Design of micro power energy harvesting by using high-powered engine noise (case study: generator set itk)," Journal of Physics Conference Series **2243**, 012042 (2022).
[393] J. Choi, I. Jung, and C.-Y. Kang, "A brief review of sound energy harvesting," Nano energy **56**, 169–183 (2019).
[394] M. Weiner, X. Ni, M. Li, A. Alù, and A. B. Khanikaev, "Demonstration of a third-order hierarchy of topological states in a three-dimensional acoustic metamaterial," Science Advances **6**, eaay4166 (2020).
[395] A. B. Khanikaev, R. Fleury, S. H. Mousavi, and A. Alu, "Topologically robust sound propagation in an angular-momentum-biased graphene-like resonator lattice," Nature communications **6**, 8260 (2015).
[396] X. Li, Y. Meng, X. Wu, S. Yan, Y. Huang, S. Wang, and W. Wen, "Su-schrieffer-heeger model inspired acoustic interface states and edge states," Applied Physics Letters **113** (2018), 10.1063/1.5051523.
[397] S. Yves, R. Fleury, F. Lemoult, M. Fink, and G. Lerosey, "Topological acoustic polaritons: robust sound manipulation at the subwavelength scale," New Journal of Physics **19**, 075003 (2017).
[398] Z. Yang, F. Gao, X. Shi, X. Lin, Z. Gao, Y. Chong, and B. Zhang, "Topological acoustics," Physical Review Letters **114** (2015), 10.1103/physrevlett.114.114301.
[399] J. Zhang, B. Hu, and S. Wang, "Review and perspective on acoustic metamaterials: From fundamentals to applications," Applied Physics Letters **123** (2023).
[400] N. Gao, Z. Zhang, J. Deng, X. Guo, B. Cheng, and H. Hou, "Acoustic metamaterials for noise reduction: a review," Advanced Materials Technologies **7**, 2100698 (2022).
[401] W. Zhu, "Topological phononic metamaterials," Reports on Progress in Physics **86**, 106501 (2023).
[402] C. Ding, Y. Dong, Y. Wang, J. Shi, S. Zhai, and X. Zhao, "Acoustic metamaterials and metasurfaces composed of meta-atoms and meta-molecules," Journal of Physics D: Applied Physics **55**, 253002 (2022).
[403] S. Wang, T. Zhang, K. Li, S. Ma, M. Chen, P. Lu, and L. Wei, "Flexible piezoelectric fibers for acoustic sensing and positioning," Advanced electronic materials **3**, 1600449 (2017).
[404] E. Kliewer, A. Darabi, and M. J. Leamy, "Additive manufacturing of channeled acoustic topological insulators," The Journal of the Acoustical Society of America **150**, 2461–2468 (2021).
[405] R. Fleury, D. Sounas, and A. Alu, "An invisible acoustic sensor based on parity-time symmetry," Nature communications **6**, 5905 (2015).
[406] R. Fleury, D. L. Sounas, and A. Alu, "Parity-time symmetry in acoustics: theory, devices, and potential applications," IEEE Journal of Selected Topics in Quantum Electronics **22**, 121–129 (2016).
[407] X. Zhu, H. Ramezani, C. Shi, J. Zhu, and X. Zhang, "pt-symmetric acoustics," Physical Review X **4** (2014), 10.1103/physrevx.4.031042.
[408] T. Magariyachi, H. Arias Casals, R. Herrero, M. Botey, and K. Staliunas, "Pt-symmetric helmholtz resonator dipoles for sound directivity," Physical Review B **103**, 094201 (2021).
[409] J. Liu, L. Wang, X. Zhang, M. Lu, and X. Liu, "Acoustic multifunctional logic gates and amplifier based on passive parity-time symmetry," Physical Review Applied **13** (2020), 10.1103/physrevapplied.13.034047.
[410] T. Liu, X. Zhu, F. Chen, S. Liang, and J. Zhu, "Unidirectional wave vector manipulation in two-dimensional space with an all passive acoustic parity-time-symmetric metamaterials crystal," Physical Review Letters **120** (2018), 10.1103/physrevlett.120.124502.
[411] C. Liu, J. Lan, Z. Gu, and J. Zhu, "Unidirectional negative refraction at an exceptional point of acoustic pt-symmetric systems," Chinese Physics Letters **40**, 124301 (2023).
[412] G. Liao, C. Luan, Z. Wang, J. Liu, X. Yao, and J. Fu, "Acoustic wave filtering strategy based on gradient acoustic metamaterials," Journal of Physics D Applied Physics **54**, 335301 (2021).
[413] J. Liu, X. Zhang, X. Liu, and Y. Li, "Wavefront manipulation based on transmissive acoustic metasurface with membrane-type hybrid structure," Scientific Reports **8** (2018), 10.1038/s41598-018-32547-3.
[414] L. Hao, X. Chen, X. Yan, Y. Li, L. Zhang, Y. Xie, S. Pang, and Z. Chen, "Flexible manipulation of the reflected wavefront using acoustic metasurface with split hollow cuboid," Materials **15**, 1189 (2022).
[415] Z. Wang and Y. Chu, "Research progress of acoustic metasurface in china," Epj Applied Metamaterials **6**, 5 (2019).
[416] B. Liu, W. Zhao, and Y. Jiang, "Full-angle negative reflection realized by a gradient acoustic metasurface," Aip Advances **6** (2016), 10.1063/1.4967430.
[417] Y. Su and L. Ko, "Acoustic wave splitting and wave trapping designs," Journal of Vibration and Acoustics **144** (2022), 10.1115/1.4053713.

[418]B. Liang, J.-c. Cheng, and C.-W. Qiu, "Wavefront manipulation by acoustic metasurfaces: from physics and applications," Nanophotonics **7**, 1191–1205 (2018).
[419]B. Assouar, B. Liang, Y. Wu, Y. Li, J.-C. Cheng, and Y. Jing, "Acoustic metasurfaces," Nature Reviews Materials **3**, 460–472 (2018).
[420]X. Li, Y. Wang, A. Chen, and Y. Wang, "An arbitrarily curved acoustic metasurface for three-dimensional reflected wave-front modulation," Journal of Physics D Applied Physics **53**, 195301 (2020).
[421]J. Qian, J. Xia, H. Sun, Y. Wang, Y. Ge, S. Yuan, Y. Yang, X. Liu, and B. Zhang, "Aperiodic metagratings for high-performance multifunctional acoustic lenses," Advanced Materials Technologies **5** (2020), 10.1002/admt.202000542.
[422]B. Liu, W. Zhao, and Y. Jiang, "Apparent negative reflection with the gradient acoustic metasurface by integrating supercell periodicity into the generalized law of reflection," Scientific Reports **6** (2016), 10.1038/srep38314.
[423]H. Lee, M. Jung, M. Kim, R. Shin, S. Kang, W. Ohm, and Y. Kim, "Acoustically sticky topographic metasurfaces for underwater sound absorption," The Journal of the Acoustical Society of America **143**, 1534–1547 (2018).
[424]M. D. Guild, V. M. Garcia-Chocano, W. Kan, and J. Sánchez-Dehesa, "Acoustic metamaterial absorbers based on multilayered sonic crystals," Journal of Applied Physics **117** (2015).
[425]X. Jiang, Y. Li, and L. Zhang, "Thermoviscous effects on sound transmission through a metasurface of hybrid resonances," The Journal of the Acoustical Society of America **141**, EL363–EL368 (2017).
[426]J. Guo, Y. Fang, and X. Zhang, "Forbidden transmission of broadband duct noise realized by compactly placed detuned resonators," Acoustics Australia **50**, 79–90 (2021).
[427]H. Hussain and J. Guyader, "An equivalent plate model for sandwiched panels with thermoviscous fluid core," Journal of Vibration and Acoustics **134** (2012), 10.1115/1.4005848.
[428]P. A. Cotterill, D. Nigro, I. D. Abrahams, E. Garcia-Neefjes, and W. J. Parnell, "Thermo-viscous damping of acoustic waves in narrow channels: a comparison of effects in air and water," The Journal of the Acoustical Society of America **144**, 3421–3436 (2018).
[429]C. Naify, C. Chang, G. McKnight, and S. Nutt, "Transmission loss and dynamic response of membrane-type locally resonant acoustic metamaterials," Journal of Applied Physics **108** (2010), 10.1063/1.3514082.
[430]J. Wang, J. Mei, J. Friend, and O. Vazquez-Mena, "Frequency and damping effect of suspended silicon nitride membranes in water near the megahertz range," Journal of Micromechanics and Microengineering **30**, 125006 (2020).
[431]L. Guo, S. Chen, Y. Li, and H. Tan, "Transmission loss of membrane-type acoustic metamaterial with negative effective mass," Materials Science Forum **898**, 1749–1756 (2017).
[432]J. Hao, S. Guo, C. Jian, Z. Hu, and H. Cui, "Research on the sound insulation properties of membrane-type acoustic metamaterials," E3s Web of Conferences **252**, 02028 (2021).
[433]F. Mizukoshi and H. Takahashi, "A tunable open planar acoustic notch filter utilizing a pneumatically modulated helmholtz resonator array," Ieee Access **10**, 118213–118221 (2022).
[434]Y. Wang and L. Ma, "Sound insulation performance of curved sandwich structure combined with acoustic metamaterials," Journal of Vibration and Control **30**, 2993–3005 (2023).
[435]X. Tang, S. Liang, Y. Jiang, C. Gao, Y. Huang, Y. Zhang, C. Xue, and W. Wen, "Magnetoactive acoustic metamaterials based on nanoparticle-enhanced diaphragm," Scientific Reports **11** (2021), 10.1038/s41598-021-01569-9.
[436]G. Ciaburro, R. Parente, G. Iannace, and V. Puyana-Romero, "Design optimization of three-layered metamaterial acoustic absorbers based on pvc reused membrane and metal washers," Sustainability **14**, 4218 (2022).
[437]A. Leblanc and A. Lavie, "Three-dimensional-printed membrane-type acoustic metamaterial for low frequency sound attenuation," The Journal of the Acoustical Society of America **141**, EL538–EL542 (2017).
[438]F. Langfeldt, H. Hoppen, and W. Gleine, "Resonance frequencies and sound absorption of helmholtz resonators with multiple necks," Applied Acoustics **145**, 314–319 (2019).
[439]D. Wu, N. Zhang, C. Mak, and C. Cai, "Noise attenuation performance of a helmholtz resonator array consist of several periodic parts," Sensors **17**, 1029 (2017).
[440]X. Yang, F. Yang, X. Shen, E. Wang, X. Zhang, C. Shen, and W. Peng, "Development of adjustable parallel helmholtz acoustic metamaterial for broad low-frequency sound absorption band," Materials **15**, 5938 (2022).
[441]S. Dogra and A. Gupta, "Design, manufacturing, and acoustical analysis of a helmholtz resonator-based metamaterial plate," Acoustics **3**, 630–641 (2021).
[442]D. Guan, D. Zhao, and Z. Ren, "Aeroacoustic attenuation performance of a helmholtz resonator with a rigid baffle implemented in the presence of a grazing flow," International Journal of Aerospace Engineering **2020**, 1–16 (2020).
[443]N. Papadakis, "Fem investigation of a multi-neck helmholtz resonator," Applied Sciences **13**, 10610 (2023).
[444]N. Papadakis, "Tunable helmholtz resonators using multiple necks," Micromachines **14**, 1932 (2023).
[445]D. Magliacano, S. Ashani, M. Ouisse, E. Deckers, G. Petrone, W. Desmet, and S. Rosa, "Formulation and validation of the shift cell technique for acoustic applications of poro-elastic materials described by the biot theory," Mechanical Systems and Signal Processing **147**, 107089 (2021).
[446]J. Liu, H. Guo, and T. Wang, "A review of acoustic metamaterials and phononic crystals," Crystals **10**, 305 (2020).
[447]G. Aydın and S. E. San, "Breaking the limits of acoustic science: A review of acoustic metamaterials," Materials Science and Engineering: B **305**, 117384 (2024).
[448]C. Zhang and X. Hu, "3d single-port labyrinthine acoustic metamaterial," arXiv preprint arXiv:1608.04599 (2016).
[449]X. Liu, M. Duan, M. Liu, F. Xin, and C. Zhang, "Acoustic labyrinthine porous metamaterials for subwavelength low-frequency sound absorption," Journal of Applied Physics **129** (2021).
[450]Y. Xie, C. Shen, Y. Jing, and S. Cummer, "Acoustic phase hologram with labyrinthine metamaterials," The Journal of the Acoustical Society of America **138**, 1751–1752 (2015).
[451]K. Attenborough, "Analytical approximations for sub wavelength sound absorption by porous layers with labyrinthine slit perforations," Applied Sciences **11**, 3299 (2021).
[452]A. Chen, X. Zhao, Z. Yang, S. Anderson, and X. Zhang, "Broadband labyrinthine acoustic insulator," Physical Review Applied **18**, 064057 (2022).
[453]X. Man, B. Xia, Z. Luo, J. Liu, K. Li, and Y. Nie, "Engineering three-dimensional labyrinthine fractal acoustic metamaterials with low-frequency multi-band sound suppression," The Journal of the Acoustical Society of America **149**, 308–319 (2021).
[454]I. Prasetiyo, I. Sihar, F. Brahmana, *et al.*, "Enhancing nonwoven fabric material sound absorption using embedded labyrinthine rigid structures," Applied Acoustics **195**, 108852 (2022).
[455]A. Krushynska, F. Bosia, and N. M. Pugno, "Fractal and bio-inspired labyrinthine acoustic metamaterials," The Journal of the Acoustical Society of America **143**, 1714–1714 (2018).
[456]J. Liu, L. Li, B. Xia, and X. Man, "Fractal labyrinthine acoustic metamaterial in planar lattices," International Journal of Solids and Structures **132**, 20–30 (2018).
[457]Y. Noguchi, T. Yamamoto, K. Matsushima, and T. Yamada, "Labyrinthine acoustic metamaterials with a subwavelength bandgap inspired by topology-optimized structural design," Advanced Engineering Materials **25**, 2201104 (2023).
[458]Y. Noguchi, K. Matsushima, and T. Yamada, "Level set-based topology optimization for the design of labyrinthine acoustic metamaterials," Materials & Design **219**, 110832 (2022).
[459]G. Pavan and S. Singh, "Near-perfect sound absorptions in low-frequencies by varying compositions of porous labyrinthine acoustic metamaterial," Applied Acoustics **198**, 108974 (2022).
[460]L. Liu, H. Chang, C. Zhang, and X. Hu, "Single-channel labyrinthine metasurfaces as perfect sound absorbers with tunable bandwidth," Applied Physics Letters **111** (2017).
[461]A. Krushynska, F. Bosia, M. Miniaci, and N. Pugno, "Spider web-structured labyrinthine acoustic metamaterials for low-frequency sound control," New Journal of Physics **19**, 105001 (2017).
[462]T. Frenzel, J. David Brehm, T. Bückmann, R. Schittny, M. Kadic, and M. Wegener, "Three-dimensional labyrinthine acoustic metamaterials," Applied Physics Letters **103**, 061907 (2013).

[463] J.-S. Chen, Y.-T. Chung, C.-Y. Wang, W.-Y. Lo, C.-H. Liu, C.-H. Yu, I.-L. Chang, and T.-R. Lin, "Ultrathin arch-like labyrinthine acoustic metasurface for low-frequency sound absorption," Applied Acoustics **202**, 109142 (2023).

[464] S. Han, W. Zhang, G. Ma, C. Wu, and Z. Chen, "Ultrathin reflective acoustic metasurface based on the synergetic coupling of resonant cavity and labyrinthine beams," Modern Physics Letters B **32**, 1850144 (2018).

[465] Y. Zhou, "Visco-thermal effects on anisotropic and isotropic labyrinthine acoustic metamaterials in the cascade," Journal of Vibration Engineering & Technologies , 1–10 (2023).

[466] X. Fu, G. Li, M. Lu, G. Lu, and X. Huang, "A 3d space coiling metamaterial with isotropic negative acoustic properties," Applied Physics Letters **111**, 251904 (2017).

[467] Y. Chu, T. Chen, and D. Yu, "Acoustic enhancement and weak signal detection based on the space-coiling gradient acoustic grating," Applied Physics Express **13**, 097002 (2020).

[468] B. Xia, L. Li, J. Liu, and D. Yu, "Acoustic metamaterial with fractal coiling up space for sound blocking in a deep subwavelength scale," Journal of Vibration and Acoustics **140** (2018).

[469] B. Yuan, Y. Cheng, and X. Liu, "Conversion of sound radiation pattern via gradient acoustic metasurface with space-coiling structure," Applied Physics Express **8**, 027301 (2015).

[470] S. K. Maurya, A. Pandey, S. Shukla, and S. Saxena, "Double negativity in 3d space coiling metamaterials," Scientific reports **6**, 33683 (2016).

[471] S. Chen, Y. Fan, F. Yang, Y. Jin, Q. Fu, J. Zheng, and F. Zhang, "Engineering coiling-up space metasurfaces for broadband low-frequency acoustic absorption," physica status solidi (RRL)–Rapid Research Letters **13**, 1900426 (2019).

[472] S. Tong, C. Ren, and W. Tang, "High-transmission negative refraction in the gradient space-coiling metamaterials," Applied Physics Letters **114**, 204101 (2019).

[473] W. Chen, F. Wu, J. Wen, Z. Ju, L. Yao, H. Zhao, Y. Wang, and Y. Xiao, "Low-frequency sound absorber based on micro-slit entrance and space-coiling channels," Japanese Journal of Applied Physics **59**, 045503 (2020).

[474] Y. Xie, B.-I. Popa, L. Zigoneanu, and S. A. Cummer, "Measurement of a broadband negative index with space-coiling acoustic metamaterials," Physical review letters **110**, 175501 (2013).

[475] H. Ryoo and W. Jeon, "Perfect sound absorption of ultra-thin metasurface based on hybrid resonance and space-coiling," Applied Physics Letters **113** (2018).

[476] S. K. Maurya, A. Pandey, S. Shukla, and S. Saxena, "Predicting double negativity using transmitted phase in space coiling metamaterials," Royal Society Open Science **5**, 171042 (2018).

[477] T. Chen, C. Wang, and D. Yu, "Pressure amplification and directional acoustic sensing based on a gradient metamaterial coupled with space-coiling structure," Mechanical Systems and Signal Processing **181**, 109499 (2022).

[478] W. Tang, C. Ren, S. Tong, and X. Huang, "Sandwich-like space-coiling metasurfaces for weak-dispersion high-efficiency transmission," Applied Physics Letters **115**, 134102 (2019).

[479] Z. Liang, T. Feng, S. Lok, F. Liu, K. B. Ng, C. H. Chan, J. Wang, S. Han, S. Lee, and J. Li, "Space-coiling metamaterials with double negativity and conical dispersion," Scientific reports **3**, 1–6 (2013).

[480] Z. Jia, J. Li, C. Shen, Y. Xie, and S. A. Cummer, "Systematic design of broadband path-coiling acoustic metamaterials," Journal of Applied Physics **123**, 025101 (2018).

[481] Z.-G. Geng, Y.-G. Peng, Y.-X. Shen, D.-G. Zhao, and X.-F. Zhu, "Acoustic delay-line filters based on largely distorted topological insulators," Applied Physics Letters **113**, 033503 (2018).

[482] D.-C. Chen, Q. Wei, P.-Y. Yan, X.-F. Zhu, and D.-J. Wu, "Sound insulation via a reconfigurable ventilation barrier with ultra-thin zigzag structures," Journal of Applied Physics **129** (2021).

[483] Y. Liu, W. Xu, M. Chen, T. Yang, K. Wang, X. Huang, H. Jiang, and Y. Wang, "Three-dimensional fractal structure with double negative and density-near-zero properties on a subwavelength scale," Materials & design **188**, 108470 (2020).

[484] X. Zhao, G. Liu, and D. Xia, "Maze-like acoustic metamaterial for low-frequency broadband noise suppression," Applied Physics Express **13**, 027002 (2020).

[485] S. Kumar and H. Pueh Lee, "Reconfigurable metatiles with circular maze-like space-coiling-based acoustic metastructure for low-to-mid frequency sound attenuation," Journal of Applied Physics **133** (2023).

[486] E. Panahi, A. Hosseinkhani, D. Younesian, and A. Moayedizadeh, "A new circular-maze-shaped phononic crystal with multiband and broadband vibration filtration feature: design and experiment," Acta Mechanica **233**, 4961–4983 (2022).

[487] S. K. Maurya, M. Sahay, S. Shukla, and S. Saxena, "2d and 3d acoustic metamaterials using space coil design," MRS Online Proceedings Library (OPL) **1753**, mrsf14–1753 (2015).

[488] H. Ge, M. Yang, C. Ma, M. Lu, Y. Chen, N. Fang, and P. Sheng, "Breaking the barriers: advances in acoustic functional materials," National Science Review **5**, 159–182 (2017).

[489] Y. Wu, Q. Liang, J. He, J. Feng, and T. Chen, "Deep-subwavelength broadband sound absorbing metasurface based on the update finger coiling-up method," Applied Acoustics **195**, 108846 (2022).

[490] T.-T. Wu, L.-C. Wu, and Z.-G. Huang, "Frequency band-gap measurement of two-dimensional air/silicon phononic crystals using layered slanted finger interdigital transducers," Journal of Applied Physics **97**, 094916 (2005).

[491] Y. Li, X. Jiang, B. Liang, J.-c. Cheng, and L. Zhang, "Metascreen-based acoustic passive phased array," Physical Review Applied **4**, 024003 (2015).

[492] Y. Tian, Q. Wei, Y. Cheng, and X. Liu, "Acoustic holography based on composite metasurface with decoupled modulation of phase and amplitude," Applied Physics Letters **110**, 191901 (2017).

[493] W. Kan, B. Liang, C. Tian, Z. Shen, and J. Cheng, "A broadband low-reflection bending waveguide for airborne sound," Applied Physics Letters **110**, 253502 (2017).

[494] R. Fleury and A. Alù, "Extraordinary sound transmission through density-near-zero ultranarrow channels," Physical review letters **111**, 055501 (2013).

[495] Y. Cheng, C. Zhou, B. Yuan, D. Wu, Q. Wei, and X. Liu, "Ultra-sparse metasurface for high reflection of low-frequency sound based on artificial mie resonances," Nature materials **14**, 1013–1019 (2015).

[496] B. Yuan, J. Liu, C. Liu, Y. Cheng, and X. Liu, "Resonant tunneling compression and evanescent wave amplification by an acoustic metalens," Applied Acoustics **178**, 107993 (2021).

[497] F. Rafique, J. Hui Wu, S. M. A. Naqvi, M. Waqas, and C. R. Liu, "Extremely effective broadband low-frequency sound absorption with inhomogeneous micro-perforated panel (impp) backed with spider-web designed cavities," Proceedings of the Institution of Mechanical Engineers, Part L: Journal of Materials: Design and Applications **237**, 843–858 (2023).

[498] S. Sepehri, H. Jafari, M. M. Mashhadi, M. R. H. Yazdi, and M. M. S. Fakhrabadi, "Study of tunable locally resonant metamaterials: effects of spider-web and snowflake hierarchies," International Journal of Solids and Structures **204**, 81–95 (2020).

[499] M. Miniaci, A. Krushynska, A. B. Movchan, F. Bosia, and N. M. Pugno, "Spider web-inspired acoustic metamaterials," Applied Physics Letters **109**, 071905 (2016).

[500] P. Zhao, K. Zhang, F. Hong, and Z. Deng, "A resonator inspired by spider web for wave propagation in planar periodic lattice," Thin-Walled Structures **174**, 109118 (2022).

[501] V. F. Dal Poggetto, F. Bosia, M. Miniaci, and N. M. Pugno, "Optimization of spider web-inspired phononic crystals to achieve tailored dispersion for diverse objectives," Materials & Design **209**, 109980 (2021).

[502] H. Ruan and D. Li, "Wave propagation properties of a spider-web-like hierarchical acoustic metamaterial," physica status solidi (b) , 2200341 (2022).

[503] N. Gao, H. Hou, and J. H. Wu, "A composite and deformable honeycomb acoustic metamaterial," International Journal of Modern Physics B **32**, 1850204 (2018).

[504] Y. Li, Y. Zhang, and S. Xie, "A lightweight multilayer honeycomb membrane-type acoustic metamaterial," Applied Acoustics **168**, 107427 (2020).

[505] S. Ebrahimi-Nejad and M. Kheybari, "Honeycomb locally resonant absorbing acoustic metamaterials with stop band behavior," Materials Research Express **5**, 105801 (2018).

[506] Z. Li, Y. Li, S. Kumar, and H. P. Lee, "Thermal tuning of negative effective mass density in a two-dimensional acoustic metamaterial with hexagonal lattice," Journal of Applied Physics **126**, 155102 (2019).

[507]N. Sui, X. Yan, T.-Y. Huang, J. Xu, F.-G. Yuan, and Y. Jing, "A lightweight yet sound-proof honeycomb acoustic metamaterial," Applied Physics Letters **106**, 171905 (2015).

[508]M. Kushwaha and B. Djafari-Rouhani, "Sonic stop-bands for periodic arrays of metallic rods: honeycomb structure," Journal of sound and vibration **218**, 697–709 (1998).

[509]S. Xie, D. Wang, Z. Feng, and S. Yang, "Sound absorption performance of microperforated honeycomb metasurface panels with a combination of multiple orifice diameters," Applied Acoustics **158**, 107046 (2020).

[510]P. Zhao, K. Zhang, C. Zhao, L. Qi, and Z. Deng, "In-plane wave propagation analysis for waveguide design of hexagonal lattice with koch snowflake," International Journal of Mechanical Sciences **209**, 106724 (2021).

[511]T. Grabec, M. Koller, P. Sedlák, A. Kruisová, B. Román-Manso, M. Belmonte, P. Miranzo, and H. Seiner, "Frequency-dependent acoustic energy focusing in hexagonal ceramic micro-scaffolds," Wave Motion **92**, 102417 (2020).

[512]F. Yang, E. Wang, X. Shen, X. Zhang, Q. Yin, X. Wang, X. Yang, C. Shen, and W. Peng, "Optimal design of acoustic metamaterial of multiple parallel hexagonal helmholtz resonators by combination of finite element simulation and cuckoo search algorithm," Materials **15**, 6450 (2022).

[513]Z. Zhang, Y. F. Li, F. Meng, and X. Huang, "Topological design of phononic band gap crystals with sixfold symmetric hexagonal lattice," Computational Materials Science **139**, 97–105 (2017).

[514]Y. Chen, M. Kadic, and M. Wegener, "Chiral triclinic metamaterial crystals supporting isotropic acoustical activity and isotropic chiral phonons," Proceedings of the Royal Society A **477**, 20200764 (2021).

[515]N. Jiménez, J.-P. Groby, and V. Romero-García, "Spiral sound-diffusing metasurfaces based on holographic vortices," Scientific reports **11**, 10217 (2021).

[516]W.-T. Gao, C. Yang, Y.-T. Tan, and J. Ren, "Reversible topological non-reciprocity by positive–negative poisson's ratio switch in chiral metamaterials," Applied Physics Letters **121**, 071702 (2022).

[517]A. Spadoni, M. Ruzzene, S. Gonella, and F. Scarpa, "Phononic properties of hexagonal chiral lattices," Wave motion **46**, 435–450 (2009).

[518]F. Yang, J.-S. Yang, Y. Wang, S. Li, M.-G. Zhang, R. Schmidt, and K.-U. Schröder, "Theoretical study on dispersion relations of chiral acoustic metamaterials considering mass-rotation," European Journal of Mechanics-A/Solids **100**, 105005 (2023).

[519]X. Ni, M. Weiner, A. Alu, and A. B. Khanikaev, "Observation of higher-order topological acoustic states protected by generalized chiral symmetry," Nature materials **18**, 113–120 (2019).

[520]T. Yang, M. Chen, B. Xiao, Y. Liu, H. Jiang, and Y. Wang, "Subwavelength chiral spiral acoustic metamaterials for a robust topological acoustic insulator," Applied Sciences **12**, 7778 (2022).

[521]Y. Chen, M. Kadic, S. Guenneau, and M. Wegener, "Isotropic chiral acoustic phonons in 3d quasicrystalline metamaterials," Physical Review Letters **124**, 235502 (2020).

[522]X. Fei, L. Jin, X. Zhang, X. Li, and M. Lu, "Three-dimensional anti-chiral auxetic metamaterial with tunable phononic bandgap," Applied Physics Letters **116**, 021902 (2020).

[523]L. Yu, H. Xue, and B. Zhang, "Antichiral edge states in an acoustic resonator lattice with staggered air flow," Journal of Applied Physics **129** (2021).

[524]X. Wang, W. Chen, C. Lu, X. Tian, and S. Li, "Design of low-frequency and broadband acoustic metamaterials with i-shaped antichiral units," Applied Acoustics **197**, 108946 (2022).

[525]Z. Tao, X. Ren, A. G. Zhao, L. Sun, Y. Zhang, W. Jiang, D. Han, X. Y. Zhang, and Y. M. Xie, "A novel auxetic acoustic metamaterial plate with tunable bandgap," International Journal of Mechanical Sciences **226**, 107414 (2022).

[526]J. He and H.-H. Huang, "Tunable acoustic wave propagation through planar auxetic metamaterial," Journal of Mechanics **34**, 113–122 (2018).

[527]M. Kheybari, C. Daraio, and O. R. Bilal, "Tunable auxetic metamaterials for simultaneous attenuation of airborne sound and elastic vibrations in all directions," Applied Physics Letters **121**, 081702 (2022).

[528]P. Sun, H. Guo, F. Jin, Z. Zhang, N. Liu, T. Yuan, L. Ma, and Y. Wang, "Mechanics and extreme low-frequency band gaps of auxetic hexachiral acoustic metamaterial with internal resonant unit," Applied Acoustics **200**, 109046 (2022).

[529]T. R. Neil, Z. Shen, D. Robert, B. W. Drinkwater, and M. W. Holderied, "Moth wings are acoustic metamaterials," Proceedings of the National Academy of Sciences **117**, 31134–31141 (2020).

[530]T. R. Neil, Z. Shen, D. Robert, B. W. Drinkwater, and M. W. Holderied, "Moth wings as sound absorber metasurface," Proceedings of the Royal Society A **478**, 20220046 (2022).

[531]Y.-T. Wang, Z. Shen, T. R. Neil, M. W. Holderied, E. A. Skelton, and R. V. Craster, "Models for resonant acoustic metasurfaces with application to moth wing ultrasound absorption," Philosophical Transactions of the Royal Society A **380**, 20220005 (2022).

[532]Y. Ma, "Biomimetic coupling structure increases the noise friction and sound absorption effect," Materials **16**, 7148 (2023).

[533]J. Yao, K. Xu, D. Yao, and L. Yao, "A metamaterial cylindrical shell with multiple graded resonators for broadband longitudinal wave attenuation," Frontiers in Physics **11** (2023), 10.3389/fphy.2023.1133586.

[534]Z. Guo, "Hierarchical-porous acoustic metamaterials: a synergic approach to enhance broadband sound absorption," Materials & Design **241**, 112943 (2024).

[535]M. Martínez-Magallanes, E. Cuan-Urquizo, S. E. Crespo-Sánchez, A. P. Valerga, A. Roman-Flores, E. Ramírez-Cedillo, and C. D. Treviño-Quintanilla, "Hierarchical and fractal structured materials: Design, additive manufacturing and mechanical properties," Proceedings of the Institution of Mechanical Engineers, Part L: Journal of Materials: Design and Applications **237**, 650–666 (2023).

[536]M. Miniaci, A. Krushynska, A. S. Gliozzi, N. Kherraz, F. Bosia, and N. M. Pugno, "Design and fabrication of bioinspired hierarchical dissipative elastic metamaterials," Physical Review Applied **10**, 024012 (2018).

[537]J. Fan, B. Song, L. Zhang, X. Wang, Z. Zhang, S. Wei, X. Xiang, X. Zhu, and Y. Shi, "Structural design and additive manufacturing of multifunctional metamaterials with low-frequency sound absorption and load-bearing performances," International Journal of Mechanical Sciences **238**, 107848 (2023).

[538]M. Liang, H. Wu, S. Chen, Z. Fu, R. Zhang, and Z. Xing, "Simulated and experimental research on highly efficient sound absorption of low-frequency broadband acoustic metamaterial based on coiled-up space," Advanced Engineering Materials **25**, 2301221 (2023).

[539]J. Li, H. Guo, P. Sun, Y. Wang, S. Huang, T. Yuan, and H. Zhang, "Topology optimization of anisotropy hierarchical honeycomb acoustic metamaterials for extreme multi-broad band gaps," Mechanics of Advanced Materials and Structures **30**, 3540–3552 (2022).

[540]H. Sagan, *Space-filling curves* (Springer Science & Business Media, 2012).

[541]X. Zhao, G. Liu, C. Zhang, D. Xia, and Z. Lu, "Fractal acoustic metamaterials for transformer noise reduction," Applied Physics Letters **113**, 074101 (2018).

[542]Q. J. Lim, P. Wang, S. J. A. Koh, E. H. Khoo, and K. Bertoldi, "Wave propagation in fractal-inspired self-similar beam lattices," Applied Physics Letters **107**, 221911 (2015).

[543]O. Oltulu, Z. Özer, A. M. Mamedov, and E. Özbay, "Band structures of metacomposite based phononic crystals in quasi-sierpinski fractals," Journal of Silicate Based and Composite Materials **74**, 57–60 (2021).

[544]B. Figeys, R. Jansen, S. Severi, B. Nauwelaers, H. Tilmans, and X. Rottenberg, "Study of broadband propagation characteristic of quasi-fractal phononic crystal for enhanced sensing applications," in *2015 Transducers-2015 18th International Conference on Solid-State Sensors, Actuators and Microsystems (TRANSDUCERS)* (IEEE, 2015) pp. 141–144.

[545]Y. Liu, J.-y. Su, and L. Gao, "The influence of the micro-topology on the phononic band gaps in 2d porous phononic crystals," Physics Letters A **372**, 6784–6789 (2008).

[546]H. Li, Z. Wang, Z. Wang, C. Deng, J. Luo, J. Huang, X. Wang, and H. Yang, "Acoustic multichannel transports of valley edge states in bilayer sonic crystals," Applied Physics Letters **121**, 243101 (2022).

[547]P. Sun, Z. Zhang, H. Guo, N. Liu, W. Jin, T. Yuan, and Y. Wang, "Topological optimization of hierarchical honeycomb acoustic metamaterials for low-frequency extreme broad band gaps," Applied Acoustics **188**, 108579 (2022).

[548]W. Zhang, Y. Zhao, and Y. Ou, "Design of a broadband metasurface sound absorber based on hilbert fractal," Proceedings of the Institution of Mechanical Engineers, Part C: Journal of Mechanical Engineering Science , 09544062231164511 (2023).

[549]T.-z. Wang, T. Jin, Z.-m. Lu, C. Zhang, G.-q. Liu, X. Zhao, and C. Li, "Research on active noise control method compensating for acoustic metamaterial noise barrier in transformer noise reduction," in *2018 IEEE 2nd International Electrical and Energy Conference (CIEEC)* (IEEE, 2018) pp. 648–652.

[550]K. Wang, Y. Liu, and T. Liang, "Band structures in sierpinski triangle fractal porous phononic crystals," Physica B: Condensed Matter **498**, 33–42 (2016).

[551]L. Lyamshev and I. Urusovskii, "Sound diffraction at sierpinski carpet," Acoustical Physics **49**, 700–703 (2003).

[552]L. Tan, J. Yang, J. Kang, and H. Xu, "Sound-scattering properties of sierpinski triangle fractal structures in the near field," Applied Acoustics **196**, 108892 (2022).

[553]P. Woloszyn, "Acoustic diffraction patterns from fractal to urban structures: applications to the sierpinski triangle and to a neoclassical urban facade," in *Fractals in Engineering: New Trends in Theory and Applications* (Springer, 2005) pp. 97–108.

[554]A. Elmadani, A. Idrissi, R. Braik, S. Bensallam, A. Bouaaddi, Y. Achaoui, and H. Jakjoud, "Theoretical evidence for ultrasonic insulation using a fractal-like phononic crystal membranes," European Journal of Applied Physics **4**, 1–5 (2022).

[555]J. Ding, L. Fan, S.-y. Zhang, H. Zhang, and W.-w. Yu, "Simultaneous realization of slow and fast acoustic waves using a fractal structure of koch curve," Scientific Reports **8**, 1481 (2018).

[556]X. Liu, Y. Fan, and Y. An, "The influence of t-square fractal shape holes on the band structure of two-dimensional phononic crystals," Physica B: Condensed Matter **429**, 73–78 (2013).

[557]Z.-z. Yan, C. Zhang, and Y.-s. Wang, "Elastic wave localization in layered phononic crystals with fractal superlattices," Journal of Vibration and Acoustics **135** (2013).

[558]G. d. N. Almeida, E. F. Vergara, A. Lenzi, Á. S. Alves, and J. C. de Jesus, "Low-frequency broadband sound absorption based on cantor fractal porosity," Journal of Applied Physics **133** (2023).

[559]S. H. Lee, C. M. Park, Y. M. Seo, Z. G. Wang, and C. K. Kim, "Acoustic metamaterial with negative density," Physics letters A **373**, 4464–4469 (2009).

[560]V. M. Garcia-Chocano, R. Graciá-Salgado, D. Torrent, F. Cervera, and J. Sanchez-Dehesa, "Quasi-two-dimensional acoustic metamaterial with negative bulk modulus," Physical Review B **85**, 184102 (2012).

[561]P. Li, F. Yang, P. Wang, J. Zhao, and Z. Zhong, "A novel design scheme for acoustic cloaking of complex shape based on region partitioning and multi-origin coordinate transformation," Applied Mathematics and Mechanics **43**, 1641–1656 (2022).

[562]L. Zigoneanu, B.-I. Popa, and S. A. Cummer, "Three-dimensional broadband omnidirectional acoustic ground cloak," Nature materials **13**, 352–355 (2014).

[563]T. Miyashita, R. Taniguchi, and H. Sakamoto, "Experimental full bandgap of a sonic-crystal slab made of a 2d lattice of aluminum rods in air," WCU **9**, 911–914 (2003).

[564]T. Miyashita, "Sonic crystals and sonic wave-guides," Measurement Science and Technology **16**, R47 (2005).

[565]J. Radosz, "Acoustic performance of noise barrier based on sonic crystals with resonant elements," Applied Acoustics **155**, 492–499 (2019).

[566]Z. Lu, X. Yu, S.-K. Lau, B. C. Khoo, and F. Cui, "Membrane-type acoustic metamaterial with eccentric masses for broadband sound isolation," Applied Acoustics **157**, 107003 (2020).

[567]J. M. Manimala and C. Sun, "Microstructural design studies for locally dissipative acoustic metamaterials," Journal of Applied Physics **115**, 023518 (2014).

[568]X. Zhu, K. Li, P. Zhang, J. Zhu, J. Zhang, C. Tian, and S. Liu, "Implementation of dispersion-free slow acoustic wave propagation and phase engineering with helical-structured metamaterials," Nature Communications **7**, 11731 (2016).

[569]H. Gao, Q. Yan, X. Liu, Y. Zhang, Y. Sun, Q. Ding, L. Wang, J. Xu, and H. Yan, "Low-frequency bandgaps of the lightweight single-phase acoustic metamaterials with locally resonant archimedean spirals," Materials **15**, 373 (2022).

[570]A. Shelke, S. Banerjee, T. Zhenhua, and L. Yu, "Spiral lamb waveguide for spatial filtration of frequencies in a confined space," Experimental Mechanics **55**, 1199–1209 (2015).

[571]Y. Wang, H. Zhao, H. Yang, J. Zhong, D. Zhao, Z. Lu, and J. Wen, "A tunable sound-absorbing metamaterial based on coiled-up space," Journal of Applied Physics **123** (2018).

[572]Y. Wang, H. Zhao, H. Yang, J. Zhong, and J. Wen, "A space-coiled acoustic metamaterial with tunable low-frequency sound absorption," Europhysics Letters **120**, 54001 (2018).

[573]Q. Lin and G. Di, "A high-performance sound insulation component for filter capacitors based on coiled-up acoustic metamaterials," physica status solidi (a) **219**, 2200125 (2022).

[574]G. d. N. Almeida, E. F. Vergara, L. R. Barbosa, A. Lenzi, and R. S. Birch, "A low-frequency sound absorber based on micro-slit and coiled cavity," Journal of the Brazilian Society of Mechanical Sciences and Engineering **43**, 1–9 (2021).

[575]N. Sharafkhani, "An ultra-thin multi-layered metamaterial for power transformer noise absorption," Building Acoustics **29**, 53–62 (2022).

[576]Y. Liu, S. Ren, W. Sun, Y. Lei, H. Wang, and X. Zeng, "Broadband low-frequency sound absorbing metastructures based on impedance matching coiled-up cavity," Applied Physics Letters **119** (2021).

[577]S. K. Singh, O. Prakash, and S. Bhattacharya, "Hybrid fractal acoustic metamaterials for low-frequency sound absorber based on cross mixed micro-perforated panel mounted over the fractals structure cavity," Scientific Reports **12**, 20444 (2022).

[578]G. d. N. Almeida, E. F. Vergara, L. R. Barbosa, A. Lenzi, and R. S. Birch, "Sound absorption metasurface with symmetrical coiled spaces and micro slit of variable depth," Applied Acoustics **183**, 108312 (2021).

[579]C. R. Liu, J. H. Wu, Z. Yang, and F. Ma, "Ultra-broadband acoustic absorption of a thin microperforated panel metamaterial with multi-order resonance," Composite Structures **246**, 112366 (2020).

[580]I. Prasetiyo, K. Anwar, F. Brahmana, and K. Sakagami, "Development of stackable subwavelength sound absorber based on coiled-up system," Applied Acoustics **195**, 108842 (2022).

[581]X. Xiang, H. Tian, Y. Huang, X. Wu, and W. Wen, "Manually tunable ventilated metamaterial absorbers," Applied Physics Letters **118**, 053504 (2021).

[582]S. K. Singh, O. Prakash, and S. Bhattacharya, "Novel fractal acoustic metamaterials (fams) for multiple narrow-band near-perfect absorption," Journal of Applied Physics **132** (2022).

[583]M. Yang, S. Chen, C. Fu, and P. Sheng, "Optimal sound-absorbing structures," Materials Horizons **4**, 673–680 (2017).

[584]E. Choi and W. Jeon, "Near-perfect sound absorption using hybrid resonance between subwavelength helmholtz resonators with non-uniformly partitioned cavities," Scientific Reports **14**, 3174 (2024).

[585]Q. Xu, J. Qiao, G. Zhang, and L. Li, "Low-frequency sound-absorbing metasurface constructed by a membrane-covered and coiled helmholtz resonator," Journal of Applied Physics **133** (2023).

[586]G. Hu, L. Tang, and X. Cui, "On the modelling of membrane-coupled helmholtz resonator and its application in acoustic metamaterial system," Mechanical Systems and Signal Processing **132**, 595–608 (2019).

[587]H.-Z. Li, X.-C. Liu, Q. Liu, S. Li, J.-S. Yang, L.-L. Tong, S.-B. Shi, R. Schmidt, and K.-U. Schröder, "Sound insulation performance of double membrane-type acoustic metamaterials combined with a helmholtz resonator," Applied Acoustics **205**, 109297 (2023).

[588]H. Shao, H. He, Y. Chen, X. Tan, and G. Chen, "A tunable metamaterial muffler with a membrane structure based on helmholtz cavities," Applied Acoustics **157**, 107022 (2020).

[589]M. Kim, K. Lee, E. Bok, D. Hong, J. Seo, and S. H. Lee, "Broadband muffler by merging negative density and negative compressibility," Applied Acoustics **208**, 109373 (2023).

[590]H.-B. Shao, H. He, Y. Chen, and G.-P. Chen, "A novel multi-cavity helmholtz muffler," Chinese Physics B **28**, 054303 (2019).

[591]R. Zhang, G. Wang, X. Zhou, and G. Hu, "A decoupling-design strategy for high sound absorption in subwavelength structures with air ventilation," JASA Express Letters **2** (2022).

[592]J. Ji, J. Li, S. A. Cummer, and Y. Jing, "Ultra-sparse near-perfect sound absorbers," JASA Express Letters **3** (2023).

[593]X. Liu, M. Liu, and F. Xin, "Sound absorption of a perforated panel backed with perforated porous material: Energy dissipation of helmholtz resonator cavity," Mechanical Systems and Signal Processing **185**, 109762 (2023).

[594] Y. Zhou, D. Li, Y. Li, and T. Hao, "Perfect acoustic absorption by subwavelength metaporous composite," Applied Physics Letters **115**, 093503 (2019).
[595] H. Huang, J. Chen, and S. Huo, "Recent advances in topological elastic metamaterials," Journal of Physics Condensed Matter **33**, 503002 (2021).
[596] X. Wang, "A topological valley stamping plate for low-frequency-vibration isolation and wave manipulation in helicopters," Processes (2023), 10.3390/pr11102941.
[597] R. Zhu, X. Liu, G. Hu, Y. Fang, and G. Huang, "Microstructural designs of plate-type elastic metamaterial and their potential applications: A review," International Journal of Smart and Nano Materials (2015), 10.1080/19475411.2015.1025249.
[598] A. Colombi, D. Colquitt, P. Roux, S. Guenneau, and R. V. Craster, "A seismic metamaterial: The resonant metawedge," Scientific Reports (2016), 10.1038/srep27717.
[599] Y. Achaoui, T. Antonakakis, S. Brûlé, R. Craster, S. Enoch, and S. Guenneau, "Clamped seismic metamaterials: ultra-low frequency stop bands," New Journal of Physics **19**, 063022 (2017).
[600] J. Xu, H. Lu, W. Qin, P. Wang, and J. Bian, "Mechanical shunt resonators-based piezoelectric metamaterial for elastic wave attenuation," Materials (2022), 10.3390/ma15030891.
[601] D. Mu, K. Wang, H. Shu, and J. Lu, "Low frequency broadband bandgaps in elastic metamaterials with two-stage inertial amplification and elastic foundations," Journal of Physics D Applied Physics (2022), 10.1088/1361-6463/ac7480.
[602] Flexible, fast, predictable, simple, to operate. Manufacture, R. Parts, and in a wide range of thermoplastics., "Fortus 400mctm," (9085).
[603] "Objet350 and objet500 connex and multi-color and multi-material or high quality? choose everything," (0006).
[604] A. complete additive manufacturing platform and for product development directly at your office, "Wematter gravity sls 3d printing system,".
[605] M. Saadi, A. Maguire, N. T. Pottackal, M. S. H. Thakur, M. M. Ikram, A. J. Hart, P. M. Ajayan, and M. M. Rahman, "Direct ink writing: a 3d printing technology for diverse materials," Advanced Materials **34**, 2108855 (2022).
[606] Administrator, "Flashforge corporation," (0086).
[607] D. Systems-the, inventor of stereolithography (SLA), and the only SLA, "Stereolithography printers prototypes, tools and production parts with stereolithography (sla) 3d printers,".
[608] L. Yan, Y. Chen, and F. Liou, "Additive manufacturing of functionally graded metallic materials using laser metal deposition," Additive Manufacturing **31**, 100901 (2020).
[609] F. Ning, "Ultrasonic vibration assisted manufacturing of high-performance materials," (2018).
[610] G. Fusaro, L. Barbaresi, M. Cingolani, M. Garai, E. Ida, A. Prato, and A. Schiavi, "Investigation of the impact of additive manufacturing techniques on the acoustic performance of a coiled-up resonator," The Journal of the Acoustical Society of America **153**, 2921–2921 (2023).
[611] Z. Zhou, I. Salaoru, P. Morris, and G. J. Gibbons, "Development of a direct feed fused deposition modelling technology for multi-material manufacturing," in *AIP Conference Proceedings*, Vol. 1769 (AIP Publishing, 2016).
[612] M. J. Mirzaali, A. Caracciolo, H. Pahlavani, S. Janbaz, L. Vergani, and A. Zadpoor, "Multi-material 3d printed mechanical metamaterials: Rational design of elastic properties through spatial distribution of hard and soft phases," Applied Physics Letters **113** (2018).
[613] S. G. Konarski, C. A. Rohde, R. Gotoh, S. N. Roberts, and C. J. Naify, "Acoustic measurement and statistical characterization of direct-printed, variable-porosity aluminum foams," The Journal of the Acoustical Society of America **149**, 4327–4336 (2021).
[614] V. Vaghasia, H. Parmar, R. Chaudhari, J. K. Vora, K. Abhishek, and S. Kumari, "Recent advancements in the fabrication of multi-material structures by additive manufacturing," in *AIP Conference Proceedings*, Vol. 2960 (AIP Publishing, 2024).
[615] M. C. Halbig and M. Singh, "Additive manufacturing of multi-material systems for aerospace applications," Tech. Rep. (2019).
[616] B. Tiller, A. Reid, B. Zhu, J. Guerreiro, R. Domingo-Roca, J. C. Jackson, and J. Windmill, "Piezoelectric microphone via a digital light processing 3d printing process," Materials & Design **165**, 107593 (2019).
[617] J. Zhang, Y. Yang, B. Zhu, X. Li, J. Jin, Z. Chen, Y. Chen, and Q. Zhou, "Multifocal point beam forming by a single ultrasonic transducer with 3d printed holograms," Applied Physics Letters **113** (2018).
[618] W. Elmadih, D. Chronopoulos, W. Syam, I. Maskery, H. Meng, and R. Leach, "Three-dimensional resonating metamaterials for low-frequency vibration attenuation," Scientific reports **9**, 11503 (2019).
[619] Mach and start now., "Mach 100 waterjet series,".
[620] E. precision waterjet Benefits, solution Highly, and precise waterjet solution, "be precise,".
[621] S. Spadło, D. Krajcarz, and P. Młynarczyk, "A comparison of laser cutting and water-jet cutting," Journal of Achievements in Materials and Manufacturing Engineering **66**, 87–92 (2014).
[622] L. Sabine, "Technical datasheet," (0002).
[623] H. E. Quinlan, T. Hasan, J. Jaddou, and A. J. Hart, "Industrial and consumer uses of additive manufacturing: A discussion of capabilities, trajectories, and challenges," (2017).
[624] Administrator, "Flashforge corporation," (0086).
[625] www.advancedmachinery.co.uk, "Vmc 600-30 parts manual," (0844).
[626] S. Bansal and S. Subramanian, "A microfluidic acoustic metamaterial using electrowetting: Enabling active broadband tunability," Advanced Materials Technologies **6**, 2100491 (2021).
[627] S. Schweiger and S. G. Koch, "A review of acoustic impedance matching methods to validate additive manufactured metamaterial for capacitive micromachined ultrasonic transducers," in *2018 41st International Spring Seminar on Electronics Technology (ISSE)* (IEEE, 2018) pp. 1–7.
[628] M. today's and fast paced, "Built for a smarter digital future the new slx series,".
[629] B. Ai, S. Larson, L. Bradley, and Y. Zhao, "A flexible strategy to fabricate gradient plasmonic nanostructures," Advanced Materials Interfaces **5** (2018), 10.1002/admi.201800975.
[630] W. Gao, K. Guo, J. Sun, and B. Yang, "3d printed niti alloy lattice cantilever beam acoustic metamaterial," Journal of Physics Conference Series **2252**, 012009 (2022).
[631] H. Dong, C. Shen, S. Zhao, W. Qiu, H. Zheng, Z. Chuan-zeng, S. Cummer, Y. Wang, D. Fang, and C. Li, "Achromatic metasurfaces by dispersion customization for ultra-broadband acoustic beam engineering," National Science Review **9** (2022), 10.1093/nsr/nwac030.
[632] A. Vanel, "Collimated beam formation in 3d acoustic sonic crystals," New Journal of Physics **26**, 073021 (2024).
[633] A. Almesmari, "Review of additively manufactured polymeric metamaterials: design, fabrication, testing and modeling," Polymers **15**, 3858 (2023).
[634] R. Palanisamy, "Void-engineered metamaterial delay line with built-in impedance matching for ultrasonic applications," Sensors **24**, 995 (2024).
[635] Y. Wang, X. Wang, Y. Mei, and N. Chang, "An optimization method for design of acoustic metamaterial structure," Matec Web of Conferences **175**, 01023 (2018).
[636] Q. Aumann, M. Miksch, and G. Müller, "Numerical models for evaluating the vibro-acoustic properties of acoustic metamaterials," PAMM **18**, e201800174 (2018).
[637] D. Yago, G. Sal-Anglada, D. Roca, J. Cante, and J. Oliver, "Machine learning in solid mechanics: Application to acoustic metamaterial design," International Journal for Numerical Methods in Engineering , e7476 (2024).
[638] C. Ma, Y. Chang, S. Wu, and R. Zhao, "Deep learning-accelerated designs of tunable magneto-mechanical metamaterials," Acs Applied Materials & Interfaces **14**, 33892–33902 (2022).
[639] H. Tang, Z. Chen, N. Tang, S. Li, Y. Shen, Y. Peng, X. Zhu, and J. Zang, "Hollow-out patterning ultrathin acoustic metasurfaces for multifunctionalities using soft fiber/rigid bead networks," Advanced Functional Materials **28** (2018), 10.1002/adfm.201801127.
[640] C. Choi, S. Bansal, N. Münzenrieder, and S. Subramanian, "Fabricating and assembling acoustic metamaterials and phononic crystals," advanced engineering materials **23**, 2000988 (2021).
[641] C. Shen, C. Rohde, C. Cushing, J. Li, Z. Tan, H. Du, X. Peng, P. Wilson, N. Fang, and S. Cummer, "Anisotropic metallic microlattice structures for underwater operations," Advanced Engineering Materials **25** (2022), 10.1002/adem.202201294.
[642] U. Iemma and G. Palma, "Design of metacontinua in the aeroacoustic spacetime," Scientific Reports **10** (2020), 10.1038/s41598-020-74304-5.

[643] P. Mittal, "Convergence of machine learning with microfluidics and metamaterials to build smart materials," International Journal on Interactive Design and Manufacturing (Ijidem) (2024), 10.1007/s12008-023-01707-9.

[644] X. Wu, Y. Su, and J. Shi, "Perspective of additive manufacturing for metamaterials development," Smart Materials and Structures **28**, 093001 (2019).

[645] R. M. Heeb, M. Dicker, and B. K. Woods, "Manufacturing and characterisation of 3d printed thermoplastic morphing skins," Smart Materials and Structures **31**, 085007 (2022).

[646] R. M. HEEB, *Multi-material 3D Printed Thermoplastic Morphing Aircraft Skins: Manufacturing, Testing, Analysis, and Design Space Exploration*, Ph.D. thesis, University of Bristol (2023).

[647] W. Yang, J. An, C. Chua, and K. Zhou, "Acoustic absorptions of multifunctional polymeric cellular structures based on triply periodic minimal surfaces fabricated by stereolithography," Virtual and Physical Prototyping **15**, 242–249 (2020).

[648] Z. Xin-dong, X. Wang, and F. Xin, "Ultrathin acoustic metamaterial as super absorber for broadband low-frequency underwater sound," Scientific Reports **13** (2023), 10.1038/s41598-023-34993-0.

[649] C. Wong, S. Chan, W. Wu, C. Suen, H. Yau, D. Wang, and S. Li, "Tunable high acoustic impedance alumina epoxy composite matching for high frequency ultrasound transducer," Ultrasonics **116**, 106506 (2021).

[650] P. Daly, J. Windmill, and J. Jackson, "Generating characteristic acoustic impedances with hydrogel based phononic crystals for use in ultrasonic transducer matching layers," The Journal of the Acoustical Society of America **150**, A148–A148 (2021).

[651] H. Li, B. Zheng, M. Duan, F. Hong, Y. Hu, X. Li, S. Qian, X. Chen, and S. Liu, "Helmholtz-structured two-dimensional super-diffraction metalens," Frontiers in Physics **10** (2022), 10.3389/fphy.2022.923637.

[652] Y. Jin, M. Zhou, T. Choi, and A. Neogi, "Thermally tunable acoustic beam splitter based on poly(vinyl alcohol) poly(n-isopropylacrylamide) hydrogel," Gels **7**, 140 (2021).

[653] K. Zhang, C. Ma, Q. He, S. Lin, Y. Chen, Y. Zhang, N. X. Fang, and X. Zhao, "Metagel with broadband tunable acoustic properties over air-water-solid ranges," Advanced Functional Materials **29**, 1903699 (2019).

[654] R. Rust, A. Xydis, K. Heutschi, N. Perraudin, G. Casas, C. Du, J. Strauss, K. Eggenschwiler, F. Pérez-Cruz, F. Gramazio, and M. Köhler, "A data acquisition setup for data driven acoustic design," Building Acoustics **28**, 345–360 (2021).

[655] E. Hamdan and M. Fletcher, "A compact two-loudspeaker virtual sound reproduction system for clinical testing of spatial hearing with hearing-assistive devices," Frontiers in Neuroscience **15** (2022), 10.3389/fnins.2021.725127.

[656] J. Robertson and S. Becker, "Influence of acoustic reflection on the inertial cavitation dose in a franz diffusion cell," Ultrasound in Medicine & Biology **44**, 1100–1109 (2018).

[657] M. Amorim, R. Vasconcelos, M. Bolgan, S. Pedroso, and P. Fonseca, "Acoustic communication in marine shallow waters: testing the acoustic adaptive hypothesis in sand gobies," Journal of Experimental Biology (2018), 10.1242/jeb.183681.

[658] M. Kobecki, G. Tandoi, E. Di Gaetano, M. Sorel, A. V. Scherbakov, T. Czerniuk, C. Schneider, M. Kamp, S. Höfling, A. V. Akimov, *et al.*, "Picosecond ultrasonics with miniaturized semiconductor lasers," Ultrasonics **106**, 106150 (2020).

[659] K. Loskutova, D. Nimander, I. Gouwy, H. Chen, M. Ghorbani, A. Svagan, and D. Grishenkov, "A study on the acoustic response of pickering perfluoropentane droplets in different media," Acs Omega **6**, 5670–5678 (2021).

[660] T. Weissgerber, T. Stöver, and U. Baumann, "Speech perception in noise: Impact of directional microphones in users of combined electric-acoustic stimulation," PLoS one **14**, e0213251 (2019).

[661] V. Saxena, V. Kornilov, I. Arteaga, and L. Goey, "Designing variable reflection coefficient for upstream and downstream terminations to study their effect on flame thermoacoustics," International Journal of Spray and Combustion Dynamics **14**, 251–265 (2022).

[662] R. Nuster and G. Paltauf, "Comparison of piezoelectric and optical projection imaging for three-dimensional in vivo photoacoustic tomography," Journal of Imaging **5**, 15 (2019).

[663] J. O. Vasseur, P. Deymier, A. Khelif, P. Lambin, B. Djafari-Rouhani, A. Akjouj, L. Dobrzynski, N. Fettouhi, and J. Zemmouri, "Phononic crystal with low filling fraction and absolute acoustic band gap in the audible frequency range: A theoretical and experimental study," Physical Review E **65**, 056608 (2002).

[664] H. Zhong, Y. Tian, N. Gao, K. Lu, and J. Wu, "Ultra-thin composite underwater honeycomb-type acoustic metamaterial with broadband sound insulation and high hydrostatic pressure resistance," Composite structures **277**, 114603 (2021).

[665] S. van den Broek, J. Wolff, S. Scheffler, C. Hühne, and R. Rolfes, "Improving the fatigue life of printed structures using stochastic variations," Progress in Additive Manufacturing , 1–14 (2022).

[666] J. Zhao, X. Li, Y. Wang, W. Wang, B. Zhang, and X. Gai, "Membrane acoustic metamaterial absorbers with magnetic negative stiffness," The Journal of the Acoustical Society of America **141**, 840–846 (2017).

[667] Z.-x. Xu, H.-y. Meng, A. Chen, J. Yang, B. Liang, and J.-c. Cheng, "Tunable low-frequency and broadband acoustic metamaterial absorber," Journal of Applied Physics **129** (2021).

[668] K. Zimny, A. Merlin, A. Ba, C. Aristégui, T. Brunet, and O. Mondain-Monval, "Soft porous silicone rubbers as key elements for the realization of acoustic metamaterials," Langmuir **31**, 3215–3221 (2015).

[669] X. Y. Zhang, X. Ren, Y. Zhang, and Y. M. Xie, "A novel auxetic metamaterial with enhanced mechanical properties and tunable auxeticity," Thin-Walled Structures **174**, 109162 (2022).

[670] F. Ma, M. Huang, and J. H. Wu, "Ultrathin lightweight plate-type acoustic metamaterials with positive lumped coupling resonant," Journal of Applied Physics **121**, 015102 (2017).

[671] X. Zhao, O. Kaya, M. Pirro, P. Simeoni, J. Segovia-Fernandez, and C. Cassella, "Extending the linearity of alscn contour-mode-resonators through acoustic metamaterials-based reflectors," IEEE Transactions on Ultrasonics, Ferroelectrics, and Frequency Control (2023).

[672] J. Hwang, A. Baskota, B. Davaji, J. Kuo, and A. Lal, "Gigahertz metamaterial ultrasonic lens characterization using ghz cmos integrated ultrasonic micro imager," in *2022 IEEE International Ultrasonics Symposium (IUS)* (IEEE, 2022) pp. 1–4.

[673] D. R. Schipf, G. H. Yesner, L. Sotelo, C. Brown, and M. D. Guild, "Barium titanate 3–3 piezoelectric composites fabricated using binder jet printing," Additive Manufacturing **55**, 102804 (2022).

[674] S. Rezaei, M. Eskandari-Ghadi, and M. Rahimian, "Development of an acoustic metamaterials for aero acoustic noise control," Journal of Applied Fluid Mechanics **10**, 569–579 (2017).

[675] G. Iannace, G. Ciaburro, and A. Trematerra, "Metamaterials acoustic barrier," Applied Acoustics **181**, 108172 (2021).

[676] M. M. Indaleeb, H. Ahmed, M. Saadatzi, and S. Banerjee, "Deaf band-based prediction of dirac cone in acoustic metamaterials," Journal of Applied Physics **127**, 064903 (2020).

[677] X. An, C. Lai, H. Fan, and C. Zhang, "3d acoustic metamaterial-based mechanical metalattice structures for low-frequency and broadband vibration attenuation," International Journal of Solids and Structures **191**, 293–306 (2020).

[678] S.-l. Cheng, H.-y. Yang, Q. Ding, Q. Yan, Y.-t. Sun, Y.-j. Xin, and L. Wang, "Low frequency band gap and wave propagation properties of a novel fractal hybrid metamaterial," physica status solidi (b) **259**, 2200257 (2022).

[679] C. Xu, H. Guo, Y. Chen, X. Dong, H. Ye, and Y. Wang, "Study on broadband low-frequency sound insulation of multi-channel resonator acoustic metamaterials," AIP Advances **11**, 045321 (2021).

[680] L. Zhao, E. Laredo, O. Ryan, A. Yazdkhasti, H.-T. Kim, R. Ganye, T. Horiuchi, and M. Yu, "Ultrasound beam steering with flattened acoustic metamaterial luneburg lens," Applied physics letters **116**, 071902 (2020).

[681] X. Duanqi, W. Zheng, and C. Jinjing, "Acoustic design of a reverberation chamber," Applied Acoustics **32**, 83–91 (1991).

[682] B. Standard, "Bs en iso 354: 2003," Acoustics-Measurement of sound absorption in a reverberation room (2003).

[683] E. ASTM, "1050-98," Standard Test Method for Impedance and Absorption of Acoustical Materials Using Tube, Two Microphones and A Digital Frequency Analysis System, American Society for Testing and Materials (1998).

[684] A. International, "Astm e2611-09 standard test method for measurement of normal incidence sound transmission of acoustical materials based on the transfer matrix method," (ASTM, 2009).

[685] Y. Salissou, R. Panneton, and O. Doutres, "Complement to standard method for measuring normal incidence sound transmission loss with three microphones," The Journal of the Acoustical Society of America **131**, EL216–EL222 (2012).

[686] B. Chung and H. Chuah, "Design and construction of a multipurpose wideband anechoic chamber," IEEE Antennas and Propagation Magazine **45**, 41–47 (2003).

[687] S. Gade, K. Ginn, O. Roth, and M. Brock, "Sound power determination in highly reactive environments using sound intensity measurements," in *Proceedings of Inter-Noise*, Vol. 83 (1983) pp. 1047–1050.

[688] X. Wang, Y. Chen, G. Zhou, T. Chen, and F. Ma, "Synergetic coupling large-scale plate-type acoustic metamaterial panel for broadband sound insulation," Journal of Sound and Vibration **459**, 114867 (2019).

[689] L. Wu, Z. Zhai, X. Zhao, X. Tian, D. Li, Q. Wang, and H. Jiang, "Modular design for acoustic metamaterials: Low-frequency noise attenuation," Advanced Functional Materials **32**, 2105712 (2022).

[690] M. Yang and P. Sheng, "Acoustic metamaterial absorbers: The path to commercialization," Applied Physics Letters **122** (2023).

[691] E. De Bono, *Electro-active boundary control for noise mitigation: local and advective strategie*, Ph.D. thesis, Université de Lyon (2021).

[692] W. Akl and A. Baz, "Analysis and experimental demonstration of an active acoustic metamaterial cell," Journal of Applied Physics **111** (2012).

[693] A. Baz, "The structure of an active acoustic metamaterial with tunable effective density," New Journal of Physics **11**, 123010 (2009).

[694] S. Sergeev, R. Fleury, and H. Lissek, "Ultrabroadband sound control with deep-subwavelength plasmacoustic metalayers," Nature Communications **14**, 2874 (2023).

[695] S. Sergeev, H. Lissek, A. Howling, I. Furno, G. Plyushchev, and P. Leyland, "Development of a plasma electroacoustic actuator for active noise control applications," Journal of Physics D: Applied Physics **53**, 495202 (2020).

[696] M. Collet, P. David, and M. Berthillier, "Active acoustical impedance using distributed electrodynamical transducers," The Journal of the Acoustical Society of America **125**, 882–894 (2009).

[697] K. Billon, E. De Bono, M. Perez, E. Salze, G. Matten, M. Gillet, M. Ouisse, M. Volery, H. Lissek, J. Mardjono, *et al.*, "In flow acoustic characterisation of a 2d active liner with local and non local strategies." Applied Acoustics **191**, 108655 (2022).

[698] Y. Du, W. Wu, W. Chen, Y. Lin, and Q. Chi, "Control the structure to optimize the performance of sound absorption of acoustic metamaterial: A review," AIP Advances **11** (2021).

[699] A. Jaschke and A. Bos, "Concept and considerations of a medical device: the active noise cancelling incubator," Frontiers in Pediatrics **11** (2023), 10.3389/fped.2023.1187815.

[700] J. Cheer, S. Daley, and C. McCormick, "Feedforward control of sound transmission using an active acoustic metamaterial," Smart Materials and Structures **26**, 025032 (2017).

[701] M. Iranpour, A. Loghmani, and M. Danesh, "Active noise control for global broadband noise attenuation in a cylindrical cavity using modal fxlms algorithm," Journal of Vibration and Control **30**, 266–277 (2024).

[702] Z. Li, Y. Ke, G. Wu, and M. Tao, "Topology optimization combined with a genetic algorithm to design structured materials for underwater broadband acoustic absorption," Journal of Vibration and Control **29**, 5138–5147 (2023).

[703] M. T. Akhtar, F. Albu, and A. Nishihara, "Prediction error method (pem)-based howling cancellation in hearing aids: Can we do better?" IEEE Access **11**, 337–364 (2022).

[704] S. Yan, X. Luo, X. Sun, J. Xiao, and J. Jiang, "Indoor acoustic signals enhanced algorithm and visualization analysis," Computational Intelligence and Neuroscience **2021**, 7592064 (2021).

[705] C. Zhang and X. Hu, "Three-dimensional single-port labyrinthine acoustic metamaterial: Perfect absorption with large bandwidth and tunability," Physical Review Applied **6**, 064025 (2016).

[706] C. Chen, Z. Du, G. Hu, and J. Yang, "A low-frequency sound absorbing material with subwavelength thickness," Applied Physics Letters **110** (2017).

[707] Y. Tang, F. Xin, L. Huang, and T. Lu, "Deep subwavelength acoustic metamaterial for low-frequency sound absorption," Europhysics Letters **118**, 44002 (2017).

[708] X. Cai, Q. Guo, G. Hu, and J. Yang, "Ultrathin low-frequency sound absorbing panels based on coplanar spiral tubes or coplanar helmholtz resonators," Applied Physics Letters **105** (2014).

[709] J. Lloyd, C. Ludwikowski, C. Malik, and C. Shen, "Mitigating inaudible ultrasound attacks on voice assistants with acoustic metamaterials," Ieee Access **11**, 36464–36470 (2023).

[710] M. Yuan, Z. Cao, J. Luo, and X. Chou, "Recent developments of acoustic energy harvesting: a review," Micromachines **10**, 48 (2019).

[711] C. M. K. Choi, *Design, Fabrication, and Evaluation of Reconfigurable Acoustic Metamaterials*, Ph.D. thesis, UCL (University College London) (2024).

[712] C. Rasmussen, L. Quan, and A. Alù, "Acoustic nonreciprocity," Journal of Applied Physics **129** (2021).

[713] Q. Wang, Z. Zhou, D. Liu, H. Ding, M. Gu, and Y. Li, "Acoustic topological beam nonreciprocity via the rotational doppler effect," Science advances **8**, eabq4451 (2022).

[714] B. Wu, W. Jiang, J. Jiang, Z. Zhao, Y. Tang, W. Zhou, and W. Chen, "Wave manipulation in intelligent metamaterials: recent progress and prospects," Advanced Functional Materials , 2316745 (2024).

[715] G. Cerniauskas, H. Sadia, and P. Alam, "Machine intelligence in metamaterials design: a review," Oxford Open Materials Science **4**, itae001 (2024).

[716] O. Ikechukwu, Z. Long, D. Lee, X. Zhang, W. Zhang, and O. Moses, "Fundamental issues in the qualification of smart and intelligence in building materials discourse: a systematic review," Buildings **11**, 558 (2021).

[717] A. S. Lakamanahalli, M. G. Hudedmani, G. Shweta, P. Hoskeri, and S. N. Mathad, "Metamaterials: A comprehensive review of design and applications," .

[718] N. M. Ravindra, "Recent advancements in composite materials and structures for energy applications," (2024).

[719] C. R. Liu, J. H. Wu, F. Ma, X. Chen, and Z. Yang, "A thin multi-order helmholtz metamaterial with perfect broadband acoustic absorption," Applied Physics Express **12**, 084002 (2019).

[720] X. Peng, J. Li, and S. A. Cummer, "Ultra-broadband low-frequency high-efficiency acoustic energy harvesting with metamaterial-enhanced loudspeakers," Applied Physics Letters **123** (2023).

[721] X. Cui, J. Shi, X. Liu, and Y. Lai, "A panel acoustic energy harvester based on the integration of acoustic metasurface and helmholtz resonator," Applied Physics Letters **119** (2021).

[722] H. Dai, B. Xia, and D. Yu, "Dirac cones in two-dimensional acoustic metamaterials," Journal of Applied Physics **122** (2017).

[723] B. Xia, H. Dai, and D. Yu, "Symmetry-broken metamaterial for blocking, cloaking, and supertunneling of sound in a subwavelength scale," Applied Physics Letters **108** (2016).

[724] H. Su, X. Zhou, X. Xu, and G. Hu, "Experimental study on acoustic subwavelength imaging of holey-structured metamaterials by resonant tunneling," The Journal of the Acoustical Society of America **135**, 1686–1691 (2014).

[725] Y. Cheng, F. Yang, J. Y. Xu, and X. J. Liu, "A multilayer structured acoustic cloak with homogeneous isotropic materials," Applied Physics Letters **92** (2008).

[726] Q. Li and J. S. Vipperman, "Non-singular three-dimensional arbitrarily shaped acoustic cloaks composed of homogeneous parts," Journal of Applied Physics **124** (2018).

[727] Y. Bi, H. Jia, Z. Sun, Y. Yang, H. Zhao, and J. Yang, "Experimental demonstration of three-dimensional broadband underwater acoustic carpet cloak," Applied Physics Letters **112** (2018).

[728] S. Inoue, S. Mogami, T. Ichiyama, A. Noda, Y. Makino, and H. Shinoda, "Acoustical boundary hologram for macroscopic rigid-body levitation," The Journal of the Acoustical Society of America **145**, 328–337 (2019).

[729] C. Zhang, W. K. Cao, L. T. Wu, J. C. Ke, Y. Jing, T. J. Cui, and Q. Cheng, "A reconfigurable active acoustic metalens," Applied Physics Letters **118** (2021).

[730] A. Marzo, A. Ghobrial, L. Cox, M. Caleap, A. Croxford, and B. Drinkwater, "Realization of compact tractor beams using acoustic delay-lines," Applied Physics Letters **110** (2017).

[731] L. Zhao, L. Tang, Y. Liu, Z. Sun, Q. Liu, and C. Bi, "Passive directivity detection of acoustic sources based on acoustic luneburg lens," The Journal of the Acoustical Society of America **154**, 594–601 (2023).

[732] J. W. Rouse, D. Bowman, and T. F. Walsh, "Directional infrasound sensing using acoustic metamaterials," The Journal of the Acoustical Society of America **150**, 367–375 (2021).

[733] T. Sankowsky-Rothe, M. Blau, H. Schepker, and S. Doclo, "Reciprocal measurement of acoustic feedback paths in hearing aids," The Journal of the Acoustical Society of America **138**, EL399–EL404 (2015).

[734] J. Qian, J.-p. Xia, H.-x. Sun, S.-q. Yuan, Y. Ge, and X.-z. Yu, "Broadband acoustic focusing by cavity structures with phase manipulations," Journal of Applied Physics **122** (2017).

[735] X.-y. Gao, X.-b. Cui, Y. Zhang, J.-j. Zhu, and C.-p. Huang, "Acoustoelectric conversion and deep-subwavelength acoustic focusing based on fresnel zone plates," AIP Advances **13** (2023).

[736] L. Bai, G. Y. Song, W. X. Jiang, Q. Cheng, and T. J. Cui, "Acoustic tunable metamaterials based on anisotropic unit cells," Applied Physics Letters **115** (2019).

[737] J. Lan, Y. Liu, T. Wang, Y. Li, and X. Liu, "Acoustic coding metamaterial based on non-uniform mie resonators," Applied Physics Letters **120** (2022).

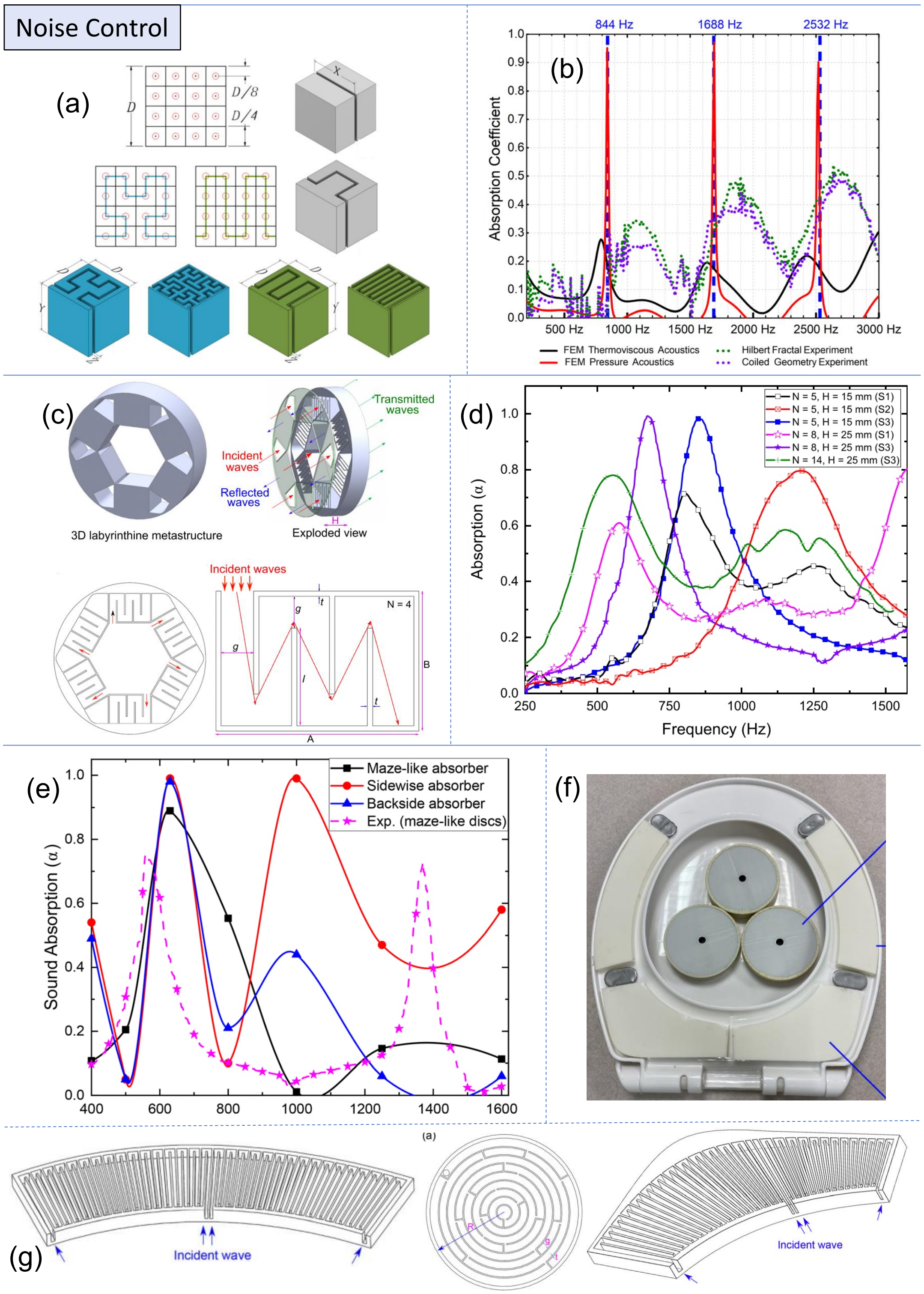

FIG. 2. Examples of noise control through the use of Hilbert fractal and coiled geometries (a)[8] to target acoustic absorption at specific frequencies (b)[8]. Reproduced from G. Comandini, C. Khodr, V. P. Ting, M. Azarpeyvand, F. Scarpa; Sound absorption in Hilbert fractal and coiled acoustic metamaterials. Appl. Phys. Lett. 7 February 2022; 120 (6): 061902, with the permission of AIP Publishing. Coiled geometries (c)[217] that can be used to target noise in HVAC systems through the coils geometry modulation. Strategies for improving low-frequency sound absorption and their measured sound absorption spectra (d)[217]. Reproduced from Sanjay Kumar, Heow Pueh Lee; Labyrinthine acoustic metastructures enabling broadband sound absorption and ventilation. Appl. Phys. Lett. 30 March 2020; 116 (13): 134103, with the permission of AIP Publishing. Water flush noise absorption (e)[56] with experimental devices applicable to a standard toilet seat (f)[56], with coiled and maze geometries (g)[56]. Reprinted with permission from Sanjay Kumar, Chua Wei Shan, Jie Wei Aow, Heow Pueh Lee; Mitigating the toilet flush noise: A psychometric analysis of noise assessment and design of labyrinthine acoustic Meta-absorber for noise mitigation. J. Acoust. Soc. Am. 1 November 2021; 150 (5): 3747-3762. Copyright 2021, Acoustical Society of America.

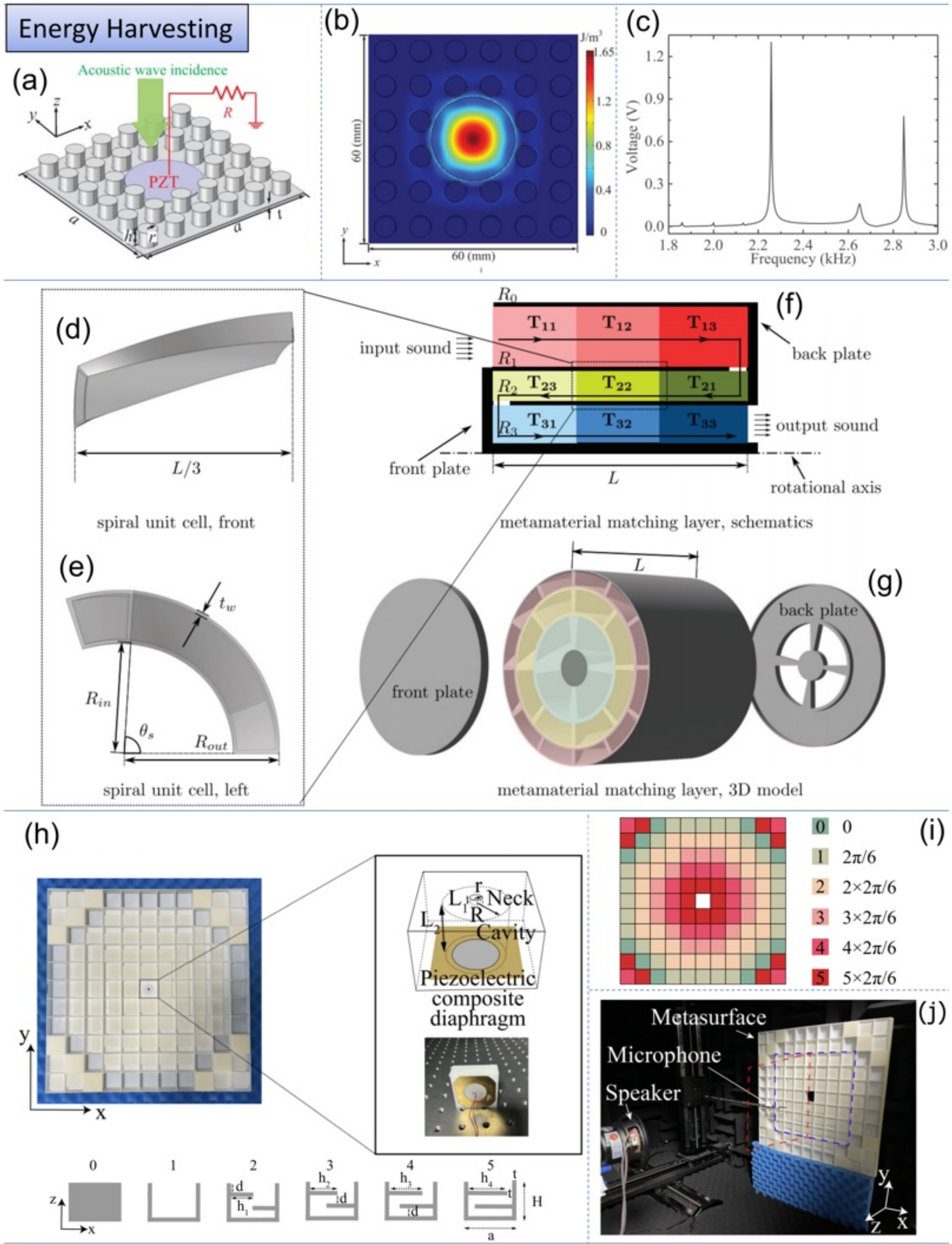

FIG. 3. Schematic representation of an acoustic energy harvesting system composed of a piezoelectric patch and an array of resonant cylinders (a)[2]. FEM analysis of the density of strain energy, in the metamaterial plate, at the frequency of 2257 Hz, with an acoustic pressure of 2 Pa (b)[2]. The harvested voltage at different frequencies by the piezoelectric acoustic metamaterial (c)[2]. Reproduced from Shuibao Qi, Mourad Oudich, Yong Li, Badreddine Assouar; Acoustic energy harvesting based on a planar acoustic metamaterial. Appl. Phys. Lett. 27 June 2016; 108 (26): 263501, with the permission of AIP Publishing. Front view of the spiral unit cell used in the metamaterial matching layer for acoustic energy harvesting (d)[720]. Side view of the spiral unit cell for broadband acoustic energy harvesting (e)[720]. Schematic of the metamaterial matching layer in the acoustic energy harvester (f)[720]. 3D rendering of the stacked spiral unit cells to enhance acoustic energy conversion (g)[720]. Reproduced from Xiuyuan Peng, Junfei Li, Steven A. Cummer; Ultra-broadband low-frequency high-efficiency acoustic energy harvesting with metamaterial-enhanced loudspeakers. Appl. Phys. Lett. 14 August 2023; 123 (7): 073903, with the permission of AIP Publishing. Acoustic metasurface, Helmholtz resonator, and piezoelectric diaphragm for energy harvesting with model, photograph, and schematics (h)[721]. Reflection-phase distribution of the discretized metasurface (i)[721]. Photograph of the experimental apparatus alongside the 3D-printed metasurface sample (j)[721]. Reproduced from Xiaobin Cui, Jinjie Shi, Xiaozhou Liu, Yun Lai; A panel acoustic energy harvester based on the integration of acoustic metasurface and Helmholtz resonator. Appl. Phys. Lett. 20 December 2021; 119 (25): 253903, with the permission of AIP Publishing.

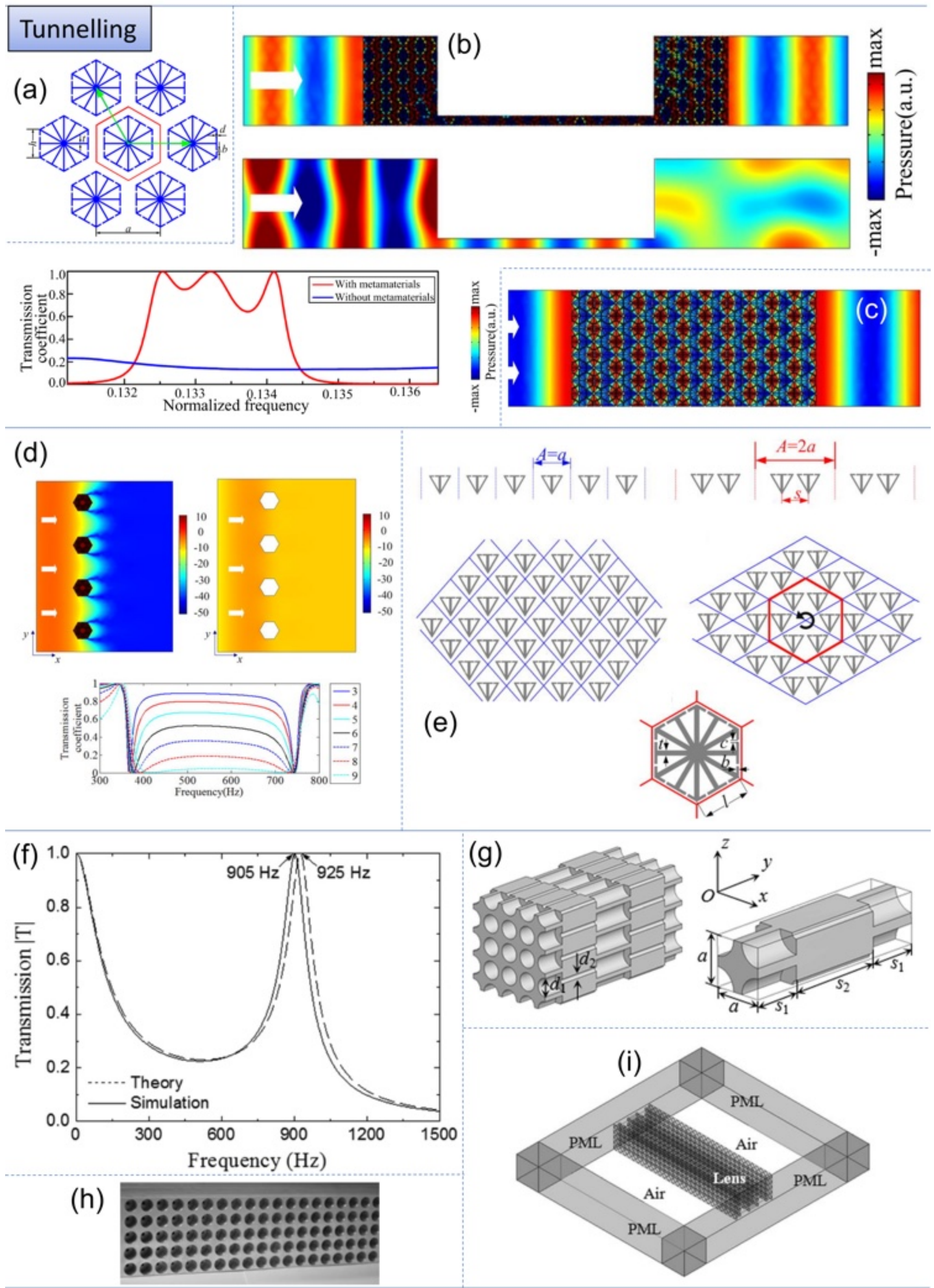

FIG. 4. Tunnelling effect due to a series of hexagonal cells formed by twelve triangular Helmholtz resonators each (a)[722]. Effects in terms of the pressure field, when inside an acoustic duct, there is a rectangular obstacle that narrows the duct geometry, with maximisation of the transmission coefficient for some selected frequencies (b)[722]. Pressure field insensitive to the presence of the acoustic metamaterial layer on both sides of the acoustic duct (c)[722]. Reproduced from Hongqing Dai, Baizhan Xia, Dejie Yu; Dirac cones in two-dimensional acoustic metamaterials. J. Appl. Phys. 14 August 2017; 122 (6): 065103, with the permission of AIP Publishing. Sound pressure distribution in a rectangular waveguide with hollow hexagonal resonators and rigid hexagonal prisms here the transmission coefficients are shown for different numbers of hollow resonators (d)[723]. Schematics of periodic and bi-periodic Helmholtz resonator arrangements, including a regular one-dimensional chain, a bi-periodic chain with varied spacing, a triangular lattice, a bi-periodic hexagonal lattice with rotational symmetry, and a symmetry-broken metamaterial (e)[723]. Reproduced from Baizhan Xia, Hongqing Dai, Dejie Yu; Symmetry-broken metamaterial for blocking, cloaking, and supertunneling of sound in a subwavelength scale. Appl. Phys. Lett. 20 June 2016; 108 (25): 251902, with the permission of AIP Publishing. Experimental and numerical transmission coefficient that underlines values near to one for frequencies around 900 Hz (f)[724]. Design of the internal part of the metamaterial array, with a detail of the single and aggregated cells (g)[724]. Frontal view of the metamaterial array (h)[724]. Sketch of the simulated test rig with boundary conditions (i)[724]. Reproduced from Haijing Su, Xiaoming Zhou, Xianchen Xu, Gengkai Hu; Experimental study on acoustic subwavelength imaging of holey-structured metamaterials by resonant tunneling. J. Acoust. Soc. Am. 1 April 2014; 135 (4): 1686-1691. Copyright 2014, Acoustical Society of America.

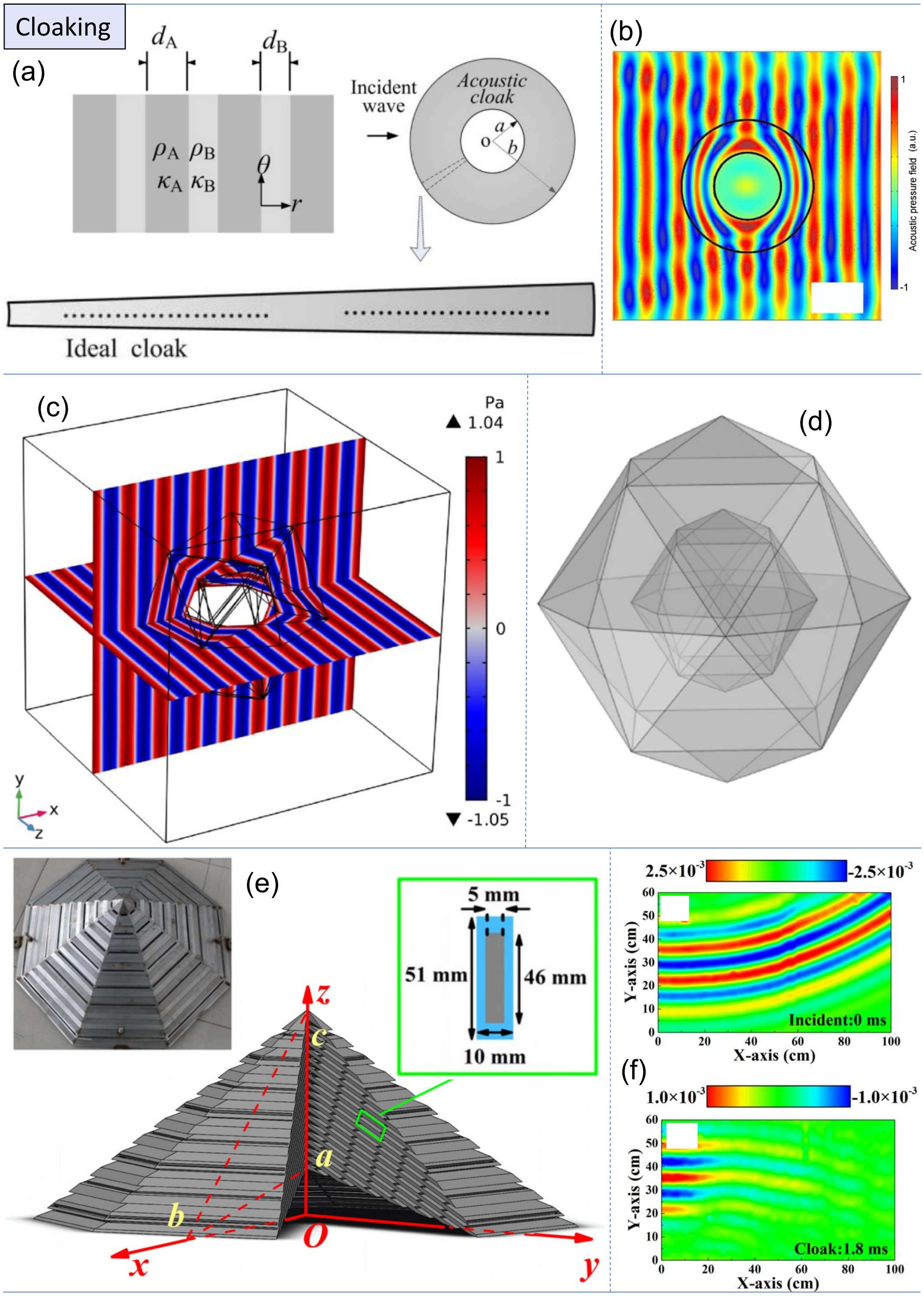

FIG. 5. 2D multilayer cloak system to make acoustically invisible an object inside a circular crown made by slices of acoustic metamaterial capable of avoiding reflections and scattering at some frequencies (a)[725]. FEM example of the interference between acoustic field and the circular metamaterial crown (b)[725]. Reproduced from Ying Cheng, Fan Yang, Jian Yi Xu, Xiao Jun Liu; A multilayer structured acoustic cloak with homogeneous isotropic materials. Appl. Phys. Lett. 14 April 2008; 92 (15): 151913, with the permission of AIP Publishing. 3D cloaking geometry that leaves unperturbed an acoustic pressure field (c)[726]. Polyhedral simulated structure with 32 faces, having cloaking capability at specific frequencies (d)[726]. Reproduced from Qi Li, Jeffrey S. Vipperman; Non-singular three-dimensional arbitrarily shaped acoustic cloaks composed of homogeneous parts. J. Appl. Phys. 21 July 2018; 124 (3): 035103, with the permission of AIP Publishing. Sketch of an underwater cloak with an octagonal pyramidal shape formed by modular inclined parallelepipedal tesserae (e)[727]. Scattered pressure field of the acoustic waves before impacting the metamaterial and after 1.8 seconds, the initially generated waves (f)[727]. Reproduced from Yafeng Bi, Han Jia, Zhaoyong Sun, Yuzhen Yang, Han Zhao, Jun Yang; Experimental demonstration of three-dimensional broadband underwater acoustic carpet cloak. Appl. Phys. Lett. 28 May 2018; 112 (22): 223502, with the permission of AIP Publishing.

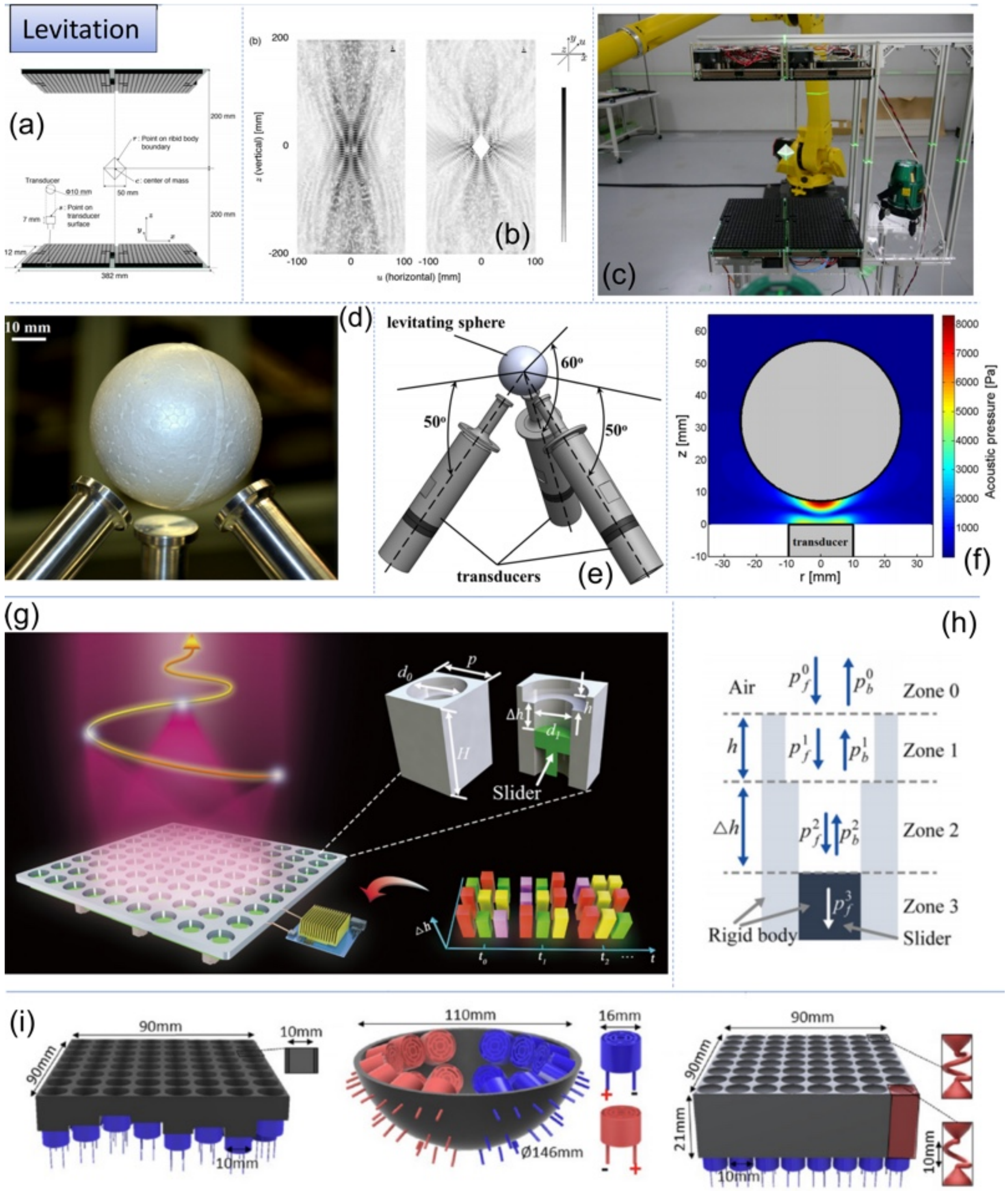

FIG. 6. Octahedron levitated 200 mm above 996-transducer arrays using 40 kHz ultrasound (a)[728]. FEM simulation of acoustic pressure fields for octahedron levitation, showing wave fields with and without the object (b)[728]. Regular octahedron levitating using a double-sided phased array at 40 kHz, demonstrating stable acoustic levitation (c)[728]. Reproduced from Seki Inoue, Shinichi Mogami, Tomohiro Ichiyama, Akihito Noda, Yasutoshi Makino, Hiroyuki Shinoda; Acoustical boundary hologram for macroscopic rigid-body levitation. J. Acoust. Soc. Am. 1 January 2019; 145 (1): 328-337. Copyright 2019, Acoustical Society of America. A 50 mm polystyrene sphere levitated by three 25 kHz ultrasonic transducers using a standing wave (d)[117]. Three 25 kHz ultrasonic transducers arranged in a tripod configuration to levitate a 50 mm polystyrene sphere (e)[117]. Simulated acoustic pressure distribution around a levitated 50 mm polystyrene sphere using 25 kHz ultrasonic transducers (f)[117]. Reproduced from Marco A. B. Andrade, Anne L. Bernassau, Julio C. Adamowski; Acoustic levitation of a large solid sphere. Appl. Phys. Lett. 25 July 2016; 109 (4): 044101, with the permission of AIP Publishing. Active acoustic metalens enabling precise acoustic levitation through dynamic phase control (g)[729]. Transmission line model of a reconfigurable unit cell, enabling dynamic phase adjustments for acoustic levitation (h)[729]. Reproduced from Cheng Zhang, Wen Kang Cao, Li Ting Wu, Jun Chen Ke, Yun Jing, Tie Jun Cui, Qiang Cheng; A reconfigurable active acoustic metalens. Appl. Phys. Lett. 29 March 2021; 118 (13): 133502, with the permission of AIP Publishing. Three designs for creating acoustic tractor beams: Straight Tubes of varying lengths, a Sculpted Surface with precisely aimed transducers, and compact Coiled Tubes. Each device uses a single driving signal for effective particle levitation (i)[730]. Reproduced from A. Marzo, A. Ghobrial, L. Cox, M. Caleap, A. Croxford, B. W. Drinkwater; Realization of compact tractor beams using acoustic delay-lines. Appl. Phys. Lett. 2 January 2017; 110 (1): 014102, with the permission of AIP Publishing.

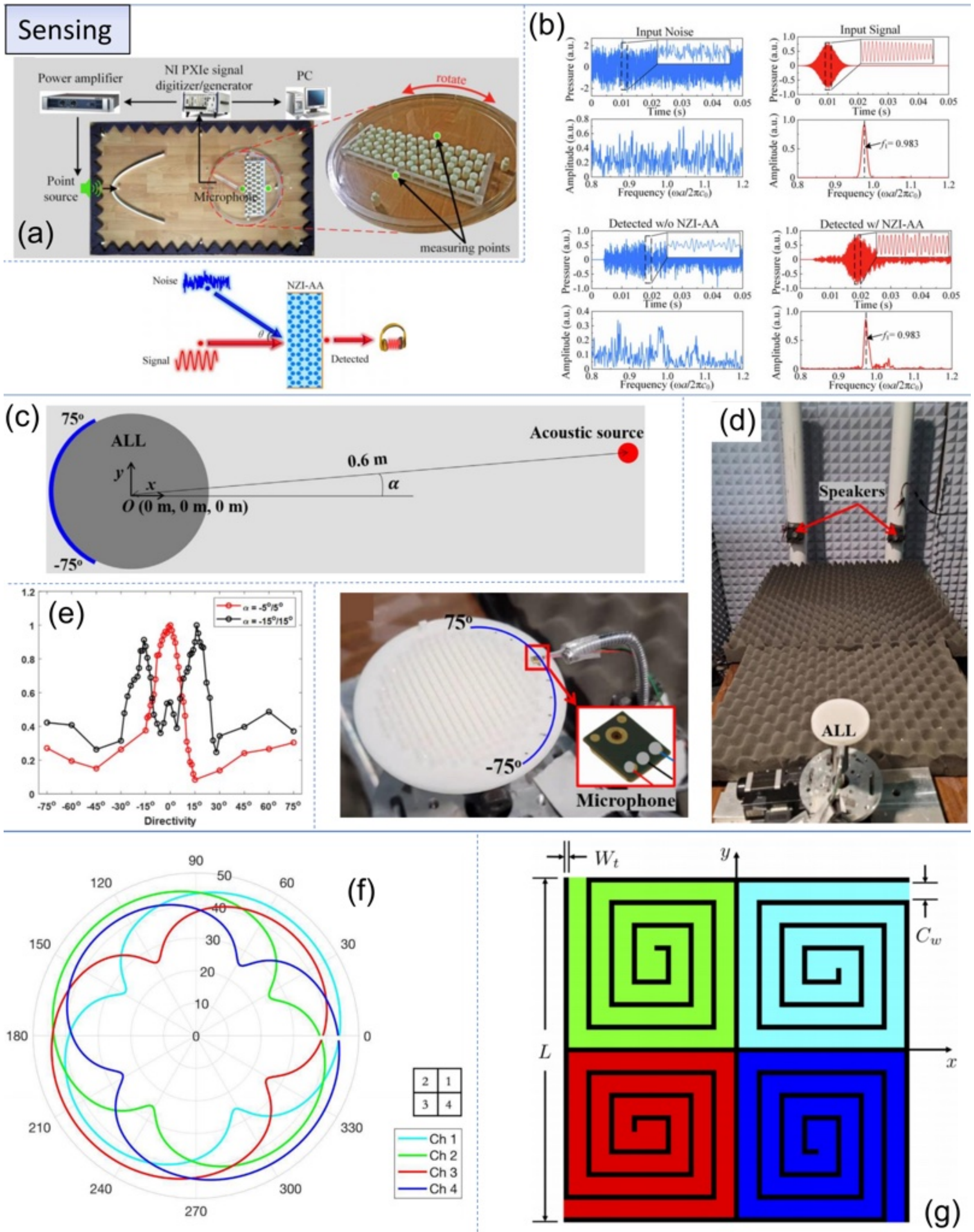

FIG. 7. Test setup of the metamaterial used to check the gain of weak signals in a noisy environment (a)[87]. Time and frequency domain of the input and detected noise, with a schematic representation for the acoustic antenna, with a sketch showing the working principle (b)[87]. Reproduced from Chengrong Ma, Shuxiang Gao, Ying Cheng, Xiaojun Liu; Acoustic metamaterial antennas for combined highly directive-sensitive detection. Appl. Phys. Lett. 29 July 2019; 115 (5): 053501, with the permission of AIP Publishing. Geometric design of noise localisation with an omnidirectional antenna (c)[731]. Laboratory setup with two acoustic sources in a semi-anechoic room (d)[731]. Directivity of the acoustic metamaterial, when the noise source is at different angles (e)[731]. Reproduced from Liuxian Zhao, Lihua Tang, Yuxin Liu, Zhaoyong Sun, Qimin Liu, Chuanxing Bi; Passive directivity detection of acoustic sources based on acoustic Luneburg lens. J. Acoust. Soc. Am. 1 August 2023; 154 (2): 594-601. Copyright 2023, Acoustical Society of America. The normalised pressure variation in sensor channels relative to the incidence angle of a 4.65 Hz plane wave. This distinctive amplitude pattern across the channels enables precise determination of the wave's direction (f)[732]. Diagram of the square coiled-space infrasound sensor, illustrating the channel layout and overall size. This sensor employs acoustic metamaterials to enable directional detection of infrasound waves, offering a much smaller footprint than conventional arrays (g)[732]. Reproduced from Jerry W. Rouse, Daniel Bowman, Timothy F. Walsh; Directional infrasound sensing using acoustic metamaterials. J. Acoust. Soc. Am. 1 July 2021; 150 (1): 367-375. Copyright 2021, Acoustical Society of America.

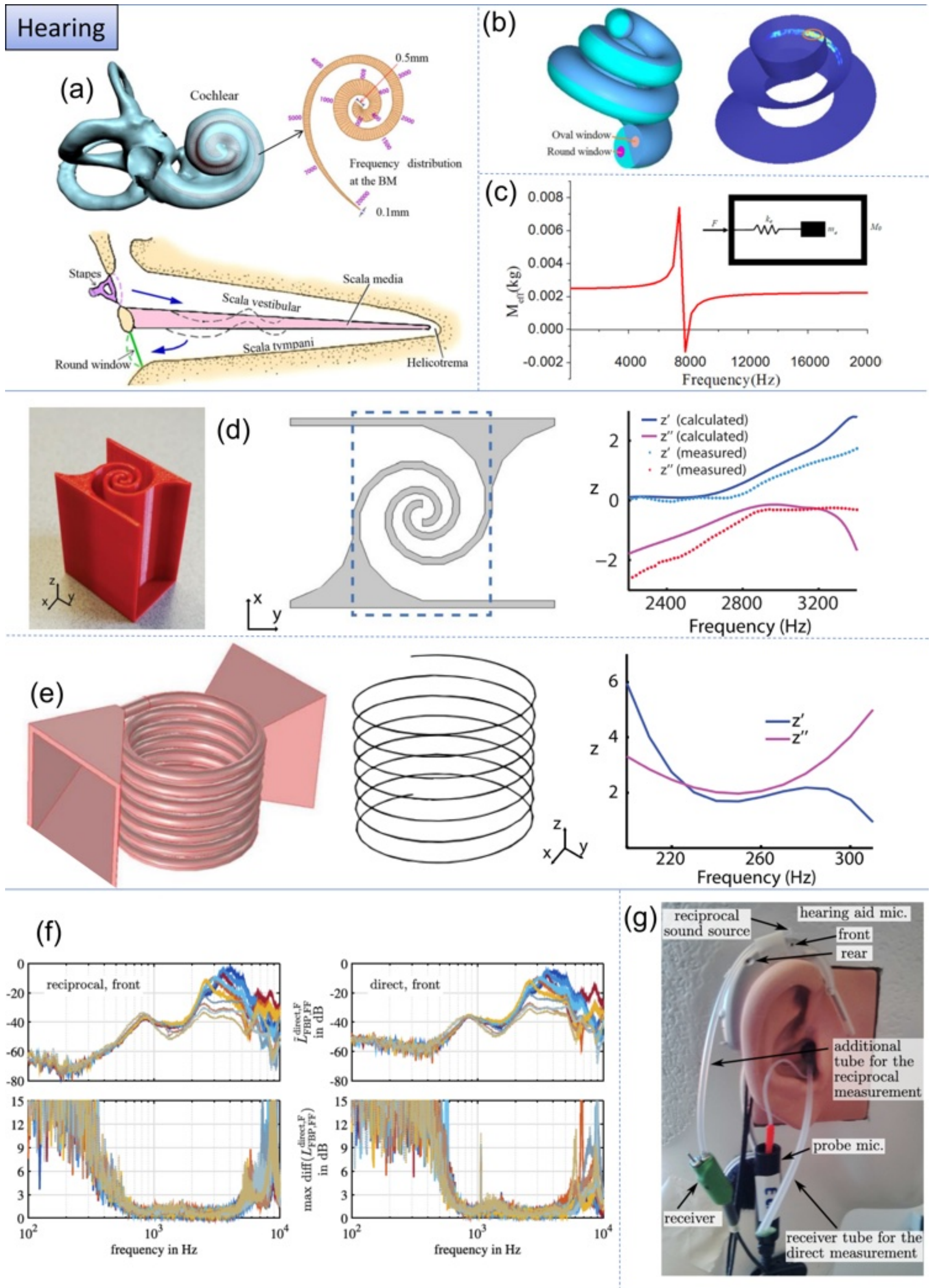

FIG. 8. Structure of the mammalian cochlear geometry with its characteristic tapering on one end of the spiral (a)[72]. Modelled cochlear geometry with a localised natural frequency of near 10 kHz (b)[72]. Model of the effective numerical dynamic mass of a cochlear bionic apparatus (c)[72]. Reproduced from Fuyin Ma, Jiu Hui Wu, Meng Huang, Gang Fu, Changan Bai; Cochlear bionic acoustic metamaterials. Appl. Phys. Lett. 24 November 2014; 105 (21): 213702, with the permission of AIP Publishing. Coiled geometry with a tapered section for impedance match consisting of a 2D extruded shape with experimental and simulated results regarding the impedance matching (d)[21]. 3D helical unit used for impedance matching between the two different mediums and relative FEM results (e)[21]. Reproduced from Yangbo Xie, Adam Konneker, Bogdan-Ioan Popa, Steven A. Cummer; Tapered labyrinthine acoustic metamaterials for broadband impedance matching. Appl. Phys. Lett. 11 November 2013; 103 (20): 201906, with the permission of AIP Publishing. Feedback path levels for venting and ear canal geometries, highlighting higher levels with open earmolds, a high-frequency minimum, and increased levels with smaller ear canals (f)[733]. Hearing aid positioned on the ear, showing the external receiver and probe microphone attached for measuring the reciprocal feedback path (g)[733]. Reproduced from Tobias Sankowsky-Rothe, Matthias Blau, Henning Schepker, Simon Doclo; Reciprocal measurement of acoustic feedback paths in hearing aids. J. Acoust. Soc. Am. 1 October 2015; 138 (4): EL399-EL404. Copyright 2015, Acoustical Society of America.

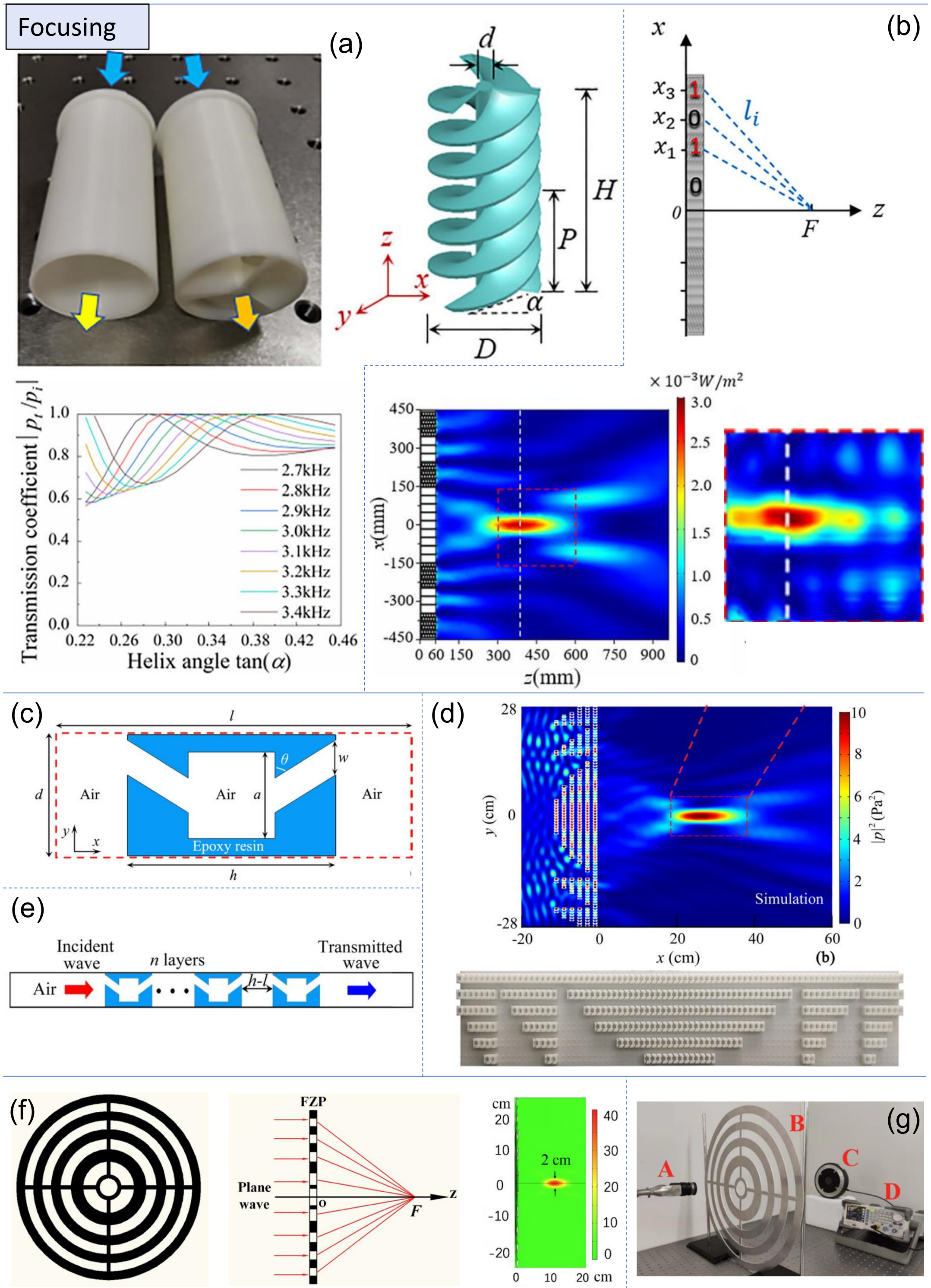

FIG. 9. Modular helix structure that is used to achieve a focusing effect at specific frequencies modulating the helix angle (a)[28]. Schematic representation of the modular metamaterial array that works as a convex lens, focusing the acoustic energy in a relatively small area (b)[28]. Reproduced from Weibai Li, Fei Meng, Xiaodong Huang; Coding metalens with helical-structured units for acoustic focusing and splitting. Appl. Phys. Lett. 13 July 2020; 117 (2): 021901, with the permission of AIP Publishing. Geometry of a single element used to produce a focusing metabehaviour (c)[734]. Simulated focusing effect and a 3D-printed array of the previous geometry (d)[734]. Design assemble of a column of single metamaterial cells (e)[734]. Reproduced from Jiao Qian, Jian-ping Xia, Hong-xiang Sun, Shou-qi Yuan, Yong Ge, Xiao-zhu Yu; Broadband acoustic focusing by cavity structures with phase manipulations. J. Appl. Phys. 28 December 2017; 122 (24): 244501, with the permission of AIP Publishing. Design and schematisation and simulation of a Fresnel lens that, as a recursive structure, is capable of acoustic focusing at specific frequencies (f)[735]. Testing setup of the Fresnel lens (g)[735]. Reproduced from Xue-ying Gao, Xiao-bin Cui, Yong Zhang, Jie-jun Zhu, Cheng-ping Huang; Acoustoelectric conversion and deep-subwavelength acoustic focusing based on Fresnel zone plates. AIP Advances 1 March 2023; 13 (3): 035336, with the permission of AIP Publishing.

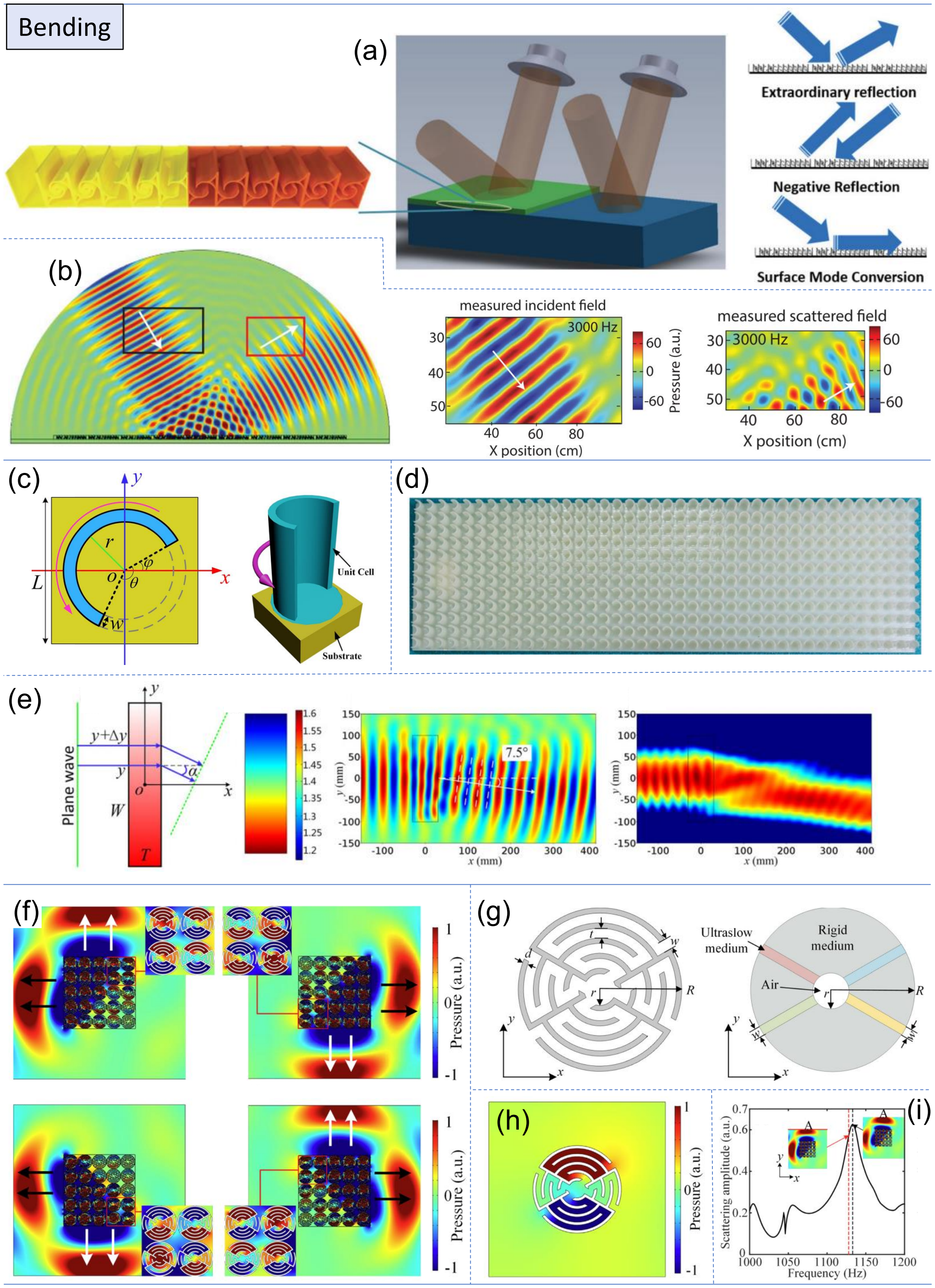

FIG. 14. Coiled 3D-printed metamaterial that allows different steering angles for the acoustic waves (a)[317]. FEM results at a specific frequency where the wave bending is more prominent (b)[317]. Reproduced from Wenqi Wang, Yangbo Xie, Bogdan-Ioan Popa, Steven A. Cummer; Subwavelength diffractive acoustics and wavefront manipulation with a reflective acoustic metasurface. J. Appl. Phys. 21 November 2016; 120 (19): 195103, with the permission of AIP Publishing. Unit cell that can be modified acting on its rotational angle (c)[736]. 3D-printed array of single metamaterial cells having different relative rotations to achieve wave steering (d)[736]. Simulation of the array lens effect, steering the acoustic field by 7.5 degrees (e)[736]. Reproduced from Lin Bai, Gang Yong Song, Wei Xiang Jiang, Qiang Cheng, Tie Jun Cui; Acoustic tunable metamaterials based on anisotropic unit cells. Appl. Phys. Lett. 2 December 2019; 115 (23): 231902, with the permission of AIP Publishing. Simulation of a 90 degrees bending of the pressure field, passing through an array of circular acoustic metamaterial (f)[737]. Circular metamaterial cell, with maze design inside and its respective effective medium (g)[737]. Pressure field that underlines a dipolar mode inside a single metamaterial cell and effective medium (h)[737]. Frequency-dependent normalized amplitude of the scattering pressure (i)[737]. Reproduced from Jun Lan, Yunpeng Liu, Tao Wang, Yifeng Li, Xiaozhou Liu; Acoustic coding metamaterial based on non-uniform Mie resonators. Appl. Phys. Lett. 18 April 2022; 120 (16): 163501, with the permission of AIP Publishing.